ABSTRACT

Title of dissertation: UTILITY DRIVEN SAMPLED DATA CONTROL UNDER IMPERFECT INFORMATION

Pavankumar Tallapragada,
Doctor of Philosophy, 2013

Dissertation directed by: Dr. Nikhil Chopra
Department of Mechanical Engineering

Computer based control systems, which are ubiquitous today, are essentially sampled data control systems. In the traditional *time-triggered* control systems, the sampling period is conservatively chosen, based on a worst case analysis. However, in many control systems, such as those implemented on embedded computers or over a network, parsimonious sampling and computation is helpful. In this context, state/data based aperiodic utility driven sampled data control systems are a promising alternative. This dissertation is concerned with the design of utility driven event-triggers in certain classes of problems where the information available to the triggering mechanisms is imperfect. In the first part, the problem of utility driven event-triggering under partial state information is considered - specifically in the context of (i) decentralized sensing and (ii) dynamic output feedback control. In the case of full state feedback, albeit with decentralized sensing, methods are developed for designing local and asynchronous event-triggers for asymptotic stabilization of an equilibrium point of a general nonlinear system. In the special case of

Linear Time Invariant (LTI) systems, the developed method also holds for dynamic output feedback control, which extends naturally to control over Sensor-Controller-Actuator Networks (SCAN), wherein even the controller is decentralized. The second direction that is pursued in this dissertation is that of parsimonious utility driven sampling not only in time but also in space. A methodology of co-designing an event-trigger and a quantizer of the sampled data controller is developed. Effectively, the proposed methodology provides a discrete-event controller for asymptotic stabilization of an equilibrium point of a general continuous-time nonlinear system. In the last part, a method is proposed for designing utility driven event-triggers for the problem of trajectory tracking in general nonlinear systems, where the source of imperfect information is the exogenous reference inputs. Then, specifically in the context of robotic manipulators we develop utility driven sampled data implementation of an adaptive controller for trajectory tracking, wherein imperfect knowledge of system parameters is an added complication.

UTILITY DRIVEN SAMPLED DATA CONTROL UNDER IMPERFECT INFORMATION

by

Pavankumar Tallapragada

Dissertation submitted to the Faculty of the Graduate School of the
University of Maryland, College Park in partial fulfillment
of the requirements for the degree of
Doctor of Philosophy
2013

Advisory Committee:
Assistant Professor Nikhil Chopra, Chair/Advisor
Professor Balakumar Balachandran
Professor Amr M. Baz
Associate Professor Jaydev P. Desai
Professor P. S. Krishnaprasad, Dean's Representative

Acknowledgments

I owe my gratitude to all the people who made this dissertation possible and who have made my graduate studies a memorable learning experience. First and foremost, I am grateful to my advisor Dr. Nikhil Chopra for his continuous support, patience and encouragement during my PhD. I also thank him for providing an open and free environment that allowed me to explore and pursue various research problems.

I also thank Prof. P. S. Krishnaprasad, Prof. Balakumar Balachandran, Prof. Amr M. Baz and Prof. Jaydev P. Desai for serving on my committee and for their valuable inputs that improved the quality of the dissertation.

I am grateful to all my colleagues and friends for helping me in various ways and for making my time at UMD memorable. Specifically, I want to thank Yen-Chen Liu, Rubyca Jaai, David Berman, Eliot Rudnick, Mohamed Raafat, Atul Thakur, Anupam Anand and Sabyasachee Mishra. I also thank the ME administrative staff for all their help in making my stay at UMD smooth.

Lastly, I thank my parents and my brother for their unconditional love and support, without which this dissertation would not have been possible.

I acknowledge support for my research by the National Science Foundation under the grants numbered 0931661 and 1232127; and by the Office of Naval Research under the grant numbered N000141310160.

Table of Contents

List of Figures

Chapter 1

Introduction

The subject of this dissertation is the designing of utility driven sampling mechanisms in sampled data control systems, specifically under some kind of imperfect information. In this chapter, the broader motivation for utility driven sampled data control is provided. Then, an outline of the dissertation and a summary of the contributions is given. The final section paves the way for the subsequent chapters by introducing the notation commonly used in the dissertation and by highlighting the factors that affect the design of utility driven sampled data control systems.

1.1 Motivation

Computer based control systems, which are ubiquitous today, are essentially sampled data control systems, wherein the control input to a 'plant' is computed based on a sampled version of, often continuously varying, signals. In traditional *time-triggered* control systems, this sampling of the sensor data and computation/execution of the control is done periodically. A basic time-triggered sampled data control system is shown in Figure 1.1 (for simplicity time-triggering has been shown only on the actuation side). The control input to the plant is updated at discrete time instants and it is held constant between updates. At discrete (and usually periodic) time instants, the 'external' clock *triggers* the updates of the control input to the plant.

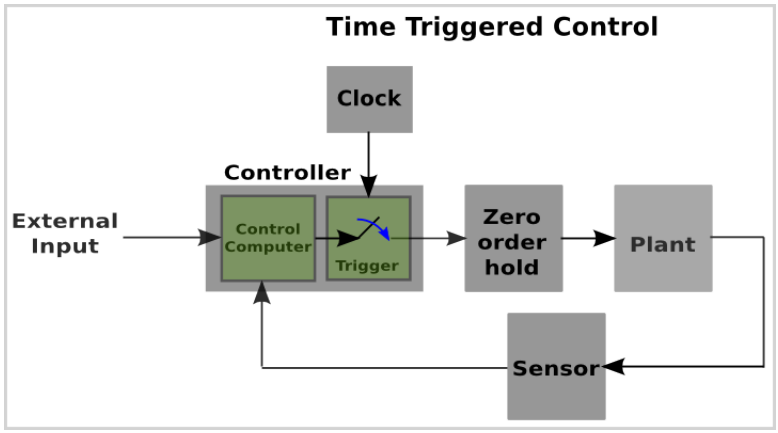

Figure 1.1: Time-triggered sampled data control.

The reasons for the popularity of this paradigm are ease of implementation and applicability to a wide range of systems. However, such sampled data control systems come at the cost of increased inefficiency from a sampling and computational perspective. This is because the period for sampling and control execution has to be determined by a worst case analysis and is independent of the system's state. This issue assumes even greater significance in the context of Cyber Physical Systems. For example, for control systems implemented on embedded computers with low computational capabilities, or for control systems implemented over a network with data rate constraints, parsimonious sampling and computation is helpful.

In this context, state based aperiodic sampling is a promising alternative. In sampled data control systems, the requirement of a sampling mechanism is not usually reconstruction of the analog signal. Rather, it is to sufficiently serve the overall control goal - such as stabilization of a fixed point (equilibrium point). Thus, state based aperiodic sampling techniques have been explored over the years in different

forms and under different names [1–5], [6, 7] (Lebesgue sampling), [8] (interrupt-based control or feedback triggered control), [9] (state-triggered control). More recently, research in these directions has become focused as 'event-triggered' or 'event based' control [10–22], which is a representative list of some early papers. A basic *event-triggered* sampled data control system is shown in Figure 1.2. The triggering

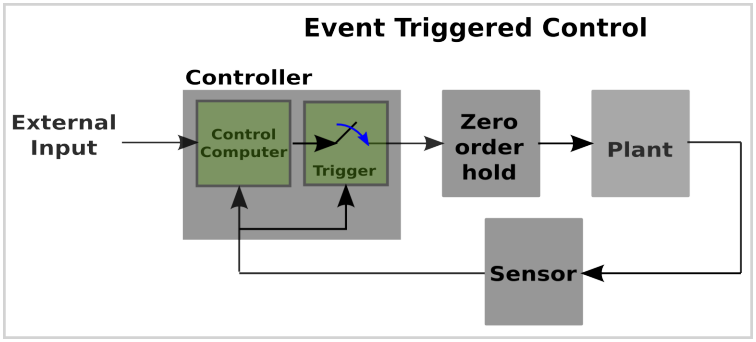

Figure 1.2: Event-triggered sampled data control.

in this paradigm is, in general, aperiodic and is determined by a state/data dependent event-triggering condition that explicitly encodes the control goal. Thus, by appropriately designing the event-trigger, the control system samples only when necessary - when the last sampled data is deemed no longer useful towards meeting the control goal specifications. Thus, such control systems may be called 'utility driven sampled data control systems'.

Although this dissertation is closely related to the event-triggered control literature, we often (specially in this chapter) refer to our own work and that of others in the literature by the phrases 'utility driven sampled data control', 'utility driven event-triggering' and their variants. This has been done for two main reasons. First, these phrases emphasise the explicit encodement of the control goal in the event-

triggering conditions. Second, the term 'event' in the control community has other, well established connotations - such as in Discrete Event Systems [23] and in the area of robotics, where the controller responds to events such as the robot encountering an obstacle in its path. In each of these cases, the term 'event' is referred to something that is external to the control system. On the other hand, in the event-triggered control paradigm of Figure 1.2 and in much of the literature on the subject, 'events' and 'event' generation are internal mechanisms of the control system. Thus, to highlight this important distinction, the phrase 'utility driven ...' and its variants are used in this dissertation.

At this stage a further clarification is needed. The sampled data control systems that we consider are based on emulating a given continuous time controller. That is, the 'control computer' in Figure 1.2 is assumed to be given. The proposed design methods simply prescribe the event-triggers that determine the sampling time instants based on a notion of utility towards fulfilling a control goal. Indeed, this is the approach adopted in much of event-triggered control literature. Moreover, in this dissertation we restrict the control goal specifications to asymptotic stabilization of an equilibrium point or a reference trajectory with a prescribed (state dependent) minimum convergence rate. Our guiding principle during the design of the event-triggers is to ensure the sampling instances to be as parsimonious as possible while also ensuring that the event-triggering condition is sufficiently simple enough. Obviously, each of these two requirements is in conflict with the other. However, a precise mathematical formulation of a trade-off is beyond the scope of this dissertation. Thus, the term 'utility' is also used in a somewhat mathematically

imprecise manner.

1.2 Outline and Contributions of the Dissertation

Much of the emerging area of utility driven event-triggered control and the closely related field of self-triggered control [24–28] is applicable for fixed-point stabilization under full state feedback. However, in practice, there are many applications where there is some imperfection in the information available to an event-trigger. This imperfection in the information may be due to varied factors such as exogenous reference signals, quantization, imperfect knowledge of system's dynamic parameters or lack of full state feedback at an event-trigger either due to decentralization or simply due to inherent lack of full state feedback in the system. This dissertation addresses each of these issues in settings of varying generality. An outline and a summary of the contributions of the dissertation follows.

The dissertation is broadly divided into three parts. The first part of the dissertation is utility driven event-triggering under partial state information. Much of the existing literature on event-triggered control assumes the availability of the full state information to event-trigger. This assumption fails to be satisfied in two very important scenarios - decentralized control systems and dynamic output feedback control. The first scenario is addressed in Chapter 2, where in a control system with decentralized sensors and a central controller is considered. The decentralized sensors together are assumed to sense the complete state of the system, which however transmit data to the central controller intermittently and asynchronously at time

instants determined by local utility driven event-triggers. In the literature, some approached this problem with restrictive assumptions. Others proposed event-triggers that could guarantee only semi-global practical stability even for linear systems if the sensors did not listen to the central controller. In contrast, the event-triggering scheme that we propose guarantees semi-global asymptotic stability for nonlinear systems and global asymptotic stability for linear systems without the sensors having to listen to the controller. However, in the nonlinear case the design is conservative. Thus, we also propose a modification, wherein the sensors occasionally receive updates from the controller.

Chapter 3 addresses the scenario where a system inherently lacks full state feedback and instead an output feedback dynamic (for example, observer based) controller has to be used. This chapter is concerned solely with Multi Input Multi Output (MIMO) Linear Time Invariant (LTI) systems. As one might expect, this problem is closely related to the subject matter of Chapter 2 and naturally extends to the case where the sensors are decentralized and not co-located with the controller. In this chapter, we in fact progress from a centralized architecture where the sensors, controller and the actuators are co-located to a fully decentralized control system - a Sensor-Controller-Actuator Network (SCAN). Again, the existing results in the literature guarantee only semi-global practical stability, while the proposed utility driven event-triggering scheme guarantees global asymptotic stability. Even in the most general of the architectures considered in this chapter, Sensor-Controller-Actuator Network (SCAN), the assumptions on the system matrices are fairly simple. Portions of this chapter have been published in [29, 30].

The second part expands the definition of utility driven sampling to include sampling in both time and space. The fields of event-triggered control and coarsest quantization have very similar motivations, although they are aimed at 'coarse sampling' in time and space, respectively. In Chapter 4, we exploit the common principle behind two fields, which is robustness/tolerance to measurement errors, to design implicitly verified discrete-event emulation based controllers for asymptotic stabilization of general nonlinear systems. In comparison to the coarsest quantization literature, our quantizer design holds for general multi-input nonlinear continuous time systems. A significant portion of the work in this chapter has been published in [31].

The third part is on utility driven sampled data control for trajectory tracking. Tracking a time varying trajectory or even a set-point is of tremendous practical importance in many control applications. In these applications, the goal is to make the state of the system follow a reference or desired trajectory, which is usually specified as an exogenous input to the system. In Chapter 5, a method for designing utility driven event-triggered controllers for trajectory tracking in nonlinear systems is proposed. Parts of the work in this chapter have been published in [32,33], which are also the first to consider this important problem.

In Chapter 6, we propose a utility driven sampled data implementation of an adaptive controller for trajectory tracking in robot manipulators. This is motivated by the fact that commonly, utility driven event-triggered controllers such as the one presented in Chapter 5 rely on the knowledge of an accurate model of the system. However, building a model of high accuracy is a time consuming process and in

many cases, it may not even be possible. Therefore, it is important to extend the design of implicitly verified event based controllers to cases where only a poor model of the system is available. In this work, we propose an event-triggered emulation of an adaptive controller from the existing literature. The proposed controller is tested through simulations and experiments performed on a PHANToM Omni robotic manipulator. The contribution of this chapter is two fold. It is only the second work to consider an event-triggered implementation of an adaptive controller and, further, the only work applicable to a nonlinear and continuous time system. This chapter also contributes to the as yet limited body of experimental results on utility driven event-triggered control.

Finally, the dissertation is concluded in Chapter 7 with a summary and some possible directions for future research.

1.3 Preliminaries

The aim of this section is to introduce the preliminaries of utility driven sampled data control and highlight some important issues/factors affecting the design process. To this end, we introduce some basic mathematical notation and consider the problem of asymptotic stabilization of Multi Input Multi Output (MIMO) Linear Time Invariant (LTI) systems.

Now, in sampled data control systems, the controller and/or the actuator make use of sampled versions of continuous-time signals. Thus, let ζ be any continuous-time signal (scalar or vector) and let $\{t_i^{\zeta}\}$ be the increasing sequence of discrete time

instants at which ζ is sampled. Then we denote the resulting piecewise constant sampled signal by ζ_s, that is,

$$\zeta_s \triangleq \zeta(t_i^\zeta), \quad \forall t \in [t_i^\zeta, t_{i+1}^\zeta) \tag{1.1}$$

Often it is useful to view the sampled data, ζ_s, as resulting from an error in the the measurement of the continuous-time signal, ζ, which is denoted by

$$\zeta_e \triangleq \zeta_s - \zeta = \zeta(t_i^\zeta) - \zeta, \quad \forall t \in [t_i^\zeta, t_{i+1}^\zeta) \tag{1.2}$$

Note that ζ_e is discontinuous at $t = t_i^\zeta$, for each i, because $\zeta_e(t_i^\zeta) = \zeta(t_i^\zeta) - \zeta(t_i^\zeta) = 0$ while $\lim_{t \uparrow t_i^\zeta} \zeta_e(t) = \lim_{t \uparrow t_i^\zeta} (\zeta(t_{i-1}^\zeta) - \zeta(t))$.

In time-triggered implementations, the time instants t_i^ζ in (1.1) are pre-determined and are commonly a multiple of a fixed sampling period. On the other hand, in event-triggered implementations the time instants t_i^ζ are determined implicitly by a state/data based triggering condition that is checked online. Consequently, an event-triggering condition may result in the inter sampling times $t_{i+1}^\zeta - t_i^\zeta$ to be arbitrarily close to zero or it may even result in the limit of the sequence $\{t_i^\zeta\}$ to be a finite number (*Zeno* behavior). Thus for practical utility, an event-trigger has to ensure that these scenarios do not occur. The event-triggering condition may be as simple as a threshold crossing of the measurement error, ζ_e. In utility driven sampled data control, implicitly verified (guaranteed to meet the control goal) task specific event-triggering conditions are designed so that the sampling is parsimonious.

Now, consider the continuous-time system

$$\dot{x} = Ax + Bu_s$$

where $x \in \mathbb{R}^n$, and $u_s \in \mathbb{R}^m$, are the plant state and the control input to the plant, respectively. The matrices A and B are of appropriate dimensions. The subscript s in u_s indicates that the controller is a sampled data controller. In this dissertation, we are interested in emulation based utility driven sampled data control. That is, the controller is a sampled data version of a given continuous-time controller. Our job then is to design a utility driven event-trigger that determines when the piecewise constant sampled data signal u_s is updated.

Thus in the current example, let the control goal is global asymptotic stabilization of the origin of the closed loop system and let the continuous-time controller $u = Kx$ be given to us. In other words, suppose that the gain matrix K renders the matrix $\bar{A} = (A + BK)$ Hurwitz. Then, the closed loop system with the sampled data controller is given by

$$\dot{x} = Ax + Bu_s, \quad u_s = Kx_s \tag{1.3}$$

where x_s is defined as in (1.1).

Now, given an $n \times n$ symmetric positive definite matrix Q, there exists a symmetric positive definite matrix P that satisfies

$$P\bar{A} + \bar{A}^T P = -Q.$$

Then, consider the Lyapunov function $V = x^T P x$ and its derivative along the flow

of the closed loop system

$$\begin{aligned}\dot{V} &= x^T[P\bar{A} + \bar{A}^T P]x + 2x^T PBK(x_s - x) \\ &= -x^T Qx + 2x^T PBKx_e \\ &= -(1-\sigma)x^T Qx - \sigma x^T Qx + 2x^T PBKx_e \end{aligned} \tag{1.4}$$

where $\sigma \in (0,1)$ is a design parameter. This suggests that

$$\dot{V} \leq -(1-\sigma)x^T Qx < 0, \quad \text{if} \;\; 2x^T PBKx_e \leq \sigma x^T Qx$$

Thus, global asymptotic stability of the origin is guaranteed if, for example, the time instants at which $u_s = Kx_s$ are given by

$$\begin{aligned} t_0^x &= 0 \\ t_{i+1}^x &= \min\{t \geq t_i^x : 2x^T PBKx_e \geq \sigma x^T Qx\} \end{aligned} \tag{1.5}$$

Thus, the sampling time instants are given implicitly in terms of the last sampled data and the current state of the system. Of course, the initial sampled data or the first sampling instant is to be specified explicitly. The inter-sample times implicitly defined by (1.5) can be shown to have a positive lower bound [14,34]. Now, note that this state dependent event-trigger is designed specifically for the task of asymptotic stabilization with a desired minimum rate of convergence. As one might expect, there is a direct trade-off between the desired minimum rate of convergence (higher is desirable) and the average sampling rate (lower is desirable). In the event-trigger (1.5), there is a tunable design parameter σ that lets us trade the desired minimum rate of convergence with the average sampling rate. Smaller σ value means a higher

desired minimum rate of convergence as well as a higher average sampling rate. On another note, in practice, there may be time delays in the control system which may adversely affect the system. Although in the above example and in the rest of the dissertation we do not explicitly address the issue of time delays, one may follow the standard procedure in the literature (see [14] for example) to provide a bound on safely tolerable time delays (higher is desirable). It suffices to say that the parameter σ affects the bound on safely tolerable time delays - smaller σ allows larger time delays. Therefore, there is again a trade-off between the average sampling rate and tolerable time delays, or alternatively, there is a trade-off between the desired minimum rate of convergence and tolerable time delays. In each of the proposed event-triggers, in the forthcoming chapters of the dissertation, there is a tunable parameter σ that analogously provides a trade-off between various characteristics.

In the example, the event-trigger is designed specifically for the task of asymptotic stabilization with a desired minimum rate of convergence. In other words, the event-trigger explicitly encodes the control goal and triggers the sampling of the signals only when it is necessary - when the last sampled data is no longer useful. It is in this sense that (1.3)-(1.5) is called a utility driven sampled data control system. This basic idea can be extended to design utility driven event-triggers for more sophisticated control goals such as asymptotic stabilization, but without the requirement of monotonically decreasing Lyapunov function V (see [34] for example). In this dissertation, the control goals are restricted to the simpler variety presented in the example, but, in scenarios where the information available to the event-trigger is imperfect. Chapters 2 and 3 are concerned with designing event-triggers that

have access only to partial state information. In Chapter 4, quantization is considered in addition to sampling in time and proposes a method for co-designing the event-trigger and the quantizer. In Chapter 5, it is in the form of exogenous reference trajectory. Chapter 6 explores the case where the dynamic parameters of the robotic system are unknown and adaptively estimated. Finally, we recall the guiding principle in our proposed designs - in addition to requiring the sampling to be parsimonious, we also want the event-triggers to be simple enough. Notice that in (1.5), the complexity of the event-trigger increases with the state space dimension. For example, each of the expressions in the inequality requires n^3 multiplications to be computed, where n is the state space dimension. Hence, the proposed event-triggers are usually simpler and conservative than the "coarsest" possible event-triggers.

Part I

Event-Triggering Under Partial State Information

Chapter 2

Decentralized Utility Driven Event-Triggering for Control of Nonlinear Systems

2.1 Introduction

Much of the literature on event-triggered control utilizes the full state information in the triggering conditions. However, in two very important classes of problems full state information is not available to the event-triggers. These are systems with decentralized sensing and/or dynamic output feedback control. In the latter case, full state information is not available even when the sensors and the controller are centralized (*co-located*). In systems with decentralized sensing, each individual sensor has to base its decision to transmit data to a central controller only on locally available information. These two classes of problems are receiving attention in the community only recently - [35–39] (decentralized sensing) and [29, 30, 40–44] (output feedback control). This chapter and the next present some useful ideas towards addressing these problems.

2.1.1 Contributions

In this chapter we propose a methodology for designing implicitly verified decentralized event-triggers for control of nonlinear systems. The system architecture we

consider is one with full state feedback but with the sensors decentralized and not co-located with a central controller. The proposed design methodology provides event-triggers that determine when each sensor transmits data to a central controller. The event-triggers are designed to utilize only locally available information, making the transmissions from the sensors asynchronous. The proposed design guarantees asymptotic stability of the origin of the system with an arbitrary, but fixed *a priori*, compact region of attraction. It also guarantees a positive lower bound for the inter-transmission times of each sensor individually. In the special case of Linear Time Invariant (LTI) systems, global asymptotic stability is guaranteed and scale invariance of inter-transmission times is preserved. For nonlinear systems, we also propose a variant with event-triggered communication from the central controller to the sensors that significantly increases the average sensor inter-transmission times.

In the literature, decentralized event-triggered control was studied in [38, 39] with the assumption that the subsystems are weakly coupled, which allowed the design of event-triggers depending on only local information. Our proposed design method requires much less restrictive assumptions. In [35–37], each sensor checks a local condition (based on threshold crossing) that triggers asynchronous transmission of data by sensors to a central controller. However, this design guarantees only semi-global practical stability (even for linear systems) if the sensors do not listen to the central controller. Compared to this work, our proposed design guarantees semi-global asymptotic stability even when the sensors do not listen to the central controller. For linear systems, our proposed method gurantees global asymptotic stability without the sensors having to listen to the central controller. A similarity

between our work and [35–37] is that both are partially motivated by the need to eliminate or drastically reduce the listening effort of the sensors to save energy.

The rest of the chapter is organized as follows. Section 2.2 describes and formally sets up the problem under consideration. In Section 2.3, the design of asynchronous decentralized event-triggers for nonlinear systems is presented - without, and then with, feedback from the central controller. Section 2.4 presents the special case of Linear Time Invariant (LTI) systems. The proposed design methodology is illustrated through simulations in Section 2.5 and finally Section 2.6 provides some concluding remarks.

2.2 Problem Setup

Consider a nonlinear control system

$$\dot{x} = f(x, u), \quad x \in \mathbb{R}^n, \ u \in \mathbb{R}^m \tag{2.1}$$

with the feedback control law

$$u = k(x + x_e) \tag{2.2}$$

where x_e is the error in the measurement of x. In general, the measurement error can be due to many factors such as sensor noise and quantization. However, we consider measurement error that is purely a result of "sampling" of the sensor data x. Before going into the precise definition of this measurement error, we first describe the broader problem. First, let us express (2.1) as a collection of n scalar differential

equations

$$\dot{x}_i = f_i(x, u), \quad x_i \in \mathbb{R}, \quad i \in \{1, 2, \ldots, n\} \tag{2.3}$$

where $x = [x_1, x_2, \ldots, x_n]^T$. In this chapter we are concerned with a decentralized sensing scenario where each component, x_i, of the state vector x is sensed at a different location. Although the i^{th} sensor senses x_i continuously in time, it transmits this data to a central controller only intermittently. In other words, the controller is a sampled-data controller that uses intermittently transmitted/sampled sensor data. In particular, we are interested in designing a mechanism for asynchronous decentralized utility driven event-triggering that renders the origin of the closed loop system asymptotically stable.

To precisely describe the sampled-data nature of the problem, we now introduce the following notation. Let $\{t_j^{x_i}\}$ be the increasing sequence of time instants at which x_i is sampled and transmitted to the controller. The resulting piecewise constant sampled signal is denoted by $x_{i,s}$, that is,

$$x_{i,s} \triangleq x(t_j^{x_i}), \quad \forall t \in [t_j^{x_i}, t_{j+1}^{x_i}), \quad \forall j \in \{0, 1, 2, \ldots\} \tag{2.4}$$

As mentioned previously, the sampled data, $x_{i,s}$, may also be viewed as resulting from an error in the the measurement of the continuous-time signal, x_i. This measurement error is denoted by

$$x_{i,e} \triangleq x_{i,s} - x_i = x_i(t_j^{x_i}) - x_i, \quad \forall t \in [t_j^{x_i}, t_{j+1}^{x_i})$$

Finally, we define the sampled-data vector and the measurement error vector as

$$x_s \triangleq [x_{1,s}, x_{2,s}, \ldots, x_{n,s}]^T, \qquad x_e \triangleq [x_{1,e}, x_{2,e}, \ldots, x_{n,e}]^T$$

Note that, in general, the components of the vector x_s are asynchronously sampled components of the plant state x. The components of x_e are also defined accordingly.

Thus, the problem under consideration may be stated more precisely as follows. For the n sensors, we want to design event-triggers that depend only on local information and implicitly define the non-identical sequences $\{t_j^{x_i}\}$ such that (i) the origin of the closed loop system is rendered asymptotically stable and (ii) inter-sample (inter-transmission) times $t_{j+1}^{x_i} - t_j^{x_i}$ are lower bounded by a positive constant.

Finally, a point regarding the notation in the chapter is that the notation $|.|$ denotes the Euclidean norm of a vector. In the next section, the main assumptions are introduced and the event-triggering conditions for the decentralized sensing architecture is developed.

2.3 Decentralized Asynchronous Event-Triggering

In this section, the main assumptions are introduced and the event-triggers for the decentralized asynchronous sensing problem are developed.

(A2.1) The closed loop system (2.1)-(2.2) is Input-to-State Stable (ISS) with respect to measurement error x_e. That is, there exists a smooth function $V : \mathbb{R}^n \to \mathbb{R}$ as well as class $\mathcal{K}_\infty$ functions[1] α_1, α_2, α and γ_i for each $i \in \{1, \ldots, n\}$, such

[1] A continuous function $\alpha : [0, \infty) \to [0, \infty)$ is said to belong to the class $\mathcal{K}_\infty$ if it is strictly increasing, $\alpha(0) = 0$ and $\alpha(r) \to \infty$ as $r \to \infty$ [45].

that

$$\alpha_1(|x|) \leq V(x) \leq \alpha_2(|x|)$$
$$\frac{\partial V}{\partial x} f(x, k(x + x_e)) \leq -\alpha(|x|), \quad \text{if } \gamma_i(|x_{i,e}|) \leq |x|, \ \forall i.$$

(A2.2) The functions f, k and γ_i, for each $i \in \{1, \ldots, n\}$, are Lipschitz on compact sets.

Note that the standard ISS assumption involves a single condition $\gamma(|x_e|) \leq |x|$ instead of the n conditions: $\gamma_i(|x_{i,e}|) \leq |x|$, for $i \in \{1, \ldots, n\}$, in (A2.1). Given a function $\gamma(.)$ in the standard ISS assumption, one may define $\gamma_i(.)$ as

$$\gamma_i(|x_{i,e}|) = \gamma\left(\frac{|x_{i,e}|}{\theta_i}\right), \quad i \in \{1, \ldots, n\}$$

where $\theta_i \in (0, 1)$ such that $\theta^2 = \sum_{i=1}^{n} \theta_i^2 \leq 1$. Then, the n conditions in (A2.1) are equivalent to $|x_{i,e}| \leq \theta_i \gamma^{-1}(|x|)$. Thus,

$$|x_e| = \sqrt{\sum_{i=1}^{n} |x_{i,e}|^2} \leq \sqrt{\sum_{i=1}^{n} \theta_i^2} \gamma^{-1}(|x|) \leq \gamma^{-1}(|x|)$$

which is the condition in the standard ISS assumption. Similarly, given (A2.1) one may pick $\gamma(.) = \gamma_i(.)$ for any i to get the standard ISS assumption, although in practice it may be possible to choose a less conservative $\gamma(.)$.

In this section, our aim is to constructively show that decentralized asynchronous event-triggering can be used to asymptotically stabilize $x \equiv 0$ (the trivial solution or the origin) with a desired region of attraction while also guaranteeing positive minimum inter-sample times. Further, without loss of generality, the desired region of attraction may be assumed to be a compact sub-level set $S(c)$ of the

Lyapunov like function V in (A2.1). Specifically, $S(c)$ is defined as

$$S(c) = \{x \in \mathbb{R}^n : V(x) \leq c\} \tag{2.5}$$

2.3.1 Centralized Asynchronous Event-Triggering

The proposed design of decentralized asynchronous event-triggering progresses in stages. In the first stage, centralized event-triggers for asynchronous transmission by the sensors are proposed in the following lemma. One of the key steps in the result is choosing linear bounds on the functions $\gamma_i(.)$ on appropriately defined sets E_i. Given that $x \in S(c)$, we define the sets E_i over which the error bounds in (A2.1) are still satisfied, that is,

$$\begin{aligned} E_i(c) &= \{x_{i,e} \in \mathbb{R} : |x_{i,e}| \leq \gamma_i^{-1}(|x|),\ x \in S(c)\} \\ &= \{x_{i,e} \in \mathbb{R} : |x_{i,e}| \leq \max_{x \in S(c)} \{\gamma_i^{-1}(|x|)\}\} \end{aligned} \tag{2.6}$$

Then, by (A2.2), for each $c \geq 0$ and each $i \in \{1, \ldots, n\}$, there exist positive constants $M_i(c)$ such that

$$\gamma_i(|x_{i,e}|) \leq \frac{1}{M_i(c)}|x_{i,e}|,\ \forall x_{i,e} \in E_i(c) \tag{2.7}$$

Lemma 2.1. *Consider the closed loop system (2.1)-(2.2) and assume (A2.1) and (A2.2) hold. Suppose for each $i \in \{1, \ldots, n\}$, the sampling instants, $\{t_j^{x_i}\}$ ensure $|x_{i,e}| \leq M_i(c)|x|$ for all time $t \geq 0$, where $M_i(c)$ are given by (2.7) and $c \geq 0$ is an arbitrary constant. Then, the origin is asymptotically stable with $S(c)$, given by (2.5), as the region of attraction.*

Proof. Suppose $x(0) \in S(c)$ is an arbitrary point, we have to show that the trajectory $x(.)$ asymptotically converges to zero. Note that, by assumption, the sampling instants are such that for each $i \in \{1, \ldots, n\}$, $\frac{|x_{i,e}|}{M_i(c)} \leq |x|$ for all time $t \geq 0$. Then, for all time $t \geq 0$, (2.7) implies

$$\gamma_i(|x_{i,e}|) \leq \frac{1}{M_i(c)}|x_{i,e}| \leq |x|, \quad \forall x \in S(c)$$

Consider the ISS Lyapunov function $V(.)$ in (A2.1), which is a function of the state x. Letting $E(c) \triangleq E_1(c) \times E_2(c) \times \ldots \times E_n(c)$, the time derivative of the function V along the flow of the closed loop system, with a restricted domain, $\dot{V}(x, x_e) : S(c) \times E(c) \to \mathbb{R}$ can be upper-bounded as

$$\dot{V}(x, x_e) \leq -\alpha(|x|), \quad \forall x \in S(c), \quad \forall x_e \in E(c)$$

Thus, the flow of the closed loop system is dissipative on the sub-level set, $S(c)$, of the Lyapunov function V. Therefore, the origin is asymptotically stable with $S(c)$ as the region of attraction. □

The lemma does not mention a specific choice of event-triggers but rather a family of them - all those that ensure the conditions $|x_{i,e}| \leq M_i(c)|x|$ are satisfied. Thus, any decentralized event-triggers in this family automatically guarantee asymptotic stability with the desired region of attraction. To enforce the conditions $|x_{i,e}| \leq M_i(c)|x|$ strictly, event-triggers at each sensor would need to know $|x|$, which is possible only if we have centralized information. One obvious way to decentralize these conditions is to enforce $|x_{i,e}| \leq M_i(c)|x_i|$. However, such event-triggers cannot guarantee any positive lower bound for the inter-transmission times, which is not

acceptable. So, we take an alternative approach, in which the next step is to derive lower bounds for the inter-transmission times when the conditions in Lemma 2.1 are enforced strictly.

Before analyzing the lower bounds for the inter-transmission times that emerge from the event-triggers in Lemma 2.1, we introduce some notation. Noting that for each $c \geq 0$ the set $S(c)$ contains the origin, Assumption (A2.2) implies that there exist Lipschitz constants $L(c)$ and $D(c)$ such that

$$\left|f(x, k(x + x_e))\right| \leq L(c)|x| + D(c)|x_e| \tag{2.8}$$

for all $x \in S(c)$ and for all x_e satisfying $|x_{i,e}|/|x| \leq M_i(c)$, for each i. Similarly, there exist constants $L_i(c)$ and $D_i(c)$ for $i \in \{1, 2, \ldots, n\}$ such that

$$\left|f_i(x, k(x + x_e))\right| \leq L_i(c)|x| + D_i(c)|x_e| \tag{2.9}$$

for all $x \in S(c)$ and for all x_e satisfying $|x_{i,e}|/|x| \leq M_i(c)$, for each i.

Now, consider the differential equation

$$\dot{\phi} = a_0 + a_1\phi + a_2\phi^2 \tag{2.10}$$

where a_0, a_1, a_2 are non-negative constants. The solution of this differential equation is denoted, as a function of time t and the initial condition ϕ_0, as $\phi(t, \phi_0)$. In particular, if $a_0 > 0$ then $\phi(t, 0)$ is a strictly increasing function of time t and if $a_0 = 0$ then $\phi(t, 0) \equiv 0$. Thus, the time it takes ϕ to evolve from 0 to a non-negative constant w is expressed as

$$\tau(w, a_0, a_1, a_2) = \min\{\{t \geq 0 : \phi(t, 0) = w\} \cup \{\infty\}\} \tag{2.11}$$

Notice that

$$\tau(w, a_0, a_1, a_2) \begin{cases} = 0, & \text{if } w = 0 \\ > 0, & \text{if } w > 0 \\ = \infty, & \text{if } w > 0,\ a_0 = 0 \end{cases} \tag{2.12}$$

Remark 2.1. *Assuming a_2 is non-zero, the solutions of the quadratic differential equation (2.10) have a finite escape time. However, by definition (2.11), $\tau(w, a_0, a_1, a_2)$ is strictly less than the finite escape time of the solution $\phi(., 0)$. Thus on the time interval of interest, $[0, \tau(w, a_0, a_1, a_2)]$, the solution $\phi(., 0)$ is well defined.*

Lemma 2.2. *Consider the closed loop system (2.1)-(2.2) and assume (A2.2) holds. Let $c > 0$ be any arbitrary known constant. For $i \in \{1, \ldots, n\}$, let $0 \leq w_i \leq M_i(c)$ be any arbitrary constants and let $W_i = \sqrt{\left(\sum_{j=1}^{n} w_j^2\right) - w_i^2}$. Suppose the sampling instants are such that $|x_{i,e}|/|x| \leq w_i$ for each $i \in \{1, \ldots, n\}$ for all time $t \geq t_0$. Finally, assume that for all $t \geq t_0$, x belongs to the compact set $S(c)$. Then, for all $t \geq t_0$, the time required for $|x_{i,e}|/|x|$ to evolve from 0 to w_i is lower bounded by*

$$T_i = \tau(w_i, a_{0,i}, a_{1,i}, a_{2,i}) \tag{2.13}$$

where the function τ is given by (2.11) and

$$a_{0,i} = L_i(c) + D_i(c)W_i,$$

$$a_{1,i} = L(c) + D_i(c) + D(c)W_i, \quad a_{2,i} = D(c)$$

Further, if $w_i > 0$ then $T_i > 0$.

Proof. By assumption, for all $t \geq t_0$, x belongs to a known compact set $S(c)$ and $|x_{i,e}|/|x| \leq w_i \leq M_i(c)$ for each i. Thus, (2.8) and (2.9) hold for all $t \geq t_0$. Now,

letting $\nu_i \triangleq |x_{i,e}|/|x|$ and by direct calculation we see that for $i \in \{1, \ldots, n\}$

$$\begin{aligned}\frac{\mathrm{d}\nu_i}{\mathrm{d}t} &= \frac{(x_{i,e}^T x_{i,e})^{-1/2} x_{i,e}^T \dot{x}_{i,e}}{|x|} - \frac{x^T \dot{x} |x_{i,e}|}{|x|^3} \\ &\leq \frac{|x_{i,e}||\dot{x}_{i,e}|}{|x_{i,e}||x|} + \frac{|x||\dot{x}||x_{i,e}|}{|x|^3} \\ &\leq \frac{L_i(c)|x| + D_i(c)|x_e|}{|x|} + \frac{\big(L(c)|x| + D(c)|x_e|\big)|x_{i,e}|}{|x|^2}\end{aligned}$$

where for $x_{i,e} = 0$ the relation holds for all directional derivatives. Next, notice that

$$\frac{|x_e|}{|x|} = \sqrt{\sum_{j=1}^{j=n} \nu_j^2} \leq \sqrt{\left(\sum_{j=1}^{j=n} w_j^2\right) - w_i^2 + \nu_i^2} \leq W_i + \nu_i$$

where the condition that $\nu_i \leq w_i$, the definition of W_i and the triangle inequality property have been utilized. Thus,

$$\begin{aligned}\frac{\mathrm{d}\nu_i}{\mathrm{d}t} &\leq L_i(c) + L(c)\nu_i + \big(D_i(c) + D(c)\nu_i\big)(W_i + \nu_i) \\ &= a_{0,i} + a_{1,i}\nu_i + a_{2,i}\nu_i^2\end{aligned}$$

Now, let t_0^i be any time instant such that $\nu_i(t_0^i) = 0$. Next, consider the flow

$$\dot{\phi}_i = a_{0,i} + a_{1,i}\phi_i + a_{2,i}\phi_i$$

and its solution denoted, as a function of time t and the initial condition $\phi_{i,0}$, as $\phi_i(t, \phi_{i,0})$. Then, by the Comparison Lemma [45], it follows that

$$\nu_i(t) \leq \phi_i(t - t_0^i, 0), \quad \forall\ t \geq t_0^i$$

As a consequence T_i, given by (2.13) is a lower bound on the time it takes $\nu_i = |x_{i,e}|/|x|$ to evolve from 0 to w_i. The final claim of the Lemma follows from the property (2.12) of the function τ. □

Now, by combining Lemmas 2.1 and 2.2, we get the following result for the centralized asynchronous event-triggering.

Theorem 2.1. *Consider the closed loop system* (2.1)-(2.2) *and assume* (A2.1)-(A2.2) *hold. Suppose the* i^{th} *sensor transmits its measurement to the controller whenever* $|x_{i,e}|/|x| \geq w_i$*, where* $0 < w_i \leq M_i(c)$*, with* $M_i(c)$ *given by* (2.7) *and* $c \geq 0$ *any arbitrary constant. Then, the origin is asymptotically stable with* $S(c)$ *as the region of attraction and the inter-transmission times of each sensor have a positive lower bound given by* T_i *in* (2.13)*.*

Proof. The triggering conditions ensure that $|x_{i,e}|/|x| \leq w_i \leq M_i(c)$ for all $t > 0$. Thus, Lemma 2.1 guarantees $x \in S(c)$ for all $t \geq 0$ and that the origin is asymptotically stable with $S(c)$ included in the region of attraction. Since $S(c)$ is positively invariant, Lemma 2.2 guarantees a positive lower bound for the inter-transmission times. □

Remark 2.2. *In Lemma 2.2, the procedure for the computation of the lower bounds to the inter-transmission times is quite similar to that in [14]. The significant difference is that in Lemma 2.2, the guaranteed lower bounds are for asynchronous transmissions while [14] provides lower bounds for synchronous transmissions.*

2.3.2 Decentralized Asynchronous Event-Triggering

Now, turning to the main subject of this chapter, in the decentralized sensing case, unlike in the centralized sensing case, no single sensor knows the exact value of $|x|$ from the locally sensed data. We may let the event-trigger at the i^{th} sensor enforce

the more conservative condition $|x_{i,e}|/|x_i| \leq w_i$ and still satisfy the assumptions of Lemma 2.1, though such a choice cannot guarantee a positive minimum inter-sample time. At this stage, it might seem that Lemma 2.2 cannot be used to design an implicitly verified event-triggering mechanism in the decentralized sensing case. However, Lemma 2.2 can be interpreted in an alternative way, which would aid in our design goal.

Rather than providing a minimum inter-sampling time for an event-triggering mechanism, Lemma 2.2 can be interpreted as providing a minimum time threshold only after which it is necessary to check a data based event-triggering condition. For example, the event-triggers in Theorem 2.1,

$$t_{j+1}^{x_i} = \min\{t \geq t_j^{x_i} : \frac{|x_{i,e}|}{|x|} \geq w_i\}, \ i \in \{1, \ldots, n\} \tag{2.14}$$

can be equivalently expressed as

$$t_{j+1}^{x_i} = \min\{t \geq t_j^{x_i} + T_i : \frac{|x_{i,e}|}{|x|} \geq w_i\} \tag{2.15}$$

where T_i are the positive lower bounds for inter-sample times, that are guaranteed by Lemma 2.2 in (2.13). In the latter interpretation, a minimum threshold for inter-sample times is explicitly enforced, only after which, the state based condition is checked. Now, in order to let the event-triggers depend only on locally sensed data, one can let the sampling times, for $i \in \{1, \ldots, n\}$, be determined as

$$t_{j+1}^{x_i} = \min\{t \geq t_j^{x_i} + T_i : |x_{i,e}| \geq w_i|x_i|\} \tag{2.16}$$

where T_i are given by (2.13). This allows us to implement decentralized asynchronous event-triggering. The following theorem is the core result of this chapter

and it shows that by appropriately choosing the constants T_i and w_i, the event triggers, (2.16), guarantee asymptotic stability of the origin while also explicitly enforcing a positive minimum inter-sample time.

Theorem 2.2. *Consider the closed loop system* (2.1)-(2.2) *and assume* (A2.1) *and* (A2.2) *hold. Let* $c \geq 0$ *be an arbitrary known constant. For each* $i \in \{1, 2, \ldots, n\}$, *let* w_i *be a positive constant such that* $w_i \leq M_i(c)$, *where* $M_i(c)$ *is given by* (2.7) *and* T_i *be given by* (2.13). *Suppose the sensors asynchronously transmit the measured data at time instants determined by* (2.16) *and that* $t_0^{x_i} \leq 0$ *for each* $i \in \{1, 2, \ldots, n\}$. *Then, the origin is asymptotically stable with* $S(c)$ *as the region of attraction and the inter-transmission times of each sensor are explicitly enforced to have a positive lower threshold.*

Proof. The statement about the positive lower threshold for inter-transmission times is obvious from (2.16) and only asymptotic stability remains to be proven. This can be done by showing that the event-triggers (2.16) are included in the family of event-triggers considered in Lemma 2.1. From the equivalence of (2.14) and (2.15), it is clearly true that $|x_{i,e}|/|x| \leq w_i$ for $t \in [t_j^{x_i}, t_j^{x_i} + T_i]$, for each $i \in \{1, 2, \ldots, n\}$ and each j. Next, for $t \in [t_j^{x_i} + T_i, t_{j+1}^{x_i}]$, (2.16) enforces $|x_{i,e}|/|x_i| \leq w_i$, which implies $|x_{i,e}|/|x| \leq w_i$ since $|x_i| \leq |x|$. Therefore, the event-triggers in (2.16) are included in the family of event-triggers considered in Lemma 2.1. Hence, $x \equiv 0$ (the origin) is asymptotically stable with $S(c)$ as the region of attraction. □

Remark 2.3. *The idea of an explicit threshold for the inter-transmission times as in the event-triggers,* (2.16), *has been employed previously in [46]. However,*

in [46] such a mechanism is used to trigger the controller updates rather than the asynchronous transmissions from the sensors to the controller. Further, in [46] the controller utilizes synchronous measurements from the sensors to compute the control input to the plant, which allows the lower bound for inter-transmission times from [14] to be used. On the other hand, in the proposed decentralized asynchronous event-triggering mechanism of Theorem 2.2 the controller utilizes asynchronously received data to compute the control input to the plant and the inter-transmission time thresholds in (2.16) need to be computed as in Lemma 2.2.

Remark 2.4. *Although the assumption that $t_0^{x_i} \leq 0$, for each i, in Theorem 2.2 has not been used in the proof explicitly, it serves two key purposes - avoiding having the sensors send their first transmissions of data synchronously; and for the controller to have some latest sensor data to compute the controller output at $t = 0$.*

Remark 2.5. *In Theorem 2.2, the parameters w_i cannot be chosen in a decentralized manner unless $M_i(c)$ and hence c is fixed a priori. In other words, the desired region of attraction $S(c)$ has to be chosen at the time of the system installation. This can potentially lead to the parameters w_i to be chosen conservatively to guarantee a larger region of attraction. One possible solution is to let the central controller communicate the parameters w_i to the sensors at $t = 0$. In any case, for $t > 0$, the sensors need not listen for a communication and need only transmit their data to the controller.*

2.3.3 Decentralized Asynchronous Event-Triggering with Intermittent Communication from the Central Controller

In Theorem 2.2, apart from the fact that the set $S(c)$ is chosen *a priori*, conservativeness in transmission frequency may also be introduced. This is because the Lipschitz constants of the nonlinear functions $\gamma_i(.)$, (2.7), are not updated after their initialization, despite knowing that the system state is progressively restricted to smaller and smaller subsets of $S(c)$. Although we started from the idea that energy may be saved by making sure that sensors do not have to listen, the cost of increased transmissions may not be in its favor. Thus, we now describe a design where the central controller intermittently communicates updated w_i and T_i to the event-triggers.

The first step in this design process is to characterize the region in which the system state actually lies, given x_s, the asynchronously transmitted data available at the central controller. Since the central controller knows the parameters used by each event-trigger, it may compute an estimate of $|x|$ based on the centralized asynchronous event-triggering of Theorem 2.1, of which (2.16) is an under-approximation. Thus, we have that

$$|x_{i,s} - x_i| = |x_{i,e}| \leq w_i|x|, \quad \forall i \in \{1, \ldots, n\}$$

from which we obtain

$$\sum_{i=1}^{n} |x_{i,s} - x_i|^2 \leq W^2 \sum_{i=1}^{n} |x_i|^2, \quad \text{where } W = \sqrt{\sum_{i=1}^{n} w_i^2}$$

$$\implies (1 - W^2) \sum_{i=1}^{n} |x_i|^2 - 2 \sum_{i=1}^{n} |x_{i,s}||x_i| + \sum_{i=1}^{n} |x_{i,s}|^2 \leq 0$$

which is the equation of an n-sphere. Thus, the system state is in the n-sphere given by

$$|x - x_c| \leq R \tag{2.17}$$

$$\text{where} \quad x_c = \frac{1}{1 - W^2} x_s, \quad R = \frac{W}{1 - W^2} |x_s| \tag{2.18}$$

Obviously, for these equations to make sense, W^2 has to be strictly less than 1. However, this is not a restriction at all. Notice that, by definition, a centralized event-trigger that enforces $|x_e| = |x - x_s| \leq W|x|$ asymptotically stabilizes the origin of the system with the required convergence rate. Further, if $W \geq 1$ then $|x - 0| \leq W|x|$ for all $x \in \mathbb{R}^n$. The implication is that the constant control $u = k(0)$ is sufficient to asymptotically stabilize the origin with required convergence rate. In that case, there is no need for event-triggered control. Thus, without loss of generality, we assume that $W^2 < 1$.

The next idea is to estimate an upper bound on the value of $V(x)$. From (2.17), we know that $|x| \leq |x_c| + R$ and hence that $V(x) \leq \alpha_2(|x_c| + R)$. However, this may be conservative and a better estimate may be obtained by maximizing $V(x)$ on the set given by (2.17). In fact, on this set, $V(x)$ is maximized on the boundary of the n-sphere. This is because if the maximum does not occur on the boundary and instead occurs only in the interior of the n-sphere (2.17), then the maximizing sub-level set, S_M, of V lies strictly and completely in the interior of the n-sphere, which means S_M is not the smallest sub-level set of V that contains the complete n-sphere. Thus, an upper bound on the value of $V(x)$ is provided by

$$\mathcal{V} \geq \max\{V(x) : |x - x_c| = R\} \tag{2.19}$$

The final idea is to update sensor event-trigger parameters w_i and T_i at time instants determined by an event-trigger running at the central controller, namely,

$$t_{j+1}^{\mathcal{V}} = \min\{t \geq t_j^{\mathcal{V}} + \mathcal{T} : \mathcal{V} \leq \rho \mathcal{V}(t_j^{\mathcal{V}})\} \tag{2.20}$$

where $\mathcal{T} > 0$ and $\rho \in (0, 1)$ are arbitrary constants. To be precise, $t_{j+1}^{\mathcal{V}}$ are the time instants at which $\mathcal{V}$ is updated. In this chapter, we assume that these are also the time instants at which new values of w_i and T_i are communicated to the sensors as well as updated by the sensors in (2.16). The initial condition $\mathcal{V}(t_0^{\mathcal{V}}) = \mathcal{V}(0) = c$ may be chosen, where c determines the region of attraction $S(c)$. Thus the 'sampled' version of $\mathcal{V}$ is denoted by

$$\mathcal{V}_s \triangleq \mathcal{V}(t_j^{\mathcal{V}}), \quad \forall t \in [t_j^{\mathcal{V}}, t_{j+1}^{\mathcal{V}}), \quad \mathcal{V}_s(t_0^{\mathcal{V}}) = \mathcal{V}_s(0) = c \tag{2.21}$$

where $c > 0$ is an arbitrary constant, $t_j^{\mathcal{V}}$ are given by (2.20) and $\mathcal{V}$ is given by (2.19). Now, the ideas in this subsection are formalized in the following result.

Theorem 2.3. *Consider the closed loop system (2.1)-(2.2) and assume (A2.1) and (A2.2) hold. Let $M_i(.)$ and $\mathcal{V}_s$ be given by (2.7) and (2.21), respectively. For each $i \in \{1, 2, \ldots, n\}$, let w_i and T_i be positive piecewise-constant signals given by $w_i = M_i(\mathcal{V}_s)$ and (2.13) (with $c = \mathcal{V}_s$), respectively. Suppose the sensors asynchronously transmit the measured data at time instants determined by (2.16) and that $t_0^{x_i} \leq 0$ for each $i \in \{1, 2, \ldots, n\}$. Then, the origin is asymptotically stable with $S(c)$ as the region of attraction and the inter-execution times of each event-trigger have a positive lower bound.*

Proof. Clearly, the Lyapunov function evaluated at the state of the system is at all times lesser than the piecewise constant and non-increasing signal $\mathcal{V}_s$. Thus,

$x \in S(\mathcal{V}_s)$ at all times, where $S(.)$ is given by (2.5). Hence, $w_i = M_i(\mathcal{V}_s)$ and T_i given by (2.13) guarantee asymptotic stability of the origin of the closed loop system, with $S(\mathcal{V}_s(0))$ as the region of attraction.

The inter-transmission times $t_j^{\mathcal{V}}$ are clearly lower bounded by $\mathcal{T} > 0$. Note that given $\mathcal{V}_s$, the different parameters in Lemma 2.2 are clearly determined, as is T_i in (2.16). Thus, the inter-transmission times of the i^{th} sensor in the interval $[t_j^{\mathcal{V}}, t_{j+1}^{\mathcal{V}})$ are lower bounded by T_i calculated with $\mathcal{V}(t_j^{\mathcal{V}})$, which are guaranteed to be positive by Lemma 2.2. The different parameters in Lemma 2.2 are upper and lower bounded by positive constants determined by $\mathcal{V}_s(0)$. Thus, T_i for all time have positive lower bounds Γ_i. Each inter-transmission time of the i^{th} sensor is thus lower bounded by $\Gamma_i > 0$. □

Remark 2.6. *As $S(c_1) \subset S(c_2)$ if $c_1 \leq c_2$, $M_i(.)$ in (2.7) can be assumed to be non-increasing functions of c. Since the signal $\mathcal{V}_s$ is non-increasing, $w_i = M_i(\mathcal{V}_s)$ are non-decreasing in time. Further, note that the aim of the event-triggers (2.16) is to enforce the conditions $|x_{i,e}| \leq w_i|x|$. Thus whenever w_i and T_i are updated, the new parameters in the event-triggers are consistent with and an improvement over the previous parameters. Although w_i are non-decreasing in time, the same cannot be said about T_i. However, it is not a restriction and the inter-transmission times are still lower bounded.*

Remark 2.7. *Computing the upper bound on V, (2.19), may be computationally intensive depending on the Lyapunov function and the dimension of the system. However, since the Lyapunov function is guaranteed to decrease even with no updates*

to w_i and T_i, there is no restriction on the time needed to compute the upper bound on V and to update the parameters of the event-triggers. On the other hand, it is true that the updates to all the event-triggers have to occur synchronously.

2.4 Linear Time Invariant Systems

Now, let us consider the special case of Linear Time Invariant (LTI) systems with quadratic Lyapunov functions. Thus, the system dynamics may be written as

$$\dot{x} = Ax + Bu, \quad x \in \mathbb{R}^n, \quad u \in \mathbb{R}^m \tag{2.22}$$

$$u = K(x + x_e) \tag{2.23}$$

where A, B and K are matrices of appropriate dimensions. As in the general case, let us assume that for each $i \in \{1, 2, \ldots, n\}$, $x_i \in \mathbb{R}$ is sensed by the i^{th} sensor. Comparing with (2.22)-(2.23) we see that x_i evolves as

$$\dot{x}_i = r_i(A)x + r_i(BK)(x + x_e) \tag{2.24}$$

where the notation $r_i(H)$ denotes the i^{th} row of the matrix H. Also note that x_e and $x_{i,e}$ are defined just as in Section 2.2.

Now, suppose the matrix $(A + BK)$ is Hurwitz, which is equivalent to the following statement.

(A2.3) Suppose that for any given symmetric positive definite matrix Q, there exists a symmetric positive definite matrix P such that

$$P(A + BK) + (A + BK)^T P = -Q$$

Then, the following Lemma describes a centralized asynchronous sensing mechanism for linear systems.

Lemma 2.3. *Consider the closed loop system (2.22)-(2.23) and assume (A2.3) holds. Let Q be any symmetric positive definite matrix and let Q_m be the smallest eigenvalue of Q. For each $i \in \{1, 2, \ldots, n\}$, let*

$$\theta_i \in (0,1) \quad s.t. \quad \theta = \sum_{i=1}^{n} \theta_i \leq 1 \tag{2.25}$$

$$w_i = \frac{\sigma \theta_i Q_m}{|c_i(2PBK)|} \tag{2.26}$$

where $\sigma \in (0,1)$ is a design constant and $c_i(2PBK)$ is the i^{th} column of the matrix $(2PBK)$. Suppose the sampling instants are such that for each $i \in \{1, \ldots, n\}$, $|x_{i,e}|/|x| \leq w_i$ for all time $t \geq 0$. Then, the origin is globally asymptotically stable.

Proof. Consider the candidate Lyapunov function $V(x) = x^T P x$ where P satisfies (A2.3). The derivative of the function V along the flow of the closed loop system satisfies

$$\begin{aligned}
\dot{V} &= x^T[P(A+BK) + (A+BK)^T P]x + 2x^T PBKx_e \\
&\leq -(1-\sigma)x^T Q x + |x|\Big[|2PBKx_e| - \sigma Q_m |x|\Big] \\
&\leq -(1-\sigma)x^T Q x + |x|\Big[\sum_{i=1}^{n} |c_i(2PBK)x_{i,e}| - \sigma Q_m |x|\Big] \\
&\leq -(1-\sigma)x^T Q x + |x|\Big[\sum_{i=1}^{n} |c_i(2PBK)||x_{i,e}| - \sigma Q_m |x|\Big]
\end{aligned}$$

The sensor update instants have been assumed to be such that $|x_{i,e}|/|x| \leq w_i = \frac{\sigma \theta_i Q_m}{|c_i(2PBK)|}$ for each i and for all time $t \geq 0$. Thus,

$$\dot{V} \leq -(1-\sigma)x^T Q x$$

which implies that the origin is globally asymptotically stable. □

Lower bounds for the inter-sample times can be found in a manner analogous to the general nonlinear case in Lemma 2.2.

Lemma 2.4. *Consider the closed loop system (2.22)-(2.23). For each $i \in \{1, \dots, n\}$, let θ_i, w_i be defined as in (2.25)-(2.26) and let $W_i = \sqrt{\left(\sum_{j=1}^{n} w_j^2\right) - w_i^2}$. Suppose the sampling instants are such that $|x_{i,e}|/|x| \leq w_i$ for each $i \in \{1, \dots, n\}$ for all time $t \geq t_0$. Then, for all $t \geq t_0$, the time required for $|x_{i,e}|/|x|$ to evolve from 0 to w_i is lower bounded by $T_i > 0$, where*

$$T_i = \tau(w_i, a_0, a_1, a_2) \tag{2.27}$$

where the function τ is given by (2.11) and

$$a_0 = |r_i(A + BK)| + |r_i(BK)|W_i,$$

$$a_1 = |A + BK| + |r_i(BK)| + |BK|W_i, \quad a_2 = |BK|$$

Proof. Letting $\nu_i \triangleq |x_{i,e}|/|x|$, for $i \in \{1, \dots, n\}$, the an upper bound for the time derivative of ν_i can be found by direct calculation.

$$\begin{aligned}
\frac{\mathrm{d}\nu_i}{\mathrm{d}t} &= \frac{(x_{i,e}^T x_{i,e})^{-1/2} x_{i,e}^T \dot{x}_{i,e}}{|x|} - \frac{x^T \dot{x} |x_{i,e}|}{|x|^3} \\
&\leq \frac{|x_{i,e}||\dot{x}_{i,e}|}{|x_{i,e}||x|} + \frac{|x||\dot{x}||x_{i,e}|}{|x|^3} \\
&\leq \frac{|r_i(A + BK)||x| + |r_i(BK)||x_e|}{|x|} + \frac{\big(|A + BK||x| + |BK||x_e|\big)|x_{i,e}|}{|x|^2}
\end{aligned}$$

where for $x_{i,e} = 0$ the relation holds for all directional derivatives while the notation $r_i(H)$ denotes the i^{th} row of the matrix H. Next, notice that

$$\frac{|x_e|}{|x|} = \sqrt{\sum_{j=1}^{j=n} \nu_j^2} \leq \sqrt{\left(\sum_{j=1}^{j=n} w_j^2\right) - w_i^2 + \nu_i^2} \leq W_i + \nu_i$$

where the condition that $\nu_i \leq w_i$, the definition of W_i and the triangle inequality property have been utilized. Thus,

$$\begin{aligned}\frac{\mathrm{d}\nu_i}{\mathrm{d}t} &\leq |r_i(A+BK)| + |A+BK|\nu_i + \Big(|r_i(BK)| + |BK|\nu_i\Big)(W_i+\nu_i) \\ &= a_0 + a_1\nu_i + a_2\nu_i^2\end{aligned}$$

The claim of the Lemma now directly follows from analogous arguments as in the proof of Lemma 2.2. □

Next, the result for the centralized asynchronous event-triggering is presented, whose proof is quite analogous to Theorem 2.1.

Theorem 2.4. *Consider the closed loop system (2.22)-(2.23) and assume (A2.3) holds. Let Q be any symmetric positive definite matrix and let Q_m be the smallest eigenvalue of Q. For each $i \in \{1, 2, \ldots, n\}$, let θ_i and w_i be defined as in (2.25)-(2.26). Also suppose the i^{th} sensor transmits its measurement to the controller whenever $|x_{i,e}|/|x| \geq w_i$. Then, the origin is globally asymptotically stable and the inter-transmission times have a positive lower bound.*

The following result is analogous to Theorem 2.2 and prescribes the constants T_i and w_i in the event triggers, (2.16), that guarantee global asymptotic stability of the origin while also explicitly enforcing a positive minimum inter-sample time.

Theorem 2.5. *Consider the closed loop system (2.22)-(2.23) and assume (A2.3) holds. Let Q be any symmetric positive definite matrix and let Q_m be the smallest eigenvalue of Q. For each $i \in \{1, 2, \ldots, n\}$, let θ_i, w_i and T_i be defined as in (2.25), (2.26) and (2.27), respectively. Suppose the sensors asynchronously transmit the*

measured data at time instants determined by (2.16). *Then, the origin is globally asymptotically stable and the inter-transmission times are explicitly enforced to have a positive lower threshold.*

In the context of the results for nonlinear systems in Section 2.3, the reason we are able to achieve global asymptotic stability for LTI systems is because, the system dynamics, the functions $\gamma_i(.)$ are globally Lipschitz, thus giving us constants w_i and T_i that hold globally. In fact, for linear systems, something more is ensured - the proposed asynchronous event-triggers guarantee a type of scale invariance.

Scaling laws of inter-execution times for centralized *synchronous* event-triggering have been studied in [28]. In particular, Theorem 4.3 of [28], in the special case of linear systems, guarantees scale invariance of the inter-execution times determined by a centralized event-trigger $|x_e| = W|x|$. The centralized and decentralized asynchronous event-triggers developed in this chapter are under-approximations of this kind of central event-triggering. In the following, we show that the scale invariance is preserved in the asynchronous event-triggers. As an aside, we would like to point out that the decentralized event-triggers proposed in [35–37] are not scale invariant. In order to precisely state the notion of scale invariance and to state the result, the following notation is useful. Let $x(t)$ and $z(t)$ be two solutions to the system: (2.22)-(2.23) along with the event-triggers (2.16).

Theorem 2.6. *Consider the closed loop system* (2.22)-(2.23) *and assume* (A2.3) *holds. Let Q be any symmetric positive definite matrix and let Q_m be the smallest eigenvalue of Q. For each $i \in \{1, 2, \ldots, n\}$, let θ_i, w_i and T_i be defined as in*

(2.25), (2.26) *and* (2.27)*, respectively. Suppose the sensors asynchronously transmit the measured data at time instants determined by* (2.16)*. Assuming* b *is any scalar constant, let* $[z(0)^T, z_s(0)^T]^T = b[x(0)^T, x_s(0)^T]^T \in \mathbb{R}^n \times \mathbb{R}^n$ *be two initial conditions for the system. Further let* $t_0^{z_i} = t_0^{x_i} < 0$ *for each* $i \in \{1, \dots, n\}$*. Then,* $[z(t)^T, z_s(t)^T]^T = b[x(t)^T, x_s(t)^T]^T$ *for all* $t \geq 0$ *and* $t_j^{x_i} = t_j^{z_i}$ *for each* i *and* j*.*

Proof. First of all, let us introduce two strictly increasing sequences of time, $\{t_j^{z_s}\}$ and $\{t_j^{x_s}\}$, at which one or more components of z_s and x_s are updated, respectively. Further, without loss of generality, assume $t_0^{z_s} = t_0^{x_s}$. The proof proceeds by mathematical induction. Let us suppose that $t_j^{z_s} = t_j^{x_s} = t_j$ for each $j \in \{0, \dots, k\}$ and that $[z(t)^T, z_s(t)^T]^T = b[x(t)^T, x_s(t)^T]^T$ for all $t \in [0, t_k)$. Then, letting $\underline{t}_{k+1} = \min\{t_{k+1}^{z_s}, t_{k+1}^{x_s}\}$ the solution, z, in the time interval $[t_k, \underline{t}_{k+1})$ satisfies

$$\begin{aligned} z(t) &= e^{A(t-t_k)} z(t_k) + \int_{t_k}^{t} e^{A(t-\sigma)} BK z_s(t_k) \mathrm{d}\sigma \\ &= b e^{A(t-t_k)} x(t_k) + b \int_{t_k}^{t} e^{A(t-\sigma)} BK x_s(t_k) \mathrm{d}\sigma \end{aligned}$$

Hence,

$$z(t) = bx(t), \quad \forall t \in [t_k, \underline{t}_{k+1}) \tag{2.28}$$

Further, in the time interval $[t_k, \underline{t}_{k+1})$

$$z_{i,e}(t) = z_i(t_k) - z_i(t) = b(x_i(t_k) - x_i(t)) = b x_{i,e}(t) \tag{2.29}$$

Similarly, for all $t \in [t_k, \underline{t}_{k+1})$,

$$\frac{|z_{i,e}(t)|}{|z(t)|} = \frac{|x_{i,e}(t)|}{|x(t)|} \tag{2.30}$$

Without loss of generality, assume $z_{i,s}$ is updated at $\underline{t}_{k+1}$. Then, clearly, at least T_i amount of time has elapsed since $z_{i,s}$ was last updated. Next, by the assumption that $t_0^{z_i} = t_0^{x_i} < 0$ and the induction statement, it is clear that at least T_i amount of time has elapsed since $x_{i,s}$ was also last updated. Further, it also means that $|z_{i,s}(t_k) - z_i(\underline{t}_{k+1})| \geq w_i|z_i(\underline{t}_{k+1})|$. Then, (2.28)-(2.29) imply that $|x_{i,s}(t_k) - x_i(\underline{t}_{k+1})| \geq w_i|x_i(\underline{t}_{k+1})|$, meaning $\underline{t}_{k+1} = t_{k+1}^{z_s} = t_{k+1}^{x_s} = t_{k+1}$. Arguments analogous to the preceding also hold for multiple $z_{i,s}$ updated at $\underline{t}_{k+1}$ instead of one or even $x_{i,s}$ instead of $z_{i,s}$. Since the induction statement is true for $k = 0$, we conclude that the statement of theorem is true. □

Remark 2.8. *From the proof of Theorem 2.6, (2.30) specifically, it is clear that the centralized asynchronous event-trggers of Theorem 2.4 also guarantee scale invariance.*

Remark 2.9. *Scale invariance, as described in Theorem 2.6, means that the average inter-transmission times over an arbitrary length of time is independent of the scale (or the magnitude) of the initial condition of the system. Similarly for any given scalar, $\delta \in (0, 1)$, the time and the number of transmissions it takes for $|x(t)|$ to reduce to $\delta|x(0)|$ is independent of $|x(0)|$. So, the advantage is that the 'average' network usage remains the same over large portions of the state space.*

2.5 Simulation Results

In this section, the proposed decentralized asynchronous event-triggered sensing mechanism is illustrated with two examples. The first is a linear system and the

second a nonlinear system.

2.5.1 Linear System Example

We first present the mechanism for a linearized model of a batch reactor, [47]. The plant and the controller are given by (2.22)-(2.23) with

$$A = \begin{bmatrix} 1.38 & -0.20 & 6.71 & -5.67 \\ -0.58 & -4.29 & 0 & 0.67 \\ 1.06 & 4.27 & -6.65 & 5.89 \\ 0.04 & 4.27 & 1.34 & -2.10 \end{bmatrix}, \qquad B = \begin{bmatrix} 0 & 0 \\ 5.67 & 0 \\ 1.13 & -3.14 \\ 1.13 & 0 \end{bmatrix}$$

$$K = - \begin{bmatrix} 0.1006 & -0.2469 & -0.0952 & -0.2447 \\ 1.4099 & -0.1966 & 0.0139 & 0.0823 \end{bmatrix}$$

which places the eigenvalues of the matrix $(A+BK)$ at around $\{-2.98+1.19i, -2.98-1.19i, -3.89, -3.62\}$. The matrix Q was chosen as the identity matrix. The system matrices and Q have been chosen to be the same as in [35]. Lastly, the controller parameters were chosen as $[\theta_1, \theta_2, \theta_3, \theta_4] = [0.6, 0.17, 0.08, 0.15]$ and $\sigma = 0.95$. For the simulations presented here, the initial condition of the plant was selected as $x(0) = [4, 7, -4, 3]^T$ and the initial sampled data that the controller used was $x_s(0) = [4.1, 7.2, -4.5, 2]^T$. The zeroth sampling instant was chosen as $t_0^{x_i} = -T_i$ for sensor i. This is to ensure sampling at $t = 0$ if the local triggering condition was satisfied. Finally the simulation time was chosen as 10s.

Figures 2.1(a) and 2.1(b) show the evolution of the Lyapunov function and its derivative along the flow of the closed loop system, respectively. Figures 2.1(c) and

2.1(d) show the inter-transmission times and the cumulative frequency distribution of the inter-transmission times for each of the sensor. The cumulative frequency

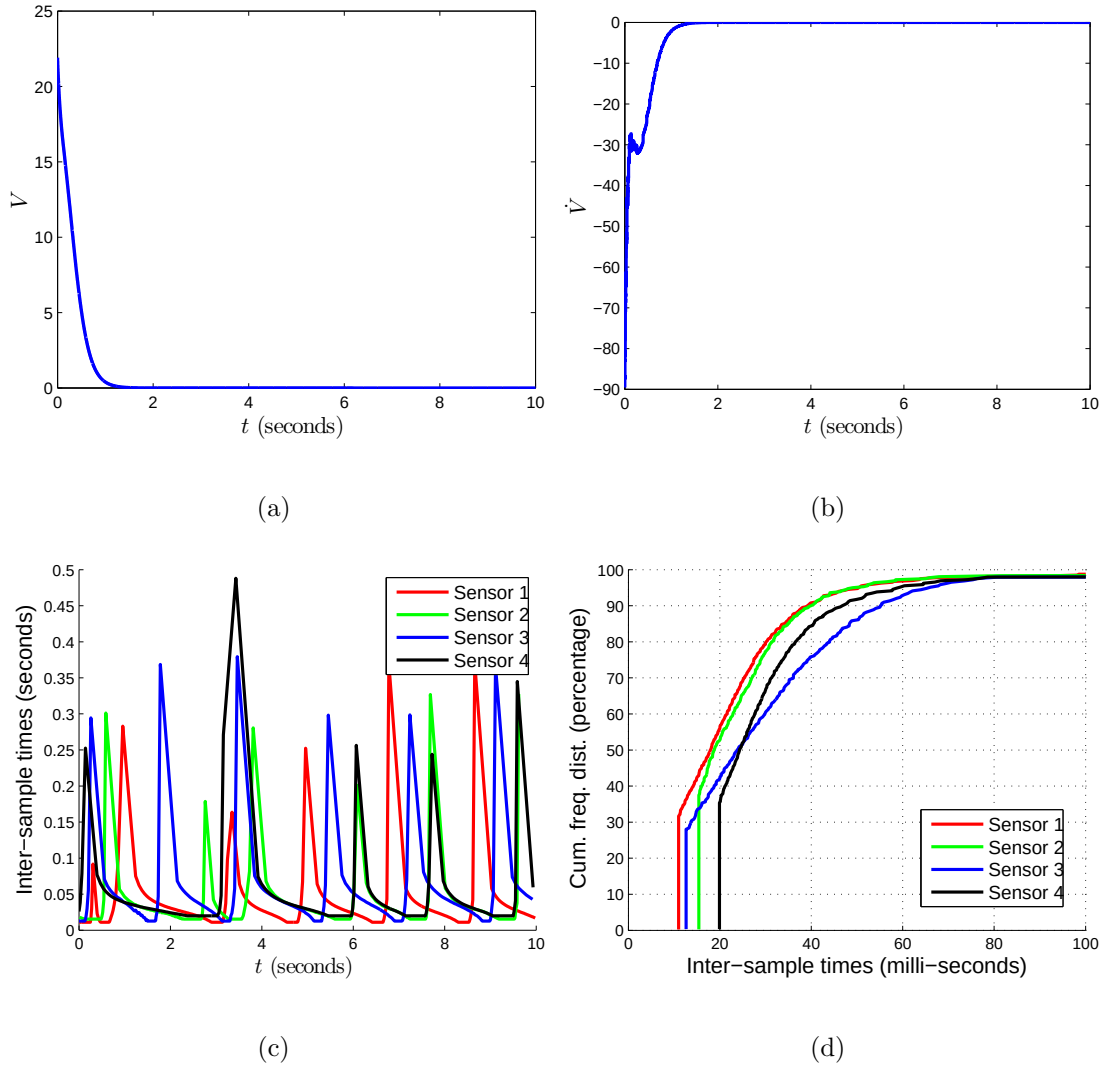

Figure 2.1: Batch reactor example: evolution of the (a) Lyapunov function, (b) time derivative of Lyapunov function, along the flow of the closed loop system. (c) Sensor inter-transmission times (d) cumulative frequency distribution of the sensor inter-transmission times.

distribution of the inter-transmission times is a measure of the performance of the event-triggers. A distribution that rises sharply to 100% indicates that event-trigger

is not much better than a time-trigger. Thus, slower the rise of the cumulative distribution curves, greater is the justification for using the event-trigger instead of a time-trigger.

The lower thresholds for the inter-transmission times T_i for the example can be computed as in Lemma 2.4 and have been obtained as

$$[T_1, T_2, T_3, T_4] = [11, 15.4, 12.6, 19.9]\text{ms}$$

which are also the minimum inter-transmission times in the simulations presented here. These numbers are a few orders of magnitude higher and an order higher than the guaranteed minimum inter-transmission times and the observed minimum inter-transmission times in [35, 36]. The average inter-transmission times obtained in the presented simulations were $[\bar{T}_1, \bar{T}_2, \bar{T}_3, \bar{T}_4] = [24.9, 27.7, 34.5, 34.2]$ms, which are about an order of magnitude lower than those reported in [35, 36]. A possible explanation for this phenomenon is that in [35, 36], the average inter-transmission times depends quite critically on the evolution of the threshold η. Although the controller gain matrix K and the matrix Q have been chosen to be the same, by inspection of the plots in [35, 36], it appears that the rate of decay of the Lyapunov function V is roughly about half of that in our simulations. However, we would like to point out that our average inter-transmission times are of the same order as in [37] by the same authors. In any case, for LTI systems, our proposed method does not require communication from the controller to sensors to achieve global asymptotic stability. Lastly, as a measure of the usefulness of the event-triggering mechanism compared to a purely time-triggered mechanism, $T_i/\bar{T}_i$ was computed

for each i and were obtained as $[T_1/\bar{T}_1, T_2/\bar{T}_2, T_3/\bar{T}_3, T_4/\bar{T}_1] = [0.44, 0.55, 0.36, 0.58]$. The lower these numbers are, the better it is.

2.5.2 Nonlinear System Example

The general result for nonlinear systems is illustrated through simulations of the following second order nonlinear system.

$$\dot{x} = f(x, x_e) = \begin{bmatrix} f_1(x, x_e) \\ f_2(x, x_e) \end{bmatrix} = Ax + \begin{bmatrix} 0 \\ x_1^3 \end{bmatrix} + Bu \tag{2.31}$$

where $A = \begin{bmatrix} 0 & 1 \\ 0 & -1 \end{bmatrix}$, $B = \begin{bmatrix} 0 \\ 1 \end{bmatrix}$

where $x = [x_1, x_2]^T$ is a vector in $\mathbb{R}^2$ and the sampled data controller (in terms of the measurement error) is given as

$$u = k(x + x_e) = K(x + x_e) - (x_1 + x_{1,e})^3 \tag{2.32}$$

where $K = [k_1, k_2]$ is a 1×2 row vector such that $\bar{A} = (A + BK)$ is Hurwitz. Then, the closed-loop tracking error system with event-triggered control can be written as

$$\begin{aligned} \dot{x} &= \bar{A}x + BKx_e + \begin{bmatrix} 0 \\ x_1^3 - (x_1 + x_{1,e})^3 \end{bmatrix} \\ &= \bar{A}x + \begin{bmatrix} 0 \\ h_1 + h_2 \end{bmatrix} \end{aligned} \tag{2.33}$$

where

$$h_1 = -\Big(x_{1,e}^3 + 3x_1x_{1,e}^2 + (3x_1^2 - k_1)x_{1,e}\Big) \tag{2.34}$$

$$h_2 = k_2x_{2,e} \tag{2.35}$$

Now, consider the quadratic Lyapunov function $V = x^T P x$ where P is a symmetric positive definite matrix that satisfies the Lyapunov equation $P\bar{A}+\bar{A}^T P = -Q$, with Q a symmetric positive definite matrix. Let p_m and p_M be the smallest and largest eigenvalues of the matrix P. Since P is a symmetric positive definite matrix, p_m and p_M are each positive real numbers. Further,

$$\alpha_1(|x|) \triangleq p_m|x|^2 \leq V(x) \leq p_M|x|^2 \triangleq \alpha_2(|x|), \quad \forall x \in \mathbb{R}^2$$

The time derivative of V along the flow of the closed loop system (2.33) can be shown to satisfy

$$\begin{aligned}\dot{V} &= -x^T Q x + 2x^T P B(h_1 + h_2) \\ &\leq -(1-\sigma)Q_m|x|^2 + |x|\big(|2PB(h_1+h_2)| - \sigma Q_m|x|\big)\end{aligned}$$

where Q_m is the smallest eigenvalue of the symmetric positive definite matrix Q and σ is a parameter satisfying $0 < \sigma < 1$.

Suppose that the desired region of attraction be $S(c)$, for some non-negative c (see (2.5) for the definition of $S(c)$). Let μ_1 be the maximum value of x_1 on the sub-level set $S(c)$. Then, we let

$$\begin{aligned}h_1^c &= |x_{1,e}|^3 + 3\mu_1|x_{1,e}|^2 + \max_{|x_1|\leq\mu_1}\{3x_1^2 - k_1\}|x_{1,e}| \\ \gamma_1(|x_{1,e}|) &\triangleq \frac{|2PB|h_1^c}{\sigma\theta_1 Q_m}, \quad \gamma_2(|x_{2,e}|) \triangleq \frac{|2PBk_2||x_{2,e}|}{\sigma\theta_2 Q_m}\end{aligned}$$

where θ_1 and θ_2 are positive constants such that $\theta_1 + \theta_2 = 1$. It is clear that Assumption (A2.1) is satisfied and we have

$$\dot{V} \leq -(1-\sigma)Q_m|x|^2, \quad \text{if } \gamma_i|x_{i,e}| \leq |x|, \quad i \in \{1,2\}$$

Now, $\mu \triangleq \alpha_1^{-1}(c) = \sqrt{c/p_m}$ is the maximum value of $|x|$ on the set $S(c)$. Hence, $M_1(c)$ in (2.7) has to be defined for the set on which $|x_{1,e}| \leq R_1 \triangleq \gamma_1^{-1}(\mu)$. Thus, we have that

$$\frac{1}{M_1(c)} = \frac{|2PB|}{\sigma\theta_1 Q_m}\Big(R_1^2 + 3\mu_1 R_1 + \max_{|x_1|\leq\mu_1}\{3x_1^2 - k_1\}\Big)$$

while $\dfrac{1}{M_2(c)} = \dfrac{|2PBk_2|}{\sigma\theta_2 Q_m}$.

Now, only T_i for each i need to be determined. To this end, the closed loop system dynamics (2.33) are bounded as in (2.8) and (2.9).

$$|f_1(x, x_e)| \leq L_1|x| + D_1|x_e|$$

$$|f_2(x, x_e)| \leq L_2|x| + D_{2,\mu}|x_e|, \quad \forall x \text{ s.t. } |x| \leq \mu$$

Comparing with (2.33) the following can be arrived at.

$$L_1 = |r_1(\bar{A})|, \quad D_1 = 0, \quad L_2 = |r_2(\bar{A})|$$

$$D_{2,\mu} = \sqrt{\Big(R_1^2 + 3\mu_1 R_1 + \max_{|x_1|\leq\mu_1}\{3x_1^2 - k_1\}\Big)^2 + k_2^2}$$

In the example simulation results presented here, the following gains and parameters were used.

$$K = -\begin{bmatrix}5 & 3\end{bmatrix}, \quad Q = \begin{bmatrix}1 & 0\\ 0 & 1\end{bmatrix}, \quad \theta_1 = 0.9, \quad \theta_2 = 0.1$$

$$\sigma = 0.9, \quad c = 10, \quad \mu_1 = \mu$$

$$x(0) = [2.8, -2.6]^T, \quad x_s(0) = [2.9, -2.7]^T \tag{2.36}$$

Notice that $M_2(c)$ is a constant independent of c. That is why θ_2 has been chosen much smaller than θ_1. The parameter μ_1 has been chosen to be equal to

μ. To be consistent with asynchronous transmissions, the initial value of $x_s(0)$ has been chosen to be different from $x(0)$.

For the chosen parameters and the initial conditions, the initial value of the Lyapunov function is $V(0) = 8.574$. Thus the initial state of the system is well within the region of attraction, given by $S(c) = S(10)$. The event-trigger parameters were obtained as $[w_1, w_2] = [M_1(c), M_2(c)] = [0.0102, 0.0832]$ and $[T_1, T_2] = [9, 5]$ms, which were also the minimum inter-transmission times. The average inter-transmission times of the sensors for the duration of the simulated time were obtained as $[\bar{T}_1, \bar{T}_2] = [9.6, 25.8]$ms. Thus for sensor 1, the average inter-transmission interval is only marginally better than the minimum. The number of transmissions by sensors 1 and 2 were 1041 and 388, respectively.

Figures 2.2(a) and 2.2(b) show the evolution of the Lyapunov function and its derivative along the flow of the closed loop system, respectively. Figures 2.2(c) and 2.2(d) show the inter-transmission times and the cumulative frequency distribution of the inter-transmission times for each of the sensor. The sharp rise of the cumulative distribution curve for Sensor 1 clearly indicates that the event-triggered transmission is nearly equivalent to time-triggered transmission. On the other hand, the slow rise of the cumulative distribution curve of Sensor 2 demonstrates the usefulness of event-triggering in its case.

Simulations were also performed for the case when the central controller intermittently sends updates to the parameters of the sensor event-triggers, as in Theorem 2.3. For the simulation results presented here, the controller gains, parameters and the initial conditions have been chosen the same as in (2.36). Additionally, the

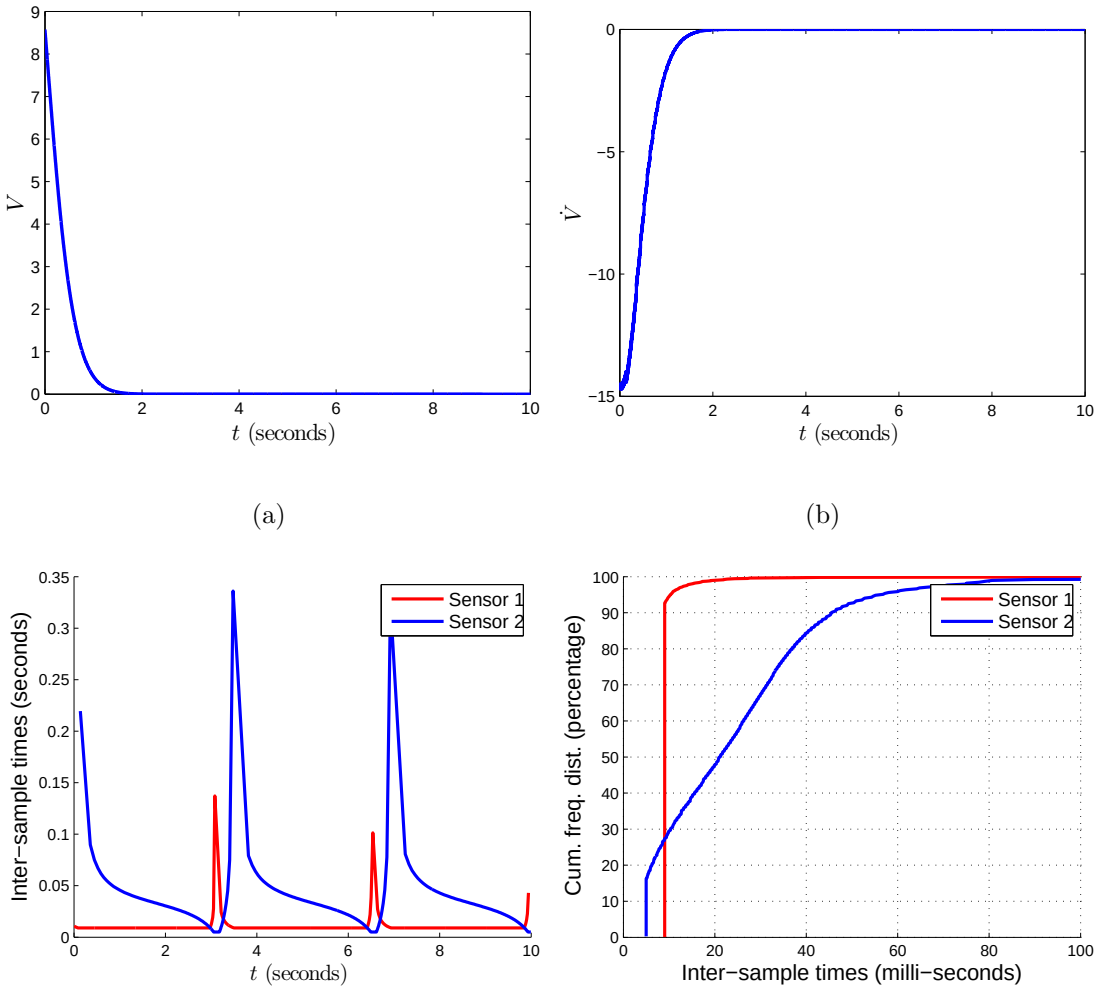

Figure 2.2: Nonlinear system example: evolution of the (a) Lyapunov function, (b) time derivative of Lyapunov function, along the flow of the closed loop system. (c) Sensor inter-transmission times (d) cumulative frequency distribution of the sensor inter-transmission times.

parameters in (2.20) were chosen as $\mathcal{T} = 0.5$ and $\rho = 0.5$. The initial condition $\mathcal{V}_s(0) = c = 10$ was chosen. For the 2 dimensional system in this example, $\mathcal{V}$ in (2.19) is the maximum value of V along a circle. $\mathcal{V}$ was then found in MATLAB by maximization of V on the circle, which was parametrized by a single angle variable

varying on the closed interval $[0, 2\pi]$.

In this case, the number of transmissions by Sensor 1 were much lower at 106 while those by Sensor 2 were 324. Notice that $w_2 = M_2(c)$ is a constant, independent of the value of c. Thus, we see that the reduction in the number of transmissions by Sensor 2 is only marginal while that of Sensor 1 is huge. The average inter-transmission times of the sensors for the duration of the simulated time were obtained as $[\bar{T}_1, \bar{T}_2] = [94.3, 30.9]$ms. The minimum inter-transmission times were observed as 9.4ms and 9ms for Sensors 1 and 2, respectively. The number of times the parameters of the sensor event-triggers were updated was 15.

The evolution of the Lyapunov function and its derivative along the flow of the closed loop system were very similar to that in Figures 2.2(a) and 2.2(b), respectively. Hence, they have not been presented here again. Figures 2.3(a) and 2.3(b) show the inter-transmission times and the cumulative frequency distribution of the inter-transmission times for each of the sensor. These two plots clearly show the usefulness of the event-triggered transmissions. Figure 2.3(c) shows the evolution of the w_i parameters of the event-triggers at each of the sensors. As mentioned earlier, w_2 is independent of c and hence is a constant. The evolution of w_1 shows that it is a non-decreasing function of time. Finally, Figure 2.3(d) shows the evolution of the T_i parameters of the event-triggers at the sensors (for clarity T_2 has been scaled by 20 times). Although, T_1 evolves in a non-decreasing manner, the same is not the case with T_2. However, as mentioned in Remark 2.6, this does not pose any problem and the inter-transmission times of the sensor are still lower bounded by a positive constant.

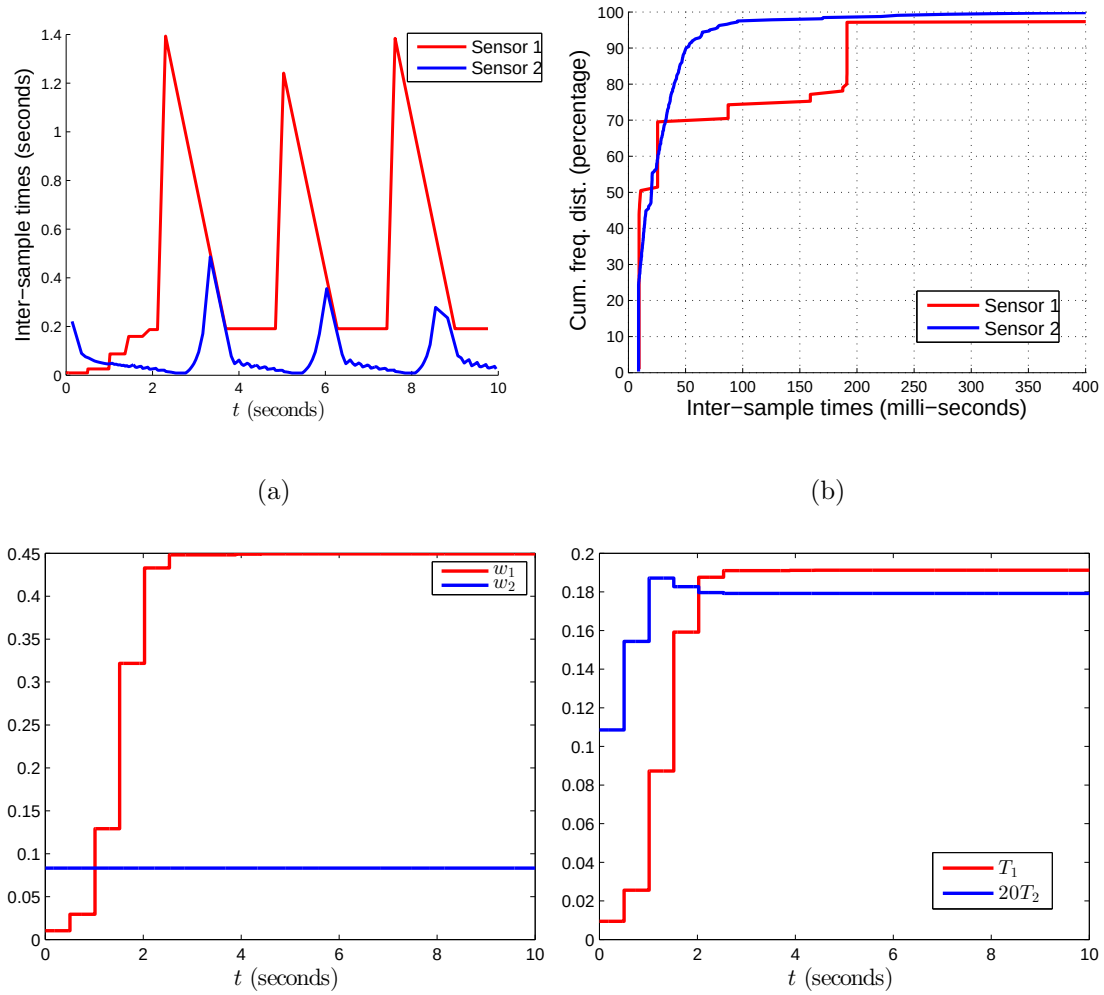

Figure 2.3: Nonlinear system example with event-triggered communication from the controller to the sensor event-triggers: (a) Sensor inter-transmission times (b) cumulative frequency distribution of the sensor inter-transmission times. Evolution of (c) w_i, (d) T_i parameters of the sensor event-triggers.

2.6 Conclusions

In this chapter, we have developed a method for designing decentralized event-triggers for control of nonlinear systems. The architecture of the systems considered

in this chapter included full state feedback, a central controller and decentralized sensors not co-located with the central controller. The aim was to develop event-triggers for determining the time instants of transmission from the sensors to the central controller. The proposed design ensures that the event-triggers at each sensor depend only on locally available information, thus allowing for asynchronous transmissions from the sensors to the central controller. Further, the design aimed at completely eliminating (or drastically reducing) the need for the sensors to listen to other sensors and/or the controller.

The proposed design was shown to guarantee a positive lower bound for inter-transmission times of each sensor (and of the controller in one of the special cases). The origin of the closed loop system is also guaranteed to be asymptotically stable with an arbitrary, but priorly fixed, region of attraction. In the special case of linear systems, the region of attraction was shown to be global with absolutely no need for the sensors to listen. Finally, the proposed design method was illustrated through simulations of a linear and a nonlinear example.

In the system architecture considered in this chapter, although the control input to the plant is updated intermittently, it is not exactly event-triggered. In fact, in all the results the inter-transmission times of each sensor individually have been shown to have a positive lower bound. And the time interval between receptions of the central controller from two different sensors can be arbitrarily close to zero. Since the control input to the plant is updated each time the controller receives some information, no positive lower bound can be guaranteed for the inter-update times of the controller. However, it is not very tough to incorporate event-triggering

(with guaranteed positive minimum inter-update times) or explicit thresholds on inter-update times of the control by choosing smaller σ values in the event-triggers for the sensors. Future work will include results with event-triggered actuation in addition to event-triggered communication on the sensing side.

Next, although the transmissions of sensors have been designed to be asynchronous, the communication from the central controller to the sensors in Section 2.3.3 have been assumed to be synchronous. In future, we aim to allow these communications also to be asynchronous. Although time delays have not been considered explicitly, they may be handled as in most event-triggered control literature (see [14] for example). Finally, it is worthwhile to investigate more sophisticated triggers for updating the parameters w_i and T_i (Section 2.3.3) as is a thorough study and quantification of sensor listening effort.

Chapter 3

Utility Driven Sampled Data Control of LTI Systems over Sensor-Controller-Actuator Networks

3.1 Introduction

As mentioned in the beginning of the previous chapter, much of the event-triggered control literature assumes the availability of full state information. However, in many practical applications only a part of the state information can be directly measured and a dynamic (for example, observer based) output feedback controller must be utilized. Thus, it is important to develop utility driven event-triggered implementations of dynamic output feedback controllers and this chapter is a contribution towards this aim. The work in this chapter is closely related to that of the previous chapter. As far as the individual decentralized event-triggers of the previous chapter are concerned, each has access only to a partial output of the system. Thus, the proposed centralized event-triggered implementation of a dynamic output feedback controller naturally extends to the decentralized event-triggering scenario. In fact, in this chapter, we go one step further. We address the problem of utility driven sampled data control over Sensor-Controller-Actuator Networks (SCAN).

Motivated by this, we group the nodes in a SCAN into three functional layers - sensor layer, controller/observer layer and the actuator layer, with no two nodes

being co-located. In practice though, several nodes from the same or different layers may be co-located. Any such scenario can simply be treated as a special case of the general framework of this chapter. The sensor nodes intermittently broadcast their data to the nodes in the observer (dynamic controller) layer. The nodes in the observer layer compute the state of the observer in a decentralized manner, with each node in the observer layer intermittently broadcasting its data to other nodes in the same layer. Each of the actuator nodes also intermittently receives data from a corresponding unique observer node. Thus, communication between the layers is unidirectional.

Sensor-Controller-Actuator Networks (SCAN) consist of physically distributed nodes, each of which performs one or more of sensing, control computation and actuation tasks in order to control a plant. If the aggregate feedback provided by the sensor nodes does not constitute full state feedback, then the controller nodes may also have to distributively estimate the state of the plant. Interest in such networked control systems has been rising steadily, specially, in the context of large scale systems such as power grids, building HVAC and even in vehicles. Some of the challenges in SCAN are asynchronous transmission of data; asynchronous and decentralized computation; decision making based only on local information and time delays. Many of these features can be thought of as a manifestation of asynchronously sampled data. Further, in SCAN there are constraints on data rate, resources and energy. Given these factors, utility driven event-triggering techniques have great potential for analyzing and designing SCAN.

3.1.1 Contributions

The fundamental contribution of this chapter is a methodology for designing implicitly verified utility driven event-triggered dynamic output feedback controllers for Linear Time Invariant (LTI) systems. The proposed methodology provides a means to achieve global asymptotic stability of the origin of the closed loop system. The methodology naturally extends to a decentralized sensing scenario (as in Chapter 2) and to the completely decentralized Sensor-Controller-Actuator Network (SCAN) control system. Each of these architectures is important in its own right and thus we address architectures where the sensors and the dynamic controller are co-located (centralized event-triggering), one where they are not co-located (decentralized sensing and actuation) and finally SCAN. In the latter architectures, all the transmissions are asynchronous. The proposed event-triggering conditions depend only on local information and include explicit positive lower thresholds for inter-sampling times that are designed to ensure global asymptotic stability of the closed loop system.

In the literature, among the few works that consider the problem of event-triggered dynamic output feedback control, [40, 41] proposed an event-triggered implementation that can guarantee uniform ultimate boundedness of the plant state and provided an estimate of minimum inter-communication time that holds semi-globally (dependent on the initial state of the dynamic controller and the unknown state of the plant). In comparison, the proposed controller guarantees asymptotic stability and an estimate of inter-communication times that holds globally.

In [42], a model based output feedback controller was proposed, where the communication from the observer subsystem to the system model subsystem is triggered by a condition that compares the observer state with that of a local copy of system model subsystem. Again, the controller guarantees only uniform ultimate boundedness of the closed loop state. In [43, 48] an output feedback control implementation for *discrete-time* systems is considered as an optimal control problem. The proposed architecture includes a Kalman filter in the sensor subsystem and identical observers in the sensor as well as actuator subsystems. The results provide an upper bound on the optimal cost attained by the event-triggered system. In comparison to [42, 43, 48], we do not require identical observers/models to be run at different locations.

Recently, [49] proposed a method for designing continuous time decentralized observers with discrete communication, wherein the sensor and the observer for each subsystem are co-located. In addition, an observability condition for each of the individual subsystems was assumed. Compared to [49], we consider non-co-located sensor and observer nodes, require an observability condition only for the overall system and further, incorporate decentralized dynamic control. Parts of the work in this chapter have appeared in [29, 30].

The rest of the chapter is organized as follows. Section 3.2 describes the main problem under consideration and establishes the mathematical notation used in the chapter. In Section 3.3, the design of decentralized event-triggering is presented in a general setting, which is then applied to specific dynamic output feedback control architectures in Section 3.4. The proposed design methodology is illustrated through

simulations in Section 3.5 and finally Section 3.6 provides some concluding remarks.

In this chapter, the notation $|.|$ is used to represent the Euclidean norm of a vector and also the induced Euclidean norm of a matrix.

3.2 Problem Setup

Consider the closed loop system consisting of a Multi Input Multi Output (MIMO) Linear Time Invariant (LTI) plant and an observer based dynamic controller

$$\dot{x} = Ax + Bu, \quad y = Cx \tag{3.1}$$

$$\dot{\hat{x}} = (A + FC)\hat{x} + BK\hat{x} - Fy, \quad u = K\hat{x} \tag{3.2}$$

where $x \in \mathbb{R}^n$, $\hat{x} \in \mathbb{R}^n$, $y \in \mathbb{R}^p$ and $u \in \mathbb{R}^m$, are the plant state, the observer state, the output of the plant and the control input to the plant, respectively. The matrices A, B, C, F and K are of appropriate dimensions. Denoting the *observer estimation error* and the state of the closed loop system, respectively, as

$$\tilde{x} \triangleq \hat{x} - x, \quad \psi \triangleq [x^T, \tilde{x}^T]^T$$

where the notation $[x^T, \tilde{x}^T]^T$ denotes the vector formed by concatenating the column vectors x and $\tilde{x}$, the closed loop system may be written as

$$\dot{\psi} = \begin{bmatrix} \dot{x} \\ \dot{\tilde{x}} \end{bmatrix} = \begin{bmatrix} A + BK & BK \\ \mathbf{0}_{n,n} & A + FC \end{bmatrix} \begin{bmatrix} x \\ \tilde{x} \end{bmatrix} \triangleq \bar{A}\psi \tag{3.3}$$

where $\mathbf{0}_{n,n}$ represents an $n \times n$ matrix of zeroes. The dynamic controller (3.2) renders the origin of the closed loop system (3.1)-(3.2) globally asymptotically stable if and only if the matrix $\bar{A}$ is Hurwitz. Typically, (A, B) and (A, C) are assumed to

be controllable and observable, respectively. This is sufficient to design the gain matrices F and K (which exist) such that $(A+FC)$, $(A+BK)$ and hence $\bar{A}$ are Hurwitz. For our purpose here, it is sufficient to assume that $\bar{A}$ is Hurwitz. In this chapter, we are interested in event-triggered implementation of the dynamic controller (3.2).

Before proceeding, we recall some of the notation introduced in Section 1.3. Let ζ be any continuous-time signal (scalar or vector) and let $\{t_i^\zeta\}$ be the increasing sequence of time instants at which ζ is sampled. Then we define the resulting piecewise constant sampled signal, ζ_s, and the 'measurement error', ζ_e, as

$$\zeta_s \triangleq \zeta(t_i^\zeta), \quad \forall t \in [t_i^\zeta, t_{i+1}^\zeta) \tag{3.4}$$

$$\zeta_e \triangleq \zeta_s - \zeta = \zeta(t_i^\zeta) - \zeta, \quad \forall t \in [t_i^\zeta, t_{i+1}^\zeta) \tag{3.5}$$

In the sequel, it is sometimes convenient (and intuitive) to group together asynchronously transmitted signals into a single vector. Let $\zeta_{j,s} \in \mathbb{R}^{d_j}$, for $j \in \{1, \ldots, q\}$, be q piecewise constant sampled data signals defined as in (3.4). Further, suppose that the q signals are asynchronously sampled. That is, the q sequences $\{t_i^{\zeta_j}\}$ are not necessarily identical. Then, the collection of q asynchronously sampled signals is compactly represented as

$$\zeta_s^* = [\zeta_{1,s}^T, \ldots, \zeta_{q,s}^T]^T \in \mathbb{R}^d, \quad \text{where } d = \sum_{j=1}^{q} d_j \tag{3.6}$$

The measurement error is correspondingly defined as

$$\zeta_e^* \triangleq \zeta_s^* - \zeta \tag{3.7}$$

The specific form of event-triggering depends on the architecture of the closed

loop system. In this chapter, we consider several different architectures ranging from the centralized case (sensors and the controller are *co-located*) to the completely decentralized Sensor-Controller-Actuator Network (SCAN) control system. We would like to clarify that *Co-located* components are assumed to have access to each others' outputs at all times. Note that in this chapter, the terms 'transmit', 'update' and 'sample' are used interchangeably.

In this chapter, the sampled data control systems are designed to satisfy: (i) global asymptotic stability of the closed loop system and (ii) a positive lower bound for the inter-transmission times that holds globally. The proposed design procedure can be divided into two major stages. In the first stage, utility driven event-triggers are designed for asynchronous transmissions using centralized information (norm of the complete state of the system). In the second stage, realizable event-triggers that depend only on local information are derived by appropriately under-approximating the centralized asynchronous event-triggers. The next section describes this procedure in a general setting and in the subsequent section, it is applied to different architectures.

3.3 Design of Decentralized Asynchronous Event-Triggering

This section presents the design of decentralized asynchronous event-triggering in a general setting. Similarities may be found with the material of Section 2.4. Consider the system

$$\dot{\xi} = \mathcal{A}\xi + \sum_{j=1}^{q} \mathcal{B}_j \zeta_{j,s} = \mathcal{A}\xi + \mathcal{B}\zeta_s^* \tag{3.8}$$

$\zeta_{j,s} \in \mathbb{R}^{d_j}$ is the sampled-data version of ζ_j, $\mathcal{B}_j \in \mathbb{R}^{n_\xi} \times \mathbb{R}^{d_j}$ is the j^{th} input matrix, $\zeta_s^* = [\zeta_{1,s}^T, \ldots, \zeta_{q,s}^T]^T \in \mathbb{R}^d$ is the asynchronously sampled-data version of ζ and is defined according to (3.6), $\mathcal{B} = [\mathcal{B}_1, \ldots, \mathcal{B}_q] \in \mathbb{R}^{n_\xi} \times \mathbb{R}^m$. With the continuous-time feedback control law

$$\zeta = \mathcal{K}\xi, \quad \zeta_j = \mathcal{K}_j\xi, \quad j \in \{1, \ldots, q\} \tag{3.9}$$

where $\mathcal{K}_j$ are appropriately defined block row matrices of $\mathcal{K}$, the closed loop system with the sampled-data controller can be expressed as

$$\dot{\xi} = (\mathcal{A} + \mathcal{B}\mathcal{K})\xi + \mathcal{B}\zeta_e^* = \bar{\mathcal{A}}\xi + \mathcal{B}\zeta_e^* \tag{3.10}$$

where $\bar{\mathcal{A}} = (\mathcal{A} + \mathcal{B}\mathcal{K})$ and $\zeta_e^* = (\zeta_s^* - \zeta) \in \mathbb{R}^d$ is the measurement error due to sampling. Finally, suppose that the continuous time control law would have stabilized the closed loop system, that is,

(A3.1) Suppose that the matrix $\bar{\mathcal{A}}$ is Hurwitz, which ensures that for each symmetric positive definite matrix Q, there exists a symmetric positive definite matrix P such that $P\bar{\mathcal{A}} + \bar{\mathcal{A}}^T P = -Q$.

Note that the design of the event-triggered controller is completed only with the implicit specification of the sampling time instants, $\{t_i^{\zeta_j}\}$, through the event-triggers. In order to develop the decentralized asynchronous event-triggers, let us first consider the following stability result.

Lemma 3.1. *Consider the sampled-data system* (3.8) *and assume* (A3.1) *holds. Let* Q *be any symmetric positive definite matrix and* Q_m *its smallest eigenvalue. For*

each $j \in \{1, \ldots, q\}$, *let* $\theta_j \in (0,1)$, *s.t.* $\theta = \sum_{j=1}^{q} \theta_j \leq 1$ *and*

$$w_j = \frac{\sigma \theta_j Q_m}{|2P\mathcal{B}_j|} \tag{3.11}$$

where $\sigma \in (0,1)$ *is a design parameter. Suppose that for each* $j \in \{1, \ldots, q\}$, *the sampling instants* $t_i^{\zeta_j}$ *are such that* $|\zeta_{j,e}| \leq w_j |\xi|$ *for all time* $t \geq 0$. *Then,* $\xi \equiv 0$ *(the origin) is globally asymptotically stable.*

Proof. Consider the candidate Lyapunov function $V(\xi) = \xi^T P \xi$ where P satisfies (A3.1). Utilizing the measurement error interpretation, (3.10), of the system (3.8), the derivative of the function V along the flow of the system is expressed as

$$\begin{aligned}
\dot{V} &= \xi^T [P\bar{\mathcal{A}} + \bar{\mathcal{A}}^T P]\xi + 2\xi^T P \mathcal{B} \zeta_e^* \\
&\leq -(1-\sigma)\xi^T Q \xi + |\xi| \Big[|2P\mathcal{B}\zeta_e^*| - \sigma Q_m |\xi| \Big] \\
&\leq -(1-\sigma)\xi^T Q \xi + |\xi| \Big[\sum_{j=1}^{q} |2P\mathcal{B}_j \zeta_{j,e}| - \sigma Q_m |\xi| \Big] \\
&\leq -(1-\sigma)\xi^T Q \xi + |\xi| \Big[\sum_{j=1}^{q} |2P\mathcal{B}_j| |\zeta_{j,e}| - \sigma Q_m |\xi| \Big]
\end{aligned}$$

The sampling instants have been assumed to be such that the conditions $|\zeta_{j,e}|/|\xi| \leq w_j = \frac{\sigma \theta_j Q_m}{|2P\mathcal{B}_j|}$ for each j are satisfied for all time $t \geq 0$. Thus,

$$\dot{V} \leq -(1-\sigma)\xi^T Q \xi$$

which implies that $\xi \equiv 0$ (the origin) is globally asymptotically stable. □

Note that Lemma 3.1 holds for a family of asynchronous event-triggers, all satisfying the conditions $|\zeta_{j,e}| \leq w_j |\xi|$. In order to enforce these conditions strictly, each event-trigger requires centralized (non-local) information, in the form of $|\xi|$.

Our aim now is to derive realizable decentralized asynchronous event-triggers that belong to the family considered in Lemma 3.1. To this end, consider the q centralized asynchronous event-triggers for the sampled-data system (3.8)

$$t_{i+1}^{\zeta_j} = \min\left\{t \geq t_i^{\zeta_j} : |\zeta_{j,e}| \geq w_j|\xi|\right\},\ j \in \{1,\ldots,q\} \tag{3.12}$$

where w_j are given by (3.11). From (3.9), we have that $\zeta_j = \mathcal{K}_j\xi$, where $\mathcal{K}_j \in \mathbb{R}^{d_j} \times \mathbb{R}^{n_\xi}$ is the j^{th} block-row matrix of $\mathcal{K}$. Since $|\zeta_j| \leq |\mathcal{K}_j||\xi|$, enforcing the conditions $|\zeta_{j,e}| \leq w_j|\zeta_j|/|\mathcal{K}_j|$ satisfies the requirements of Lemma 3.1. Although these conditions utilize only locally available data, they fail to guarantee positive minimum inter-sampling times. In order to design event-triggers that utilize only locally available data while also guaranteeing minimum inter-sample times, let us first analyze the emergent inter-sample times of the centralized asynchronous event-triggers (3.12).

Now, consider the differential equation

$$\dot{\phi} = \big(k + \phi\big)\big(a + b\phi\big) \tag{3.13}$$

where k, a, b are non-negative constants. The solution of this differential equation is denoted, as a function of time t and the initial condition ϕ_0, as $\phi(t, \phi_0)$. In particular, if $ka > 0$ then $\phi(t, 0)$ is a strictly increasing function of time t and if $ka = 0$ then $\phi(t, 0) \equiv 0$. Thus, the time it takes ϕ to evolve from 0 to a non-negative constant w is expressed as

$$\tau(w, a, b, k) = \min\{\{t \geq 0 : \phi(t, 0) = w\} \cup \{\infty\}\} \tag{3.14}$$

Notice that

$$\tau(w,a,b,k)\begin{cases}=0, & \text{if } w=0\\ >0, & \text{if } w>0\\ =\infty, & \text{if } w>0,\ ka=0\end{cases} \tag{3.15}$$

Remark 3.1. *Assuming b is non-zero, the solutions of the quadratic differential equation (3.13) have a finite escape time. However, by definition (3.14), $\tau(w,a,b,k)$ is strictly less than the finite escape time of the solution $\phi(.,0)$. Thus on the time interval of interest, $[0,\tau(w,a,b,k)]$, the solution $\phi(.,0)$ is well defined.*

The following lemma guarantees positive lower bounds for the emergent inter-sample times for the system (3.8) with the event-triggers (3.12).

Lemma 3.2. *Consider the closed loop system given by (3.8) and the event-triggers (3.12). Let $w_j > 0$ for $j \in \{1,\dots,q\}$ be given by (3.11) and let $W = \sum_{i=j}^{q} |\mathcal{B}_j| w_j$. Then for $j \in \{1,\dots,q\}$, the inter-sample times $\{t_{i+1}^{\zeta_j} - t_i^{\zeta_j}\}$ are lower bounded by the positive constants*

$$T_j = \tau(w_j, |\bar{\mathcal{A}}| + W - |\mathcal{B}_j| w_j, |\mathcal{B}_j|, |\mathcal{K}_j|). \tag{3.16}$$

where the function τ is given by (3.14).

Proof. Letting $\nu_j \triangleq |\zeta_{j,e}|/|\xi|$ and by direct calculation we see that for $j \in \{1,\dots,q\}$

$$\begin{aligned}\frac{\mathrm{d}\nu_j}{\mathrm{d}t} &= \frac{-(\zeta_{j,e}^T\zeta_{j,e})^{-1/2}\zeta_{j,e}^T\mathcal{K}_j\dot{\xi}}{|\xi|} - \frac{\xi^T\dot{\xi}|\zeta_{j,e}|}{|\xi|^3}\\ &\le \big(|\mathcal{K}_j| + \nu_j\big)\frac{|\dot{\xi}|}{|\xi|}\\ &\le \big(|\mathcal{K}_j| + \nu_j\big)\frac{|\bar{\mathcal{A}}\xi| + \sum_{j=1}^{q}|\mathcal{B}_j||\zeta_{j,e}|}{|\xi|}\end{aligned}$$

where for $\zeta_{j,e} = 0$ the relation holds for all directional derivatives. This relation is further simplified by considering (3.12), which ensures that the sampling instants are such that for all time $\nu_j \leq w_j$ for each $j \in \{1, \ldots, q\}$.

$$\frac{\mathrm{d}\nu_j}{\mathrm{d}t} \leq \big(|\mathcal{K}_j| + \nu_j\big)\big(|\bar{\mathcal{A}}| + W - |\mathcal{B}_j|w_j + |\mathcal{B}_j|\nu_j\big)$$

Now, by definition, $\nu_i(t_i^{\xi_j}) = 0$ for every sampling time instant $t_i^{\xi_j}$. Next, consider the flow

$$\dot{\phi}_j = \big(|\mathcal{K}_j| + \phi_j\big)\big(|\bar{\mathcal{A}}| + W - |\mathcal{B}_j|w_j + |\mathcal{B}_j|\phi_j\big)$$

and its solution denoted, as a function of time t and the initial condition $\phi_{j,0}$, as $\phi_j(t, \phi_{j,0})$. Then, by the Comparison Lemma [45], it follows that

$$\nu_j(t) \leq \phi_j(t - t_i^{\xi_j}, 0), \quad \forall\ t \geq t_i^{\xi_j}$$

As a consequence T_j, given by (3.16) is a lower bound on the inter-sample times $\{t_{i+1}^{\zeta_j} - t_i^{\zeta_j}\}$. The fact that $T_j > 0$ follows from the property (3.15). □

Remark 3.2. *In Lemma 3.2, the procedure for the computation of the lower bounds to the inter-transmission times is quite similar to that in [14]. The significant difference is that in Lemma 3.2, the guaranteed lower bounds are for asynchronous sampling while [14] provides lower bounds for synchronous sampling.*

Lemma 3.2 says that the inter-sample times that emerge from the event-triggers (3.12) have positive lower bounds, given by (3.16). An exactly equivalent method of implementing the event-triggers (3.12), for each $j \in \{1, \ldots, q\}$, is as follows.

$$t_{i+1}^{\zeta_j} = \min\Big\{t \geq t_i^{\zeta_j} + T_j : |\zeta_{j,e}| \geq w_j|\xi|\Big\} \tag{3.17}$$

In these event-triggers, the lower thresholds for the iner-sample times is explicitly enforced, although the actual inter-sample times that emerge from (3.17) may have lower bounds greater than T_j. The advantage with this implementation is that T_j depends only on the system matrices and hence is locally known at the corresponding event-trigger. In other words, the j^{th} event-trigger (3.17) uses only locally available information for time T_j after each of its transmissions. Thus, having guaranteed a positive lower bound for inter-sample times, it is sufficient to under-approximate $|\xi|$ to guarantee global asymptotic stability of the closed loop system. One obvious choice is to use the bound $|\zeta_j|/|\mathcal{K}_j| \leq |\xi|$ in the event-triggers, for $j \in \{1, \ldots, q\}$,

$$t_{i+1}^{\zeta_j} = \min \left\{ t \geq t_i^{\zeta_j} + T_j : |\zeta_{j,e}| \geq w_j \frac{|\zeta_j|}{|\mathcal{K}_j|} \right\}. \tag{3.18}$$

A better option is to use the bound $|\mathcal{K}_j^+ \zeta_j| \leq |\xi|$, where the notation $.^+$ denotes the pseudo-inverse of the matrix. In fact, this is the greatest lower bound for $|\xi|$ given ζ_j. Hence the event-triggers, for $j \in \{1, \ldots, q\}$,

$$t_{i+1}^{\zeta_j} = \min \left\{ t \geq t_i^{\zeta_j} + T_j : |\zeta_{j,e}| \geq w_j |\mathcal{K}_j^+ \zeta_j| \right\} \tag{3.19}$$

use only locally available information and achieve all the design requirements. While the event-triggers we have described in [29, 30] are based on (3.18), the ones that are described in this chapter utilize the improved version (3.19). Note, however, that if ζ_j is scalar then (3.18) and (3.19) are equivalent. The following theorem prescribes the constants T_j and w_j in the event triggers, (3.19), that guarantee global asymptotic stability of the origin.

Theorem 3.1. *Consider the closed loop system* (3.10) *and assume* (A3.1) *holds. Let* Q *be any symmetric positive definite matrix and let* Q_m *be the smallest eigenvalue*

of Q. For each $j \in \{1, 2, \ldots, q\}$, let w_j and T_j be defined as in (3.11) and (3.16), respectively. Suppose ζ_j are asynchronously updated at time instants determined by (3.19). Then, the origin is globally asymptotically stable and the inter-transmission times are explicitly enforced to have a positive lower threshold.

Proof. The statement about the positive lower threshold for inter-transmission times is obvious from (3.19) and only asymptotic stability remains to be demonstrated. This can be done by showing that the event-triggers (3.19) are included in the family of event-triggers considered in Lemma 3.1. From the equivalence of (3.12) and (3.17), it is clearly true that $|\zeta_{j,e}| \leq w_j|\xi|$ for $t \in [t_i^{\zeta_j}, t_i^{\zeta_j} + T_j]$, for each $j \in \{1, 2, \ldots, q\}$ and each i. Next, for $t \in [t_i^{\zeta_j} + T_j, t_{i+1}^{\zeta_j}]$, (3.19) enforces $|\zeta_{j,e}| \leq w_j|\mathcal{K}_j^+\zeta_j| \leq w_j|\xi|$. Therefore, the event-triggers, (3.19), are included in the family of event-triggers considered in Lemma 3.1. Hence, $\xi \equiv 0$ (the origin) is globally asymptotically stable. □

In the next section, this general formulation is applied to specific architectures of the control system.

3.4 Event-Triggered Implementations of The Dynamic Controller

In this section, the dynamic controllers and the event-triggering conditions are developed for different architectures.

3.4.1 Architecture I - Centralized

In Architecture I, Figure 3.1, the observer and the sensor are co-located, which means the observer has access to the sensor's output at all times. The closed loop

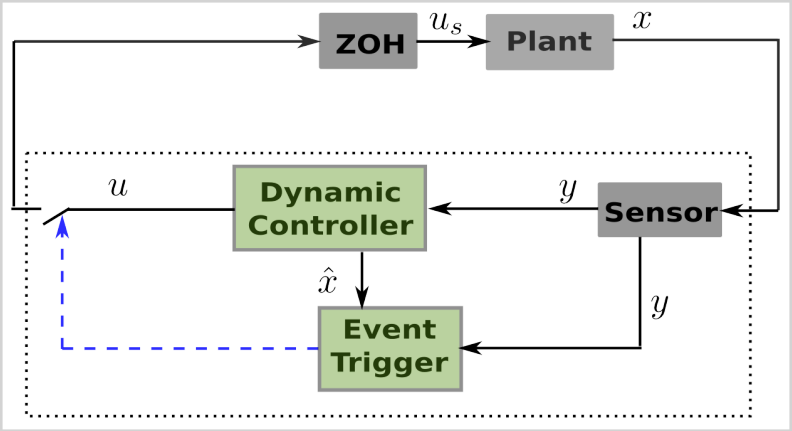

Figure 3.1: Architecture I: Sensor output available to the controller at all time. Co-located components have access to the others' output at any given time.

system with the sampled data implementation of the observer and the controller is given by

$$\dot{x} = Ax + Bu_s, \quad y = Cx \tag{3.20}$$

$$\dot{\hat{x}} = (A + FC)\hat{x} + BK\hat{x}_s - Fy, \quad u = K\hat{x} \tag{3.21}$$

where the subscript s denotes the sampled versions of the corresponding continuous-time signals. The second term, $BK\hat{x}_s$, in the observer, (3.21), is the natural choice to model the effect of the sampled data control $u_s = K\hat{x}_s$ in the plant dynamics (3.20).

The closed loop system can be written in terms of the measurement error,

$\hat{x}_e = \hat{x}_s - \hat{x}$, as

$$\dot{\psi} = \bar{A}\psi + \begin{bmatrix} BK \\ \mathbf{0}_{n,n} \end{bmatrix} \hat{x}_e \tag{3.22}$$

where $\psi = [x^T, \tilde{x}^T]^T = [x^T, (\hat{x} - x)^T]^T$, $\bar{A}$ is as defined in (3.3), $\mathbf{0}_{n,n}$ is the $n \times n$ matrix of zeroes. Note that the sampled-data nature of the system is implicit in the measurement error term, $\hat{x}_e$ (or ψ_e).

In the notation of Section 3.3, $\xi = \psi$, $\zeta = \hat{x}$, $\bar{\mathcal{A}} = \bar{A}$, $\mathcal{B} = G_1$, $\mathcal{K} = H_1$, where

$$\text{where } G_1 \triangleq \begin{bmatrix} BK \\ \mathbf{0}_{n,n} \end{bmatrix}, \quad H_1 \triangleq \begin{bmatrix} I_n & I_n \end{bmatrix} \tag{3.23}$$

so that $\hat{x} = H_1\psi$. Here, the notation I_n denotes the $n \times n$ identity matrix. Since there is only one event-trigger, $q = 1$, $\zeta_s = \zeta_s^* = \hat{x}_s$ and similarly, $\zeta_e = \zeta_e^* = \hat{x}_e$. Therefore, we have the following result as a direct consequence of Theorem 3.1.

Theorem 3.2. *Consider the system given by (3.22) and assume (A3.1) is satisfied with $\bar{\mathcal{A}} = \bar{A}$. Let $Q \in \mathbb{R}^{2n}$ be any positive definite matrix and let P be defined according to (A3.1). Let the event-triggering condition be*

$$t_{i+1} = \min\left\{t \geq t_i + T : |\hat{x}_e| \geq w|H_1^+\hat{x}|\right\}$$

where $w = \dfrac{\sigma Q_m}{|2PG_1|}$, in which Q_m is the smallest eigenvalue of Q, $0 < \sigma < 1$, G_1 and H_1 are given by (3.23) while $T = \tau\big(w, |\bar{A}|, |G_1|, |H_1|\big)$, the function τ being as defined in (3.14). Then, the origin of the closed loop system is globally asymptotically stable and the inter-transmission times are lower bounded by T. □

Note that the special structure of the matrix H_1 implies that in this case, the event-triggers of the form (3.18) and (3.19) (the one in the theorem) are exactly

equivalent. Now, in Architecture I (Figure 3.1), since the sensor, the dynamic controller and the event-trigger are all co-located, the event-trigger can in fact use the additional information obtained from the sensor in determining the transmission instants. In other words, an estimate of $|\psi|$ better than $|H_1^+\hat{x}|$ may be obtained by using the sensor data. Thus, let

$$H \triangleq \begin{bmatrix} I_n & I_n \\ C & \mathbf{0}_{p,n} \end{bmatrix} \tag{3.24}$$

so that $[\hat{x}^T, y^T]^T = H\psi$. The notation I_n again denotes the $n \times n$ identity matrix. Therefore, we now have the following result.

Theorem 3.3. *Consider the system given by (3.22) and assume (A3.1) is satisfied with $\bar{\mathcal{A}} = \bar{A}$. Let $Q \in \mathbb{R}^{2n}$ be any positive definite matrix and let P be defined according to (A3.1). Let the event-triggering condition be*

$$t_{i+1} = \min\left\{t \geq t_i + T : |\hat{x}_e| \geq w\middle|H^+[\hat{x}^T, y^T]^T\middle|\right\}$$

where $w = \dfrac{\sigma Q_m}{|2PG_1|}$, in which Q_m is the smallest eigenvalue of Q, $0 < \sigma < 1$, G_1 and H_1 are given by (3.23), H is given by (3.24), while $T = \tau\big(w, |\bar{A}|, |G_1|, |H_1|\big)$, the function τ being as defined in (3.14). Then, the origin of the closed loop system is globally asymptotically stable and the inter-transmission times are lower bounded by T. □

Note that T remains the same as in Theorem 3.2.

3.4.2 Architecture II - Centralized Synchronous

In Architecture II, Figure 3.2, the observer and the sensor are again co-located, which means the observer has access to the sensor information at all times. However, the

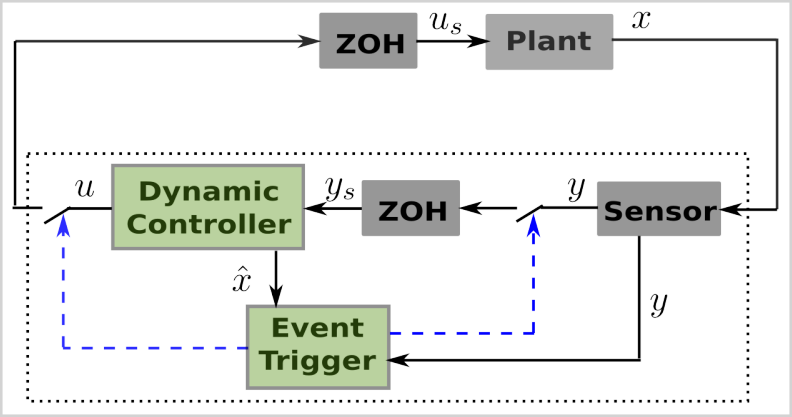

Figure 3.2: Architecture II: Synchronous transmissions by the sensor and the controller. Co-located components have access to the others' output at any given time.

observer in this architecture utilizes sampled version of the sensor output so that the dynamic controller has piecewise constant inputs (which simplifies the online computation of the observer state, $\hat{x}$). The controller and sensor outputs are sampled synchronously at time instants determined by a single event-trigger. The observer system in this case is given by

$$\dot{\hat{x}} = (A + FC)\hat{x} + BK\hat{x}_s - Fy_s \tag{3.25}$$

where the subscript s denotes the sampled versions of the corresponding continuous-time signals. The closed loop system may be written in terms of the measurement

error $\hat{x}_e = \hat{x}_s - \hat{x}$ and $y_e = y_s - y$ as

$$\dot{\psi} = \bar{A}\psi + G_s \begin{bmatrix} \hat{x}_e \\ y_e \end{bmatrix}, \quad \text{where } G_s \triangleq \begin{bmatrix} BK & \mathbf{0}_{n,p} \\ \mathbf{0}_{n,n} & -F \end{bmatrix} \tag{3.26}$$

where $\psi = [x^T, \tilde{x}^T]^T = [x^T, (\hat{x} - x)^T]^T$, $\bar{A}$ is as defined in (3.3), $\mathbf{0}_{a,b}$ represents the $a \times b$ matrix of zeroes. In the context of Section 3.3, $\xi = \psi$, $\zeta = [\hat{x}^T, y^T]^T$, $\bar{\mathcal{A}} = \bar{A}$, $\mathcal{B} = G_s$, $\mathcal{K} = H$, where H is the matrix defined in (3.24) and again $q = 1$ as there is only one event-trigger.

Theorem 3.4. *Consider the system given by (3.26) and assume (A3.1) is satisfied with $\bar{\mathcal{A}} = \bar{A}$. Let $Q \in \mathbb{R}^{2n}$ be any positive definite matrix and let P be defined according to (A3.1). Let the event-triggering condition be*

$$t_{i+1} = \min \left\{ t \geq t_i + T : \left| [\hat{x}_e^T, y_e^T]^T \right| \geq w \left| H^+ [\hat{x}^T, y^T]^T \right| \right\}$$

where $w = \dfrac{\sigma Q_m}{|2PG_s|}$, in which Q_m is the smallest eigenvalue of Q, $0 < \sigma < 1$, G_s is given by (3.26), H is given by (3.24), while $T = \tau\big(w, |\bar{A}|, |G_s|, |H|\big)$, the function τ being as defined in (3.14). Then, the origin of the closed loop system is globally asymptotically stable and the inter-transmission times are lower bounded by T. □

3.4.3 Architecture III - Decentralized Architecture

In the decentralized architecture of Figure 3.3, the sensors are decentralized. Their outputs are sampled and communicated to the central controller asynchronously by independent event-triggers that depend only on local information. Further, the different controller outputs are updated in parallel and asynchronously. The closed

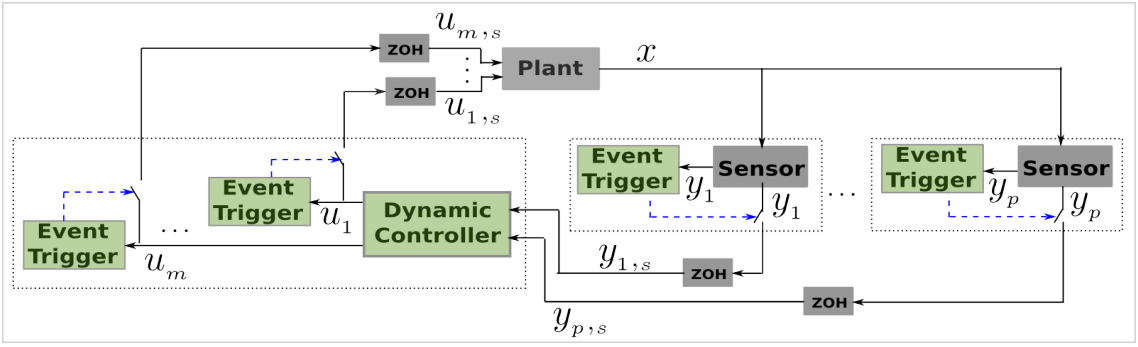

Figure 3.3: Architecture III: Centralized controller with decentralized sensors and actuators, each transmitting its data asynchronously.

loop system is given by

$$\dot{x} = Ax + Bu_s^*, \quad y = Cx$$

$$\dot{\hat{x}} = (A + FC)\hat{x} + Bu_s^* - Fy_s^*, \quad u = K\hat{x}$$

where $x \in \mathbb{R}^n$ is the state of the plant, $\hat{x} \in \mathbb{R}^n$ is the observer state, $y \in \mathbb{R}^p$ is the vector of sensed outputs, $u_s^* \in \mathbb{R}^m$ is the vector of inputs to the plant from the actuators. The vectors u_s^* and y_s^* denote the asynchronously sampled versions of the corresponding continuous-time signals as in (3.6). In other words, $u_s^* = [u_{1,s}, \ldots, u_{m,s}]$ and $y_s^* = [y_{1,s}, \ldots, y_{p,s}]$. That is, each actuator output $u_{i,s}$, for $i \in \{1, \ldots, m\}$, and each sensor output $y_{j,s}$, for $j \in \{1, \ldots, p\}$, represent asynchronously sampled signals,

$$u_{i,s} = u(t_k^{u_i}), \quad \forall t \in [t_k^{u_i}, t_{k+1}^{u_i})$$

$$y_{j,s} = y(t_k^{y_j}), \quad \forall t \in [t_k^{y_j}, t_{k+1}^{y_j})$$

It is possible to define u_i and y_j as vectors (instead of scalars) with only minor changes in notation. However, in this chapter we restrict to the scalar case for

simplicity.

In terms of the measurement error vectors $u_e^* = u_s^* - u$ and $y_e^* = y_s^* - y$, the closed loop system is

$$\dot{\psi} = \bar{A}\psi + \begin{bmatrix} B & \mathbf{0}_{n,p} \\ \mathbf{0}_{n,m} & -F \end{bmatrix} \begin{bmatrix} u_e^* \\ y_e^* \end{bmatrix}, \quad G_d \triangleq \begin{bmatrix} B & \mathbf{0}_{n,p} \\ \mathbf{0}_{n,m} & -F \end{bmatrix} \tag{3.27}$$

where $\psi = [x^T, \tilde{x}^T]^T = [x^T, (\hat{x} - x)^T]^T$, $\bar{A}$ is as defined in (3.3), $\mathbf{0}_{a,b}$ represents the $a \times b$ matrix of zeroes. In the context of Section 3.3, $\xi = \psi$, $\zeta = [u^T, y^T]^T$, $\bar{\mathcal{A}} = \bar{A}$,

$$\mathcal{B} \triangleq \begin{bmatrix} \bar{B} & \bar{F} \end{bmatrix} \triangleq \begin{bmatrix} B & \mathbf{0}_{n,p} \\ \mathbf{0}_{n,m} & -F \end{bmatrix} \tag{3.28}$$

$$\mathcal{K} \triangleq \begin{bmatrix} \bar{K} \\ \bar{C} \end{bmatrix} \triangleq \begin{bmatrix} K & K \\ C & \mathbf{0}_{p,n} \end{bmatrix} \tag{3.29}$$

where $\bar{B} \in \mathbb{R}^{2n} \times \mathbb{R}^m$, $\bar{F} \in \mathbb{R}^{2n} \times \mathbb{R}^p$, $\bar{K} \in \mathbb{R}^m \times \mathbb{R}^{2n}$ and $\bar{C} \in \mathbb{R}^p \times \mathbb{R}^{2n}$ are appropriately defined block matrices. For this architecture, the number of event-triggers is $q = p + m$. Denoting the i^{th} column of $\bar{B}$ and $\bar{F}$ by $\bar{B}_i$ and $\bar{F}_i$; and similarly, the i^{th} row of $\bar{K}$ and $\bar{C}$ by $\bar{K}_i$ and $\bar{C}_i$, respectively, we have

$$\dot{\psi} = \bar{A}\psi + \sum_{i=1}^{m} \bar{B}_i u_{i,e} + \sum_{j=1}^{p} \bar{F}_j y_{j,e} \tag{3.30}$$

$$u_i = \bar{K}_i \psi, \qquad y_j = \bar{C}_j \psi \tag{3.31}$$

We now present the result for decentralized asynchronous event-triggering in dynamic output feedback control.

Theorem 3.5. *Consider the system given by* (3.30) *and assume* (A3.1) *is satisfied with* $\bar{\mathcal{A}} = \bar{A}$. *Let* $Q \in \mathbb{R}^{2n}$ *be any positive definite matrix and let* P *be defined*

according to (A3.1). *For* $i \in \{1, \ldots, m\}$ *and* $j \in \{1, \ldots, p\}$, *let the event-triggering conditions be*

$$t_{k+1}^{u_i} = \min\{t \geq t_k^{u_i} + T_{u,i} : |u_{i,e}| \geq w_{u,i}|\bar{K}_i^+ u_i|\}$$

$$t_{k+1}^{y_j} = \min\{t \geq t_k^{y_j} + T_{y,j} : |y_{j,e}| \geq w_{y,j}|\bar{C}_j^+ y_j|\}$$

where $w_{u,i} = \dfrac{\sigma Q_m \theta_{u,i}}{2|P\bar{B}_i|}$, $w_{y,j} = \dfrac{\sigma Q_m \theta_{y,j}}{2|P\bar{F}_j|}$, *in which* Q_m *is the smallest eigenvalue of* Q, $0 < \sigma < 1$, $0 < \theta_{u,i} < 1$, $0 < \theta_{y,j} < 1$ *are design parameters such that* $\sum \theta_{u,i} + \sum \theta_{y,j} = 1$, $\bar{B}_i$ *and* $\bar{F}_j$ *are given by* (3.28). *Let the inter-sampling time thresholds be given by*

$$T_{u,i} = \tau(w_{u,i}, |\bar{A}| + W - |\bar{B}_i|w_{u,i}, |\bar{B}_i|, |\bar{K}_i|)$$

$$T_{y,j} = \tau(w_{y,j}, |\bar{A}| + W - |\bar{F}_j|w_{y,j}, |\bar{F}_j|, |\bar{C}_j|)$$

where $W = \sum |\bar{B}_i|w_{u,i} + \sum |\bar{F}_j|w_{y,j}$, *and the function* τ *is defined as in* (3.14). *Then, the origin of the closed loop system is globally asymptotically stable and the inter-sample times of* u_i *and* y_j *are lower bounded by* $T_{u,i}$ *and* $T_{y,j}$, *respectively.* □

3.4.4 Architecture IV - SCAN

Finally, we consider a Sensor-Controller-Actuator Network (SCAN) control system architecture, shown in Figure 3.4. The control system contains three functional layers - the sensor layer, the dynamic controller/observer layer and the actuator layer. Each layer consists of non-co-located (physically distributed) nodes. The sensor, observer and the actuator layers consist of p sensor nodes, n observer nodes and m actuator nodes, respectively. In Figure 3.4, the solid arrows indicate physical links,

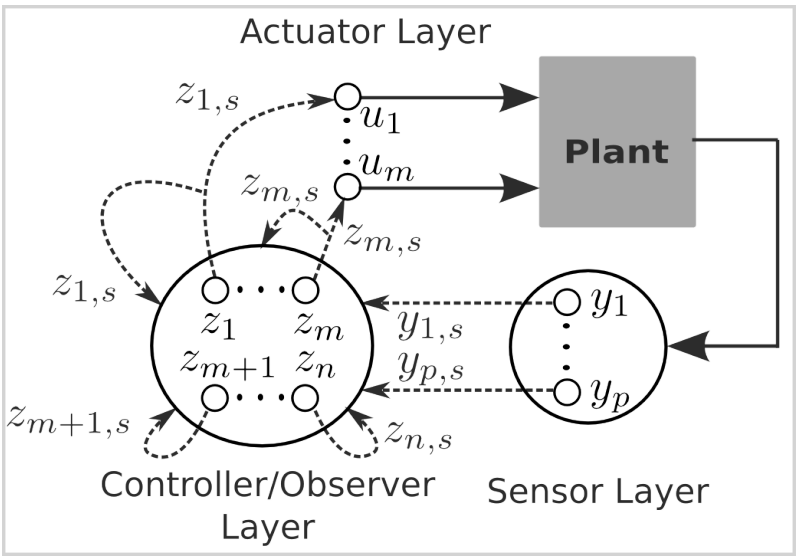

Figure 3.4: The SCAN control architecture has three functional layers. Each node in the sensor layer intermittently broadcasts its output to all the nodes in the observer layer. Each node in the observer layer intermittently broadcasts its state to every other node in that layer. Each of the first m nodes of the observer layer also transmit intermittently to one of the actuator nodes. The dotted arrows indicate even-triggered communication links, with the event-trigger running at the tail end of the arrow. The solid arrows are physical links.

while the dotted arrows indicate the links on which the communication is event-triggered. The event-trigger for each of these links is located at the tail end of the arrow and uses only information that is locally available at that node. Meanwhile, the node or the nodes at the receiving end utilize the asynchronously transmitted data (sampled data), indicated by the additional subscript s. Note that the arrows that go from an arbitrary node 'A' to a layer circle in the figure indicate broadcast communication from the node 'A' to all the nodes in the layer circle. The aggregate observer state $z = [z_1, \ldots, z_n]^T$ is simply a basis transformation of the vector $\hat{x}$ of (3.2). When this basis transformation is appropriately chosen, the communication from the observer layer to the actuator layer is simplified and the actuator inputs to the plant are $u_i = z_{i,s}$ for $i \in \{1, \ldots, m\}$.

Figure 3.4 is a functional description of the control system and also represents the most general case, where no two nodes are co-located. If some nodes (from the same or different layers) are co-located, then each collection of co-located nodes need not utilize the sampled versions of the data. Of particular interest is the case where the observer node z_i is co-located with the actuator node u_i for $i \in \{1, \ldots, m\}$. In the sequel, apart from the general case, this special case is also discussed briefly. Next, in order to keep the notation simple, the data at each node is assumed to be scalar. Our results can easily be generalized to the vector case with only minor changes to the notation.

Now, let us consider the design of event-triggered dynamic output feedback control over SCAN architecture of Figure 3.4. The heart of the SCAN architecture of Figure 3.4 is the observer layer. Once this is designed, the decentralized

asynchronous event-triggers can be designed using the results in Section 3.3. As noted earlier, the nodes in the observer layer do not compute $\hat{x}$ but rather a basis transformation of $\hat{x}$. Defining this transformation is our next task.

(A3.2) Assume that the column space of the matrix K, in (3.2), is of dimension m.

Under this assumption, the pseudoinverse $K^+ \in \mathbb{R}^n \times \mathbb{R}^m$ has only the trivial null space. Consider the mapping

$$\hat{x} = K^+ u + \hat{x}^{\mathcal{N}(K)}$$

where $\hat{x}^{\mathcal{N}(K)} \in \mathbb{R}^{n-m}$ is an element of the null space of K and by definition, K^+u is an element of the row space of K. Assumption (A3.2) implies that this mapping is one-to-one and onto. Further, since the row space and the null space of K are orthogonal to each other, the basis for the two subspaces can be chosen independently. Thus, let

$$S = \begin{bmatrix} K^+ & K_N \end{bmatrix} \tag{3.32}$$

where $K_N \in \mathbb{R}^n \times \mathbb{R}^{n-m}$ is an arbitrary matrix whose columns span the null space of K. Then, the matrix S is invertible and satisfies

$$\hat{x} = Sz \tag{3.33}$$

$$u = u_s^* = KSz_s^* = \bar{K} z_s^*, \text{ with } \bar{K} = \begin{bmatrix} I_m & \mathbf{0}_{m,n-m} \end{bmatrix} \tag{3.34}$$

where I_m is the $m \times m$ identity matrix and $\mathbf{0}_{m,n-m}$ is $m \times (n-m)$ matrix of zeroes. Note that there is no 'sampling' of the data between the actuator nodes and the

plant. However, the notation u_s^* is useful for keeping in mind that the actuation signals are the asynchronously transmitted signals $\bar{K}z_s^*$. Thus, the dynamic controller (observer), (3.2), is equivalently expressed as

$$\dot{z} = S^{-1}[(A + FC)Sz + B\bar{K}z_s^* - Fy] \tag{3.35}$$

where $\bar{K} = KS$ has been used.

Letting $H = S^{-1}(A + FC)S$, the sampled data version of the decentralized observer is given by

$$\dot{z} = D(H)z + (H - D(H))z_s^* + S^{-1}B\bar{K}z_s^* - S^{-1}Fy_s^*$$

where $D(H)$ is the diagonal matrix with its diagonal given by the diagonal of the matrix H. It is more convenient to write the observer equation in terms of the sampling induced measurement errors, as follows.

$$\dot{z} = S^{-1}[(A + FC)Sz + B\bar{K}z_s^* - Fy] + (H - D(H))z_e^* - S^{-1}Fy_e^*$$

which when expressed in terms of $\hat{x}$ is given as

$$\dot{\hat{x}} = (A + FC)\hat{x} + Bu_s^* - Fy + S(H - D(H))z_e^* - Fy_e^*$$

Let us denote the *observer estimation error* and the state of the closed loop system, respectively, as

$$\tilde{x} \triangleq \hat{x} - x, \quad \psi \triangleq [x^T, \tilde{x}^T]^T$$

Then the closed loop system may be written compactly as

$$\dot{\psi} = \bar{A}\psi + \begin{bmatrix} B\bar{K} \\ S(H - D(H)) \end{bmatrix} z_e^* - \begin{bmatrix} \mathbf{0}_{n,p} \\ F \end{bmatrix} y_e^* \tag{3.36}$$

where the matrix $\bar{A}$ is as defined in (3.3). The following theorem prescribes the decentralized asynchronous event-triggering mechanism for the SCAN control architecture in Figure 3.4.

Theorem 3.6. *Consider the closed loop system, (3.36), and assume that (A3.1) holds with $\bar{\mathcal{A}} = \bar{A}$. Also suppose (A3.2) holds. Let $\zeta = [z^T, y^T]^T$ and*

$$\mathcal{B} = \begin{bmatrix} B\bar{K} & \mathbf{0}_{n,p} \\ S(H - D(H)) & -F \end{bmatrix}, \quad \mathcal{K} = \begin{bmatrix} S^{-1} & S^{-1} \\ C & \mathbf{0}_{p,n} \end{bmatrix}.$$

Further, for each $j \in \{1, \ldots, q = n + p\}$, let $\zeta_j \in \mathbb{R}$, $\mathcal{B}_j$ is the j^{th} column of $\mathcal{B}$ and $\mathcal{K}_j$ is the j^{th} row of $\mathcal{K}$. Let $Q \in \mathbb{R}^{2n} \times \mathbb{R}^{2n}$ be any symmetric positive definite matrix and let Q_m be the smallest eigenvalue of Q. For each $j \in \{1, 2, \ldots, q\}$, let w_j and T_j be defined as in (3.11) and (3.16), respectively. Suppose ζ_j are asynchronously transmitted at time instants determined by (3.19), with $t_0^{\zeta_j} < 0$. Then, $\psi \equiv 0$ (the origin) is globally asymptotically stable and the inter-transmission times are explicitly enforced to have a positive lower threshold.

Proof. Assumption (A3.2) implies that S is invertible and that the matrices $\mathcal{B}$ and $\mathcal{K}$ are well defined. The rest of the proof follows from Theorem 3.1. □

Remark 3.3. *In case the first m nodes of the observer layer, z, are co-located with the corresponding actuator nodes, then $u = \bar{K}z$ may be used. In this case, the closed loop system equation is given by*

$$\dot{\psi} = \bar{A}\psi + \begin{bmatrix} \mathbf{0}_{n,n} \\ S(H - D(H)) \end{bmatrix} z_e^* - \begin{bmatrix} \mathbf{0}_{n,p} \\ F \end{bmatrix} y_e^* \tag{3.37}$$

and Theorem 3.6 holds for this system if $\mathcal{B}$ is appropriately chosen as

$$\mathcal{B} = \begin{bmatrix} \mathbf{0}_{n,n} & \mathbf{0}_{n,p} \\ S(H - D(H)) & -F \end{bmatrix}.$$

Remark 3.4. *In Figure 3.4 and in our results, the sensor nodes and the observer nodes have been assumed to intermittently broadcast their data to all the nodes in the controller/observer layer. However, this has been done purely for ease of presentation. In practice, a sensor node y_j need not transmit its data to the observer node z_k if the dynamics of z_k is not dependent on y_j. A similar statement for intra observer layer communication also holds.*

Remark 3.5. *As discussed in Remark 2.3 of the previous chapter, the idea of an explicit threshold for the inter-transmission times as in the event-triggers, (3.19), has been employed previously in [46]. However, in [46] such a mechanism is used to trigger the controller updates rather than the asynchronous transmissions from the sensors to the controller. Further, in [46] the controller utilizes synchronous measurements from the sensors to compute the control input to the plant, which allows the lower bound for inter-transmission times from [14] to be used.*

In Architectures I and II of this chapter, the transmissions/samplings are synchronous. As a result, the inter-transmission time thresholds are exactly as those obtained from [14]. On the other hand, in Architectures III and IV, the controller has access only to asynchronously received data and the inter-transmission time thresholds of each node need to be computed as in Lemma 3.2.

In the next section, simulation results are presented to illustrate the proposed

event-triggered controllers.

3.5 Simulation Results

In this section, the proposed event-triggered dynamic output feedback controllers are illustrated for a linearized model of a batch reactor, [47]. The plant and the dynamic controller are given by (3.1)-(3.2) with

$$A = \begin{bmatrix} 1.38 & -0.2077 & 6.715 & -5.676 \\ -0.5814 & -4.29 & 0 & 0.675 \\ 1.067 & 4.273 & -6.654 & 5.893 \\ 0.048 & 4.273 & 1.343 & -2.104 \end{bmatrix}, \quad B = \begin{bmatrix} 0 & 0 \\ 5.679 & 0 \\ 1.136 & -3.146 \\ 1.136 & 0 \end{bmatrix}$$

$$C = \begin{bmatrix} 1 & 0 & 1 & -1 \\ 0 & 1 & 0 & 0 \end{bmatrix}, \quad K = - \begin{bmatrix} 0.1768 & 0.079 & 0.0794 & -0.2464 \\ 1.0328 & 0.1896 & -0.4479 & 0.7176 \end{bmatrix}$$

$$F = - \begin{bmatrix} -2 & 0 \\ -4 & -1 \\ -2 & 2 \\ -1 & -4 \end{bmatrix}$$

In the event-triggered controllers, $Q = I_8$, the 8×8 identity matrix, $\sigma = 0.95$ were chosen. For the simulations presented here, the initial condition of the plant was chosen as $x(0) = [2, 3, -1, 2]^T$. The state of the centralized observer in Architectures I-III was chosen as $\hat{x}(0) = [0, 0, 0, 0]^T$. The simulation time for each of the simulations was $T_{\text{sim}} = 10$s.

3.5.1 Architecture I

In this architecture, the sampled data is $\hat{x}_s$ and its initial condition was chosen as $\hat{x}_s(0) = \hat{x}(0)$. The inter-event time threshold of the event-triggers in Theorems 3.2 and 3.3 was obtained as $T = 3$ms. With the event-trigger of Theorem 3.2 (which is essentially the one proposed in our previous work, [29]), the number of events, average inter-event time and minimum inter-event time were observed to be 543, 18.4ms and 3ms, respectively. With the event-trigger of Theorem 3.3 the corresponding values were 484, 20.7ms and 7.2ms, respectively. This clearly shows the improvement over our previous results in [29]. The simulation results for Theorem 3.3 are summarized in Figures 3.5 and 3.6. Figure 3.5 shows the evolution of the Lyapunov function and its derivative along the flow of the closed loop system. Figure 3.6 shows the inter-transmission times and the cumulative frequency distribution of the inter-event times.

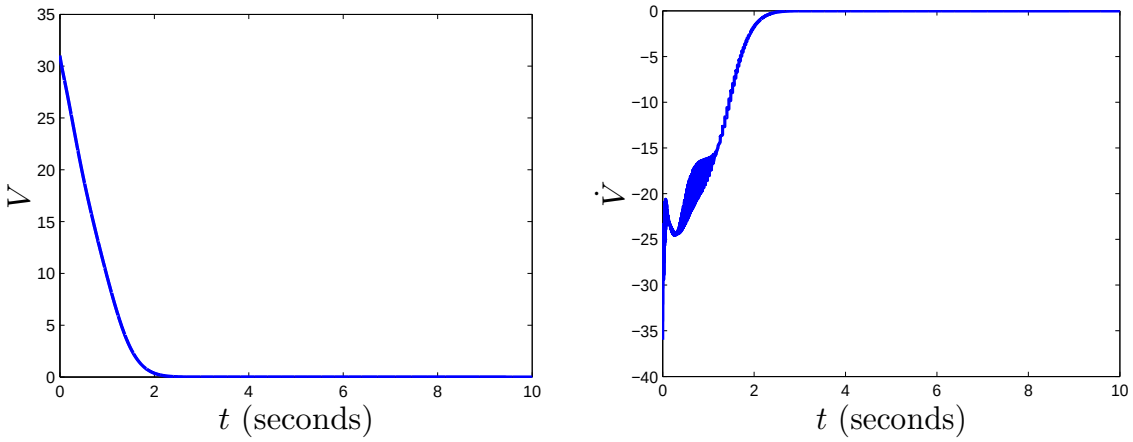

(a) (b)

Figure 3.5: Architecture I: (a) The evolution of the Lyapunov function and (b) its derivative along the flow of the closed loop system.

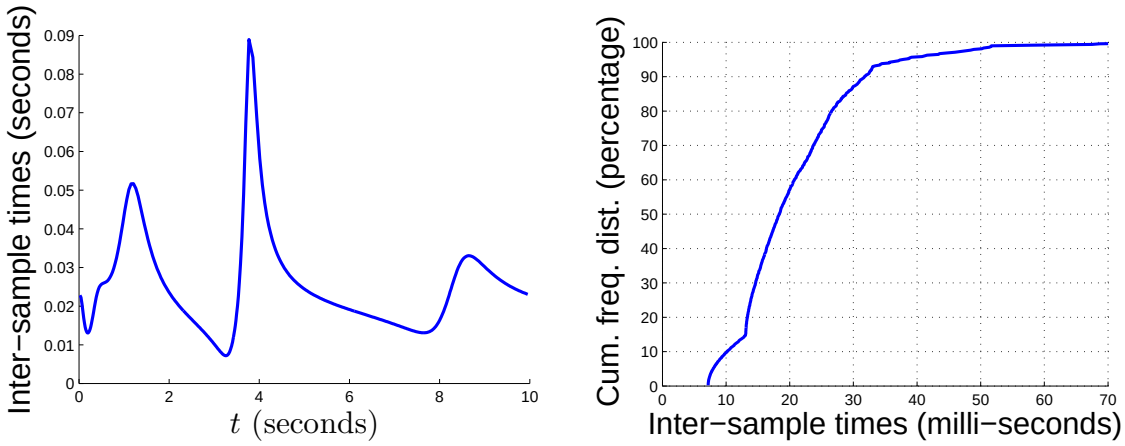

(a) (b)

Figure 3.6: Architecture I: (a) Inter-event times and (b) the cumulative frequency distribution of the inter-event times.

3.5.2 Architecture II

In this architecture, the sampled data is $[\hat{x}_s^T, y_s^T]^T$ and its initial condition was chosen as $[\hat{x}_s^T(0), y_s^T(0)]^T = [\hat{x}^T(0), y^T(0)]^T$. The inter-event time threshold of the event-trigger in Theorem 3.4 was obtained as $T = 0.9$ms. For the presented simulation, the number of events, average inter-event time and minimum inter-event time were observed to be 1081, 9.3ms and 3.2ms, respectively. To give a comparison, with the event-trigger corresponding to (3.18), these values were observed as 1548, 6.5ms and 2.2ms, respectively. Again the improvement over our previous results in [29] is clearly visible. Figure 3.7 shows the evolution of the Lyapunov function and its derivative along the flow of the closed loop system. Figure 3.8 shows the inter-transmission times and the cumulative frequency distribution of the inter-event times.

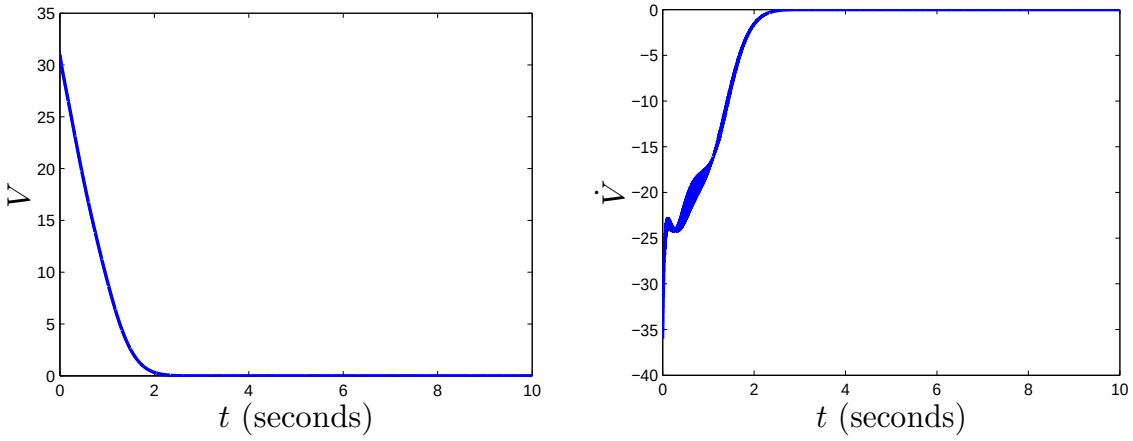

(a) (b)

Figure 3.7: Architecture II: (a) The evolution of the Lyapunov function and (b) its derivative along the flow of the closed loop system.

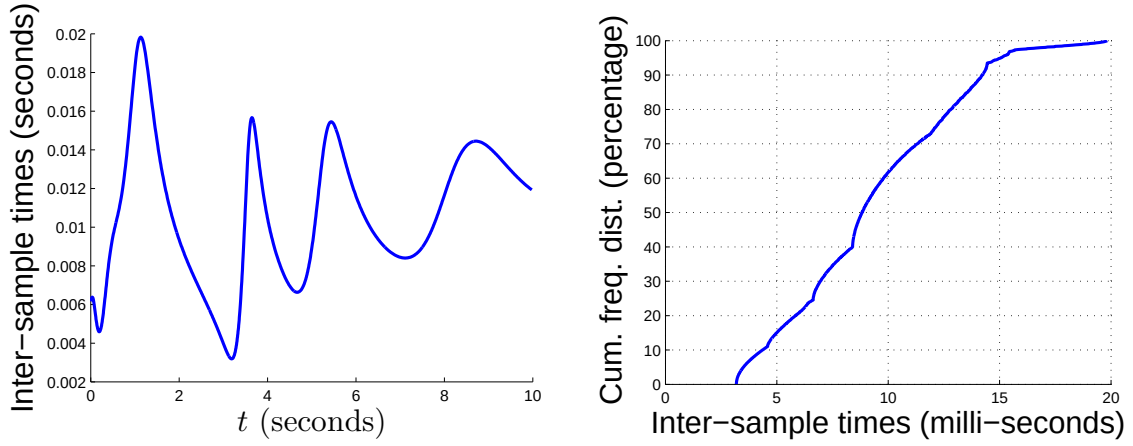

(a) (b)

Figure 3.8: Architecture II: (a) Inter-event times and (b) the cumulative frequency distribution of the inter-event times.

3.5.3 Architecture III

Finally in Architecture III, the sampled data is $\zeta_s^* = [u_s^{*T}, y_s^{*T}]^T$. Even though $y(0) = [-1, 3]^T$, the initial sampled data was chosen as

$$\zeta_s^*(0) = [0, 0, -1.005, 3.01]^T$$

to be consistent with the asynchronous transmission model. The zeroth transmission instant was chosen as $t_0^{\zeta_j} = -T_j$ for each $j \in \{1, \ldots, 4\}$. This is to ensure sampling at $t = 0$ if necessary. However, by choosing the initial sampled data sufficiently close to the actual data, the asynchronous nature of transmissions is respected, as indicated by the first transmission times by the controller and the sensors, which occur at $t_1^{\zeta} = [0, 0, 0.6, 1.5]$ms for the chosen initial conditions. The inter-transmission time thresholds in the event-triggers of Theorem 3.5 were obtained as

$$T_u = [1.1, 0.8]\text{ms}, \qquad T_y = [0.7, 0.6]\text{ms}$$

which were also the minimum inter-transmission times for the presented simulation. Over a simulation time of 10s, the average inter-transmission times were obtained as $\bar{T} = [5.3, 3.8, 3.6, 3.8]$ms, which are roughly five times larger than the inter-transmission time thresholds. Figure 3.9 shows the evolution of the Lyapunov function and its derivative along the flow of the closed loop system. Figure 3.10 shows the inter-transmission times and the cumulative frequency distribution of the inter-transmission times.

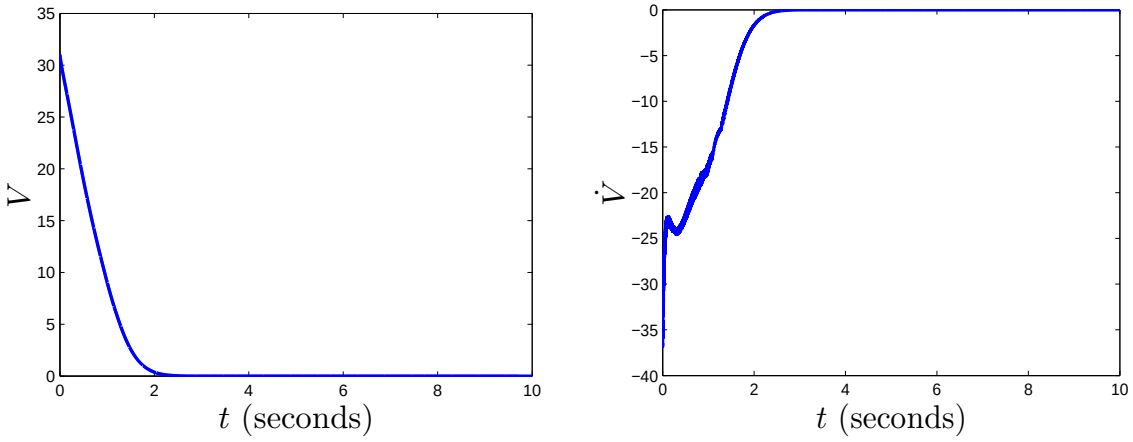

(a) (b)

Figure 3.9: Architecture III: (a) The evolution of the Lyapunov function and (b) its derivative along the flow of the closed loop system.

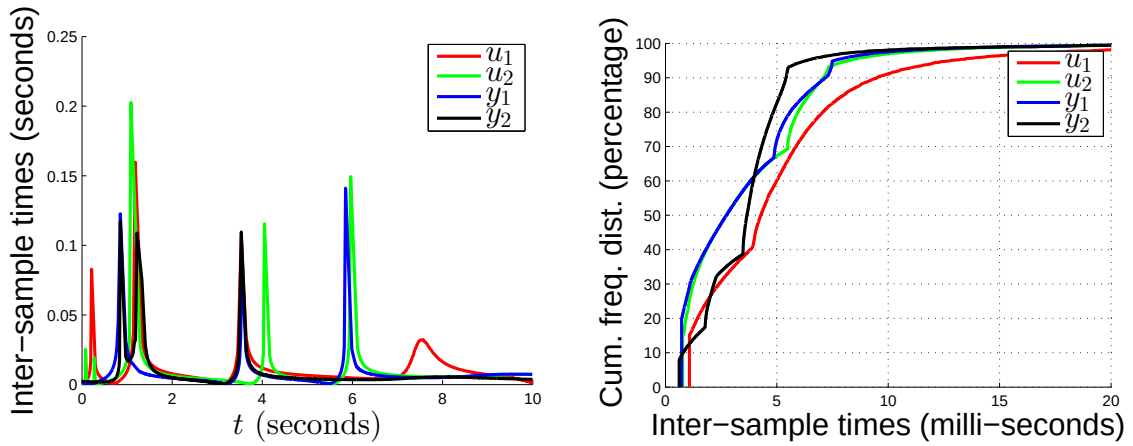

(a) (b)

Figure 3.10: Architecture III: (a) Inter-transmission times and (b) the cumulative frequency distribution of the inter-transmission times of the nodes. The curves labelled with u_i and y_j denote the relevant inter-transmission time data of the controller output u_i and the sensor output y_j, respectively.

3.5.4 Architecture IV - SCAN

In the SCAN architecture, the initial condition of the observer was chosen as $z(0) = [0, -1, 1, -1]^T$. Denoting $\zeta = [z^T, y^T]^T$ as in Theorem 3.6, the initial sampled data was chosen arbitrarily as

$$\zeta_s^*(0) = [-1.001, -1.001, 1.001, -1.001, -1.001, 3.002]^T$$

so that it is consistent with the asynchronous transmission model. The zeroth transmission instant was chosen as $t_0^{\zeta_j} = -T_j$ for each $j \in \{1, \ldots, 6\}$. This is to ensure sampling at $t = 0$ if necessary. However, by choosing the initial sampled data sufficiently close to the actual data, the asynchronous nature of transmissions is respected, as indicated by the first transmission times by the 6 nodes which occur at $t_1^{\zeta} = [6, 1.1, 0.4, 1.2, 0.4, 0.9]$ms for the chosen initial conditions. The inter-transmission time thresholds in the event-triggers, (3.19), were obtained as

$$T = 10^{-4} \times [4.886, 4.676, 5.247, 3.976, 4.12, 3.881]\text{s}$$

which were also the minimum inter-transmission times for the presented simulation. Over a simulation time of 10s, the average inter-transmission times for the nodes were obtained as $\bar{T} = [3.1, 3, 2.7, 2.6, 2.7, 3]$ms, which are roughly an order of magnitude larger than the inter-transmission time thresholds. Figure 3.11 shows the evolution of the Lyapunov function and its derivative along the flow of the closed loop system. Figure 3.12 shows the inter-transmission times and the cumulative frequency distribution of the inter-transmission times of the nodes.

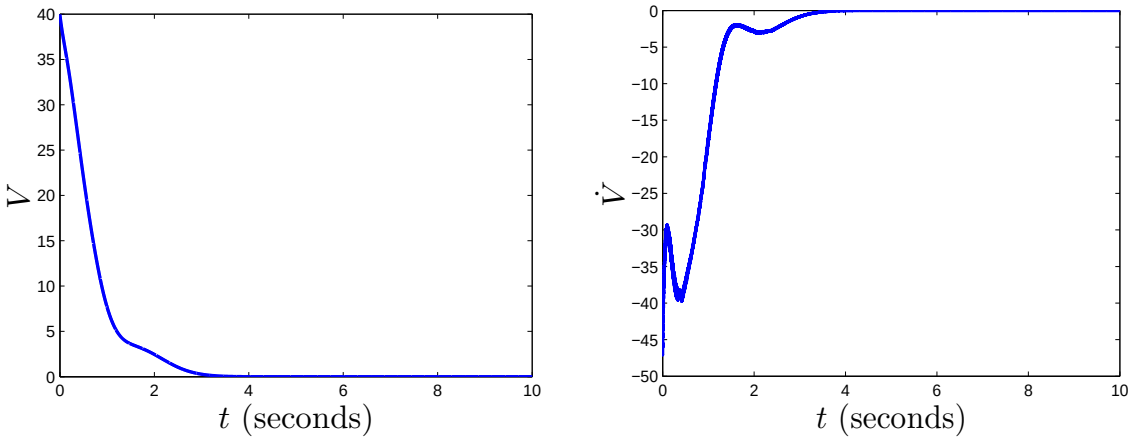

(a) (b)

Figure 3.11: Architecture IV: (a) The evolution of the Lyapunov function and (b) its derivative along the flow of the closed loop system.

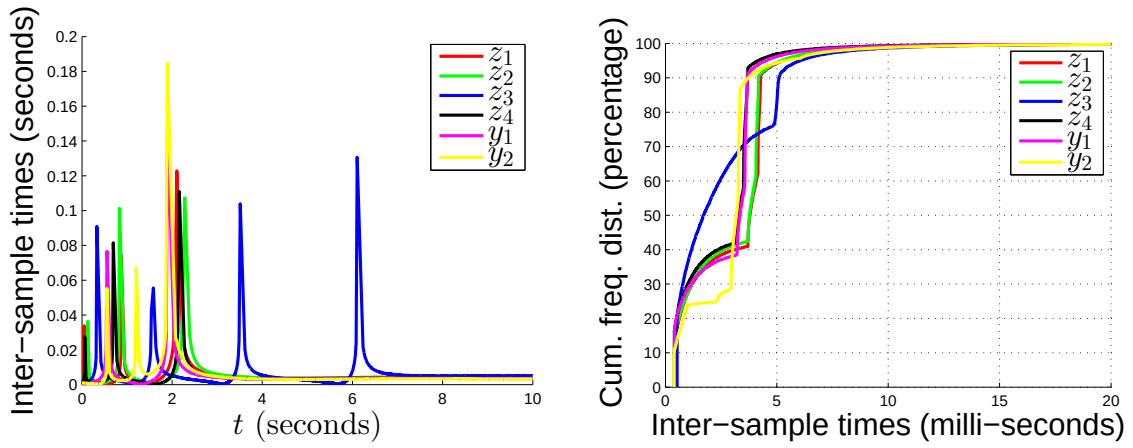

(a) (b)

Figure 3.12: Architecture IV: (a) Inter-transmission times and (b) the cumulative frequency distribution of the inter-transmission times of the nodes. The curves labelled with z_i and y_j denote the relevant inter-transmission time data of those nodes, respectively.

3.6 Conclusions

In this chapter event-triggered dynamic output feedback controllers have been developed for architectures where the controller and the sensor are co-located as well as where they are not co-located. In each case, a minimum inter-transmission time is enforced by incorporating a lower threshold on inter-transmission interval in the event-triggering conditions. The design of these thresholds was also presented. The designed event-triggering conditions have been shown to ensure global asymptotic stability of the origin of the closed loop system. The proposed controllers have been illustrated through simulations. In Architecture III, the sensors, the controller and the actuators are not co-located. Hence, the event-triggering conditions have been designed for the sensors and controller outputs to be transmitted asynchronously.

In Architecture IV, control of LTI systems over Sensor-Controller-Actuator Networks (SCAN) is considered. A SCAN is divided into three functional layers - sensor layer, controller/observer layer and the actuator layer, each layer consisting of several nodes. The communication between the nodes is intermittent and event-triggered. Further, the flow of information is only from the sensor to observer to actuator layer with the only intra-layer communication occurring in the observer layer. With a careful choice of basis for decentralized estimation of the plant state in the observer layer, each actuator node intermittently receives data from a corresponding unique observer node. The event-triggers are designed to utilize only locally available information, making the nodes' transmissions asynchronous. Some of the future work will include relaxation of assumption (A3.2), extending the design

to the case where an arbitrary communication graph is given and optimal placement of the controller/observer nodes (see Remark 3.3 for example).

In each architecture, the observer and the controller gains can be chosen independently, as in the classical case. However, their effect on the exact convergence rate and inter-sampling times has to be studied in detail. The inter-sample time thresholds can also be made less conservative. Finally, in [44] (and references therein), a self-triggered dynamic output feedback controller was presented that renders the origin of the closed loop system globally asymptotically stable under the absence of exogenous disturbances. The controller was designed by allowing the Lyapunov function to evolve non-monotonically and obtained larger inter-sample times. It would be interesting to apply the ideas from the current chapter to design event-triggered variants of [44], specially with decentralized asynchronous event-triggering.

Part II

Co-Design of Event-Triggering and Quantization

Chapter 4

Utility Driven Co-design of Event-Trigger and Quantizer

4.1 Introduction

In this chapter we revisit the problem of control under data rate constraints and limited information, a problem that has been actively researched in the last decade. A good survey paper on this and other topics is [50]. Many papers have looked at issues such as fundamental limits on communication rate for stabilization (see for example [51–55]), while others have focused on asymptotic stabilization with dynamic quantization [56–60]. Control under data rate constraints and limited information occurs frequently in Cyber Physical Systems (CPS), often with the additional constraint of limited computational capabilities.

The field of event-triggered control (example: [14, 15, 19]) also has similar motivations and seeks to systematically design controllers that update or sample the control action at low average rates. These controllers are based on the principle of updating the control only when necessary (control by exception). In other words, event-triggered control seeks to minimize the average rate of communication instances, while the amount of information that can be conveyed at each communication instance is not limited. However, in practical situations quantization is inevitable, and hence it is necessary to consider utility driven sampled data control along with quantization. The survey paper [22] makes a related remark that the con-

nection between quantized and even-triggered feedback must be studied. In [61,62] event-triggered control systems with dynamic quantization are proposed. While [61] considers a model based approach, with identical models of the plant running on the sensing and the actuation side, [62] considers a zero-order-hold actuation. Keeping in mind the limited computational resources, in this chapter we only consider static quantizers.

Starting from very similar motivations as utility driven event-triggered control, there is a body of literature that seeks to design coarsest static quantizers. Elia and his co-workers first studied this problem in the context of quadratically stabilizable linear time invariant systems [63, 64] (single input), [65] (two input), and demonstrated that the coarsest quantizer is the logarithmic quantizer. Fu and Xie [66] extended the results of [64] to linear multiple input systems by quantizing each dimension separately, and their design resulted in an infinite-density logarithmic quantizer. Finite density logarithmic quantizers for the multiple input case were designed in [67–70]. All the above references focussed on Linear Time Invariant (LTI) systems and, except for [63,64], the results were only developed for discrete time systems. While [63] designed an implicitly verified discrete-event controller, [64] studied the optimal periodic sampling time. The references [71, 72] utilized a Robust Control Lyapunov Function (RCLF) approach to characterize the coarsest quantizers for single input control affine nonlinear systems.

Systems with quantization can be viewed as switched systems [73], the switching surfaces being the boundaries of the quantization cells. In other words, a quantizer is a discrete-event encoder, whose output is the quantization state. The quan-

tization state evolves in a discrete set and the boundaries of the quantization cells determines the event-trigger. The complexity of the event-triggering condition is determined by the complexity of the shape of the quantization cells. An RCLF approach to quantization in nonlinear systems may lead to very complicated geometries (for example, see Equation (10) in [71]) and the event-triggering condition may be as computationally intensive, if not more, as the original control law.

Thus, we see that on the one hand, event-triggered control [14, 15, 19] assumes the availability of an infinite precision quantizer and on the other an RCLF quantizer assumes that the induced event-trigger is computationally inexpensive. Therefore, in the context of Cyber Physical Systems, there is a need to co-design the quantizer and the utility driven event-trigger for emulation based control.

4.1.1 Contributions

In this chapter, we exploit the common principle behind utility driven sampled data control and coarsest quantization (robustness to measurement errors) to design discrete-event controllers for semi-global asymptotic stabilization of general nonlinear systems. Specifically, we propose a methodology for co-designing the event-trigger and the quantizer in an emulation based controller. Although the resultant quantizer is not necessarily coarsest, it is however a finite density logarithmic quantizer and is easy to implement. The proposed algorithm produces an implicitly verified emulation based discrete-event controller that asymptotically stabilizes the origin with a specified arbitrary compact region of attraction. In the special case

that a certain Lipschitz constant holds globally, the origin of the closed loop system is globally asymptotically stable. In comparison to the coarsest quantization literature, our quantizer design holds for general multi-input nonlinear continuous time systems. Compared to [61, 62] we co-design the event-trigger and the static quantization, keeping in mind the applicability to control systems with low computational capabilities. Another important aspect of the proposed quantizer is the presence of hysteresis, which is utilized for guaranteeing a dwell time for the updates of the discrete event controller. A significant portion of the work in this chapter has been published in [31].

The rest of the chapter is organized as follows. Section 4.2 introduces the basic notation and states precisely the problem under study. The design of the event-trigger is discussed in Section 4.3 and the quantizer design is described in Section 4.4. An example of a two dimensional nonlinear system is provided in Section 4.5 and finally some concluding remarks are made in Section 4.6.

4.2 Problem statement

Note: The results in Sections 4.2 and 4.3 do not depend on a specific choice of a norm. However, the proposed quantizer design utilizes the max or the infinity norm. Therefore, we adopt this norm through out the chapter, and use the notation $|y|$ to denote the max norm, $||y||_\infty$, of a vector y.

Consider a nonlinear system of the form

$$\dot{x} = f(x, u),\ x \in \mathbb{R}^n,\ u \in \mathbb{R}^m \tag{4.1}$$

with feedback control $u = \kappa(x)$ that renders the origin of the closed loop system

$$\dot{x} = f(x, \kappa(x)) \tag{4.2}$$

globally asymptotically stable. Now, consider the problem of controlling the system with quantized state feedback, where the quantizer is static. A static quantizer can be modeled as a nonlinear function of the state. However, in this chapter we consider quantizers with hysteresis (hence memory). Thus, we define the quantizer function in a more general sense as follows.

Definition 4.1. *A quantizer is a function* $q : \mathbb{R}^n \times \Omega \longrightarrow \Omega$, *where* $\Omega = \{\omega^0, \omega^1, \omega^2, \dots\}$ *is a countable set, with* $\omega^k \in \mathbb{R}^n$ *for each* k *and* $\bigcup_{\omega^k \in \Omega} \{x \in \mathbb{R}^n : q(x, \omega^k) = \omega^k\} = \mathbb{R}^n$.

In this chapter ω^k are called the *generating points* and Ω is called the *generating set* (or the *set of generating points*) of the quantizer. The quantization density is defined as

Definition 4.2. *Quantization density: For* $0 < \epsilon \leq 1$, *let* $N(\epsilon)$ *be the number of elements* $\omega \in \Omega$ *such that* $\epsilon \leq |\omega| \leq 1/\epsilon$. *The quantization density of the quantizer* q *is defined as*

$$\eta_q = \limsup_{\epsilon \to 0} \frac{N(\epsilon)}{-2ln(\epsilon)}. \tag{4.3}$$

This definition is similar to the one in [64]. The presence of hysteresis in the quantization state x_q, and the interpretation of a quantizer as a discrete-event encoder necessitates the treatment of x_q as a state variable and the resultant closed loop system as a hybrid system. In this chapter, we adopt the notation and theory

described in [74] (and the references therein) to study this hybrid system. Let $\xi = [x; x_q] \in \mathbb{R}^n \times \Omega$ denote the state of the hybrid system (the notation $[x; x_q]$ denotes the concatenation of the vectors x and x_q). Then, the closed loop hybrid system may be expressed as

$$\dot{\xi} = F(\xi) := \begin{cases} \dot{x} = f(x, \kappa(x_q)) \\ \\ \dot{x}_q = 0 \end{cases} \quad , \quad \xi \in C \tag{4.4}$$

$$\xi^+ = G(\xi) := \begin{cases} x^+ = x \\ \\ x_q^+ = q(x, x_q) \end{cases} \quad , \quad \xi \in D \tag{4.5}$$

$$\mathcal{H} = (C, F, D, G) \tag{4.6}$$

where $C \subset \mathbb{R}^n \times \Omega$ and $D \subset \mathbb{R}^n \times \Omega$ are appropriately defined sets. The hybrid system $\mathcal{H}$ is the collection of the flow set, C, the flow map, F, the jump set, D, and the jump map, G. The quantizer is specified by the set Ω and the function $q(x, x_q)$. As is clear from our formulation, the updates of the quantized state information, x_q, are not periodic, unlike in [64]. Rather, the quantized state is updated whenever a state-dependent triggering condition is satisfied, that is when $\xi \in D$.

The event-trigger determines **when** the feedback is communicated and the control updated. The quantizer determines **what** is communicated. As discussed earlier, an efficient discrete event controller necessitates the co-design of the event-trigger and the quantizer. Therefore, the problem under consideration in this chapter is that of co-designing the event-trigger and the quantizer in emulation based controllers for semi-global asymptotic stability of general nonlinear systems. Specif-

ically, the problem is to design the sets Ω, C and D; and the quantizer function q such that both the event-trigger and the quantizer are efficient. In the next section, the design of the event-trigger (design of the sets C and D) is detailed.

4.3 Design of the Flow and the Jump Sets

The following are the main assumptions in the chapter.

(A4.1) The closed loop system (4.2) is input-to-state stable (ISS) with respect to measurement error, i.e., there exists a C^1 Lyapunov function, $V : \mathbb{R}^n \to \mathbb{R}$, that satisfies

$$\alpha_1(|x|) \leq V(x) \leq \alpha_2(|x|)$$
$$\frac{\partial V}{\partial x} f(x, \kappa(x+e)) \leq -\alpha(|x|), \quad \text{if } \gamma(|e|) \leq |x|$$

where $\alpha_1(.)$, $\alpha_2(.)$, $\alpha(.)$ and $\gamma(.)$ are class $\mathcal{K}_\infty$[1] functions.

(A4.2) The function γ is Lipschitz on compact sets.

It is actually sufficient to assume that the origin of the system (4.2) is asymptotically stable as opposed to the ISS assumption (A4.1). However, the ISS assumption keeps the exposition focused and simpler.

Expressing the measurement/quantization error as

$$e \triangleq x_q - x, \tag{4.7}$$

[1] A continuous function $\alpha : [0, \infty) \to [0, \infty)$ is said to belong to the class $\mathcal{K}_\infty$ if it is strictly increasing, $\alpha(0) = 0$ and $\alpha(r) \to \infty$ as $r \to \infty$ [45].

let us define the flow and the jump sets as

$$C = \{\xi \in \mathbb{R}^n \times \Omega : |e| \leq W|x|\} \tag{4.8}$$

$$D = \{\xi \in \mathbb{R}^n \times \Omega : |e| \geq W|x|\} \tag{4.9}$$

where W is a positive constant. The sets C and D capture a simple event-triggering condition. The stability aspects of the hybrid system (4.6) maybe studied through a hybrid Lyapunov function candidate [74], which is defined as follows.

Definition 4.3 (Lyapunov-function candidate)**.** *Given the hybrid system $\mathcal{H}$ with data (C, F, D, G) and the compact set $\mathcal{A} \subset \mathbb{R}^p$, the function $V_h : \ dom\ V_h \to \mathbb{R}$ is a Lyapunov-function candidate for $(\mathcal{H}, \mathcal{A})$ if (i) V_h is continous and nonnegative on $(C \cup D) \setminus \mathcal{A} \subset dom\ V_h$, (ii) V_h is continuously differentiable on an open set $\mathcal{O}$ satisfying $C \setminus \mathcal{A} \subset \mathcal{O} \subset dom\ V_h$, and (iii)* $\lim_{\{\xi \to \mathcal{A}, \xi \in (dom\ V_h) \cap (C \cup D)\}} V_h(\xi) = 0.$

For the hybrid system (4.6), let

$$\mathcal{A} \triangleq \{\xi \in \mathbb{R}^n \times \Omega : x = x_q = 0\} \tag{4.10}$$

and define the hybrid Lyapunov function candidate for the pair $(\mathcal{H}, \mathcal{A})$ as

$$V_h(\xi) = V(x) + \max\{0, |x_q - x| - 2W|x|\} \tag{4.11}$$

where V is given by (A4.1). Notice that $V_h(\xi) = V(x)$ for all $\xi \in C$. The function $V_h(\xi)$ is positive definite and its sub-level sets are compact. Also note that $\langle \nabla V_h(\xi), F(\xi) \rangle = \dfrac{\partial V}{\partial x} f(x, \kappa(x_q))$ for all $\xi \in C \setminus \mathcal{A}$ and in an open neighborhood of $C \setminus \mathcal{A}$.

4.3.1 Selection of W

Let

$$B_r = \{x \in \mathbb{R}^n : |x| \leq r\}. \tag{4.12}$$

$$E_r = \{\xi \in \mathbb{R}^n \times \Omega : |x| \leq r,\ |x_q| \leq r\}. \tag{4.13}$$

Note that for each r finite, B_r and E_r are compact sets in $\mathbb{R}^n$ and $\mathbb{R}^n \times \Omega$, respectively. For each $\mu \geq 0$ define

$$\mathcal{R} \triangleq \{\xi : \mathbb{R}^n \times \Omega : V(x) \leq \mu,\ |x_q| \leq R \triangleq \alpha_1^{-1}(\mu)\} \tag{4.14}$$

where $\alpha_1(.)$ is the function from assumption (A4.1). Then, it is clear that $\mathcal{R} \subset E_R$. For each compact set $\mathcal{B}$ that contains the origin, there is a $\mu \geq 0$ such that $\mathcal{B} \subset \mathcal{R}$. Therefore, without loss of generality it is assumed that the prescribed region of attraction is of the form (4.14). If assumption (A4.2) holds, then there exists a constant $W_R > 0$ such that

$$W_R|x| \leq \gamma^{-1}(|x|), \quad \forall x \in B_R \tag{4.15}$$

The design of the flow and the jump sets is complete if we specify how the constant W is to be chosen. The following Lemma provides a methodology for accomplishing this goal.

Lemma 4.1. *Consider the hybrid system (4.6) with C and D defined as in (4.8)-(4.9). Suppose assumptions (A4.1) and (A4.2) hold. Let the desired region of attraction be $\mathcal{R}$, (4.14), for some $\mu \geq 0$. If $W \leq W_R$ then*

$$\langle \nabla V_h(\xi), F(\xi) \rangle < 0,\ \forall \xi \in C \cap \mathcal{R} \setminus \mathcal{A} \tag{4.16}$$

Proof. By the definition of W_R and the fact that $W \leq W_R$, it follows that

$$W|x| \leq W_R|x| \leq \gamma^{-1}(|x|), \quad \forall x \in B_R$$

Recall the definition of the flow set C, (4.8). Also, $\mathcal{R}$ is a subset of E_R, (4.13). Therefore, $(C \cap \mathcal{R}) \subset \{\xi \in \mathbb{R}^n \times \Omega : |e| \leq \gamma^{-1}(|x|)\}$ and assumption (A4.1) immediately implies that (4.16) is true. □

Remark 4.1. *If the function γ is globally Lipschitz, then (4.16) holds for all $\xi \in C \setminus \mathcal{A}$ and not just for $\xi \in (C \cap \mathcal{R}) \setminus \mathcal{A}$.*

If $W_R \geq 1$ then quantization is not required and a constant control $u \equiv \kappa(0)$ asymptotically stabilizes the origin of the nonlinear system (4.1). This is made more precise in the following proposition and the subsequent discussion.

Proposition 4.1. *Consider the hybrid system (4.6) with C and D defined as in (4.8)-(4.9). If $W_R \geq W > 1$ and $\Omega = \{0\}$, then the set $\mathcal{A}$, (4.10), is asymptotically stable with $\mathcal{R}$ included in the region of attraction.*

Proof. The set $(D \cap \mathcal{R}) = \{x \in \mathbb{R}^n \times \{0\} : |x - 0| \geq W|x|\} \cap \mathcal{R} = \emptyset$, the empty set. On the other hand, $(C \cap \mathcal{R}) = \{x \in \mathbb{R}^n \times \{0\} : |x - 0| \leq W|x|\} \cap \mathcal{R} = \mathcal{R}$. Lemma 4.1 then implies that the set $\mathcal{A}$ is asymptotically stable with $\mathcal{R}$ included in the region of attraction. □

If $W_R \geq W > 1$ and $\Omega = \{0\}$, then the set D is empty. Thus, the hybrid system (4.6) is really just the continuous time system (4.4) with $x_q \equiv 0$. If $W_R \geq W = 1$ and $\Omega = \{0\}$, then $(C \cap \mathcal{R}) = (D \cap \mathcal{R}) = \mathcal{R}$ and there can be jumps in the solutions of $\mathcal{H}$, (4.6). However, the jump map is the identity map, $x^+ = x$ and $x_q^+ = x_q = 0$. Since

the jump map is induced by the controller and is not inherent in the system, the identity jump map can be ignored by the controller and we can focus only on purely flowing solutions that start in $\mathcal{R} \setminus \mathcal{A}$. All such solutions asymptotically converge to the set $\mathcal{A}$.

Therefore, in the sequel we assume that $W = W_R < 1$ unless specifically mentioned otherwise. In the next section the design process of the quantizer is detailed.

4.4 Design of The Quantizer

Now, all that is left to be designed is the quantizer. Our goal here is the following. Given an event-trigger, (4.8)-(4.9), satisfying Lemma 4.1, design an efficient quantizer that semi-globally asymptotically stabilizes the origin of the system with a prescribed compact region of attraction.

In the coarsest quantizer literature, robustness to measurement errors is exploited to design finite density logarithmic quantizers and in single input LTI systems the coarsest quantizer. The quantizer in this chapter also utilizes the same principle, although indirectly through the simplified event triggering condition designed in Section 4.3. In our opinion, this approach is better suited for continuous time nonlinear systems for two reasons. Considering general nonlinear systems, the set $\{x \in \mathbb{R}^n : \frac{\partial V}{\partial x} f(x, \kappa(x_q)) < 0\}$ for an arbitrary x_q can have a complicated shape. This can potentially lead to a complex design process, that requires significant customization for individual systems. The second drawback is that of implementation

- checking, in real time, whether the state belongs to a particular quantization cell can be as intensive, if not more, as computing the control itself. This defeats our motivation of designing controllers that require low rate of communication and low computation capabilities.

The proposed quantizer design is much simpler and applicable to a wide range of nonlinear systems. The chief features of the proposed quantizer design are as follows. The quantization cells are determined by the simplified triggering condition, (4.8)-(4.9). In the triggering condition, the *max or the infinity norm* is used, leading to a very easily implementable triggering condition and quantizer. The quantization cells are allowed to be overlapped, and the resulting hysteresis is utilized to avoid chattering of the controller.

Definition 4.4. *For each* $k \in \{0, 1, 2, \ldots\}$*, the quantization cell generated by* ω^k *is the set* $C^k = \{x \in \mathbb{R}^n : q(x, \omega^k) = \omega^k\}$.

In the hybrid system (4.6), x_q changes only during jumps. In order to minimize the number of control updates or jumps, it is necessary to ensure that at each jump the state is mapped outside the jump set D, or more precisely, it is required that

$$\xi^+ = G(\xi) \in (C \setminus D) \cap E_R, \quad \forall \xi \in (D \cap E_R) \setminus \mathcal{A} \tag{4.17}$$

However, x does not change during jumps, and $x_q^+ = q(x, x_q)$. Hence, the quantizer needs to be designed such that $x_q^+ \neq x_q$. Therefore, by the definition of a quantization cell it is necessary that $\left(C^k \times \{\omega^k\}\right) \cap (D \cap E_R) \setminus \mathcal{A} = \emptyset$ for each $k \in \{0, 1, 2, \ldots\}$.

In other words, the quantizer must be defined such that for each $k \in \{0, 1, 2, \ldots\}$

$$\left(C^k \times \{\omega^k\}\right) \cap (C \cap E_R) = (C^k \times \{\omega^k\}) \cap E_R \tag{4.18}$$

Finally, $\mathcal{A} \subset C$, $\mathcal{A} \subset D$ and $\mathcal{A} \cap C^k = \emptyset$ if $\omega^k \neq 0$. Hence, it is necessary to choose $\omega^0 = 0$. Therefore, the quantizer has to satisfy the following constraints.

$$\omega^k \in \mathbb{R}^n \text{ and } |\omega^k| \leq R,\ k \in \{1, 2, \ldots\} \tag{4.19}$$

$$C^k = \{x \in \mathbb{R}^n : |\omega^k - x| < W_R|x|\},\ k \in \{1, 2, \ldots\} \tag{4.20}$$

$$\omega^0 = 0 \tag{4.21}$$

$$C^0 = \{0\} \cup \{x \in \mathbb{R}^n : |x| > R\} \tag{4.22}$$

$$C^0 \cup \left(\bigcup_{k=1}^{k=\infty} \overline{C_\rho^k} \right) = \mathbb{R}^n, \quad 0 < \rho < 1 \tag{4.23}$$

where $C_\rho^k = \{x \in \mathbb{R}^n : |\omega^k - x| \leq \rho W_R|x|\}$ and $\overline{C_\rho^k}$ denotes the closure of the set C_ρ^k. Note that $C_\rho^k \subset C^k$ for each k. The constraint (4.23) has been introduced so that the resultant quantizer is over designed and the quantization cells overlap. In other words, the final constraint induces hysteresis in the quantizer, which is useful for avoiding chattering. Moreover, excluding C^0, each cell C^k is such that in the region where C^k overlaps with no other cell, $|\omega^k - x| \leq \rho W_R|x|$. Next, notice that the cell C^0 includes the region outside B_R. Any arbitrary nominal value could have been chosen as the quantization state for the region outside B_R, and we have selected it to be 0.

We define the quantizer function as follows.

$$q(x,\omega^k) = \begin{cases} \omega^k, & \text{if } x \in C^k \\ \underset{\omega^j}{\operatorname{argmin}} \dfrac{|\omega^j - x|}{W_R|x|}, & \text{if } x \notin C^k,\ x \neq 0 \\ \omega^0, & \text{if } x = 0 \end{cases} \tag{4.24}$$

In the second case there can be more than one solution. Note that the quantizer function satisfies (4.17).

The following theorem demonstrates that a quantizer that satisfies (4.19)-(4.24) asymptotically stabilizes the set $\mathcal{A}$ with $\mathcal{R}$ in the region of attraction.

Theorem 4.2. *Consider the hybrid system* (4.6) *with* C *and* D *defined as in* (4.8)-(4.9)*, and suppose assumptions* (A4.1) *and* (A4.2) *hold. Let the desired region of attraction be* $\mathcal{R}$*,* (4.14)*, for some* $\mu \geq 0$*. Suppose that* $W \leq W_R$ *and that the quantizer is designed to satisfy* (4.19)-(4.24)*. Then, the set* $\mathcal{A}$ *is asymptotically stable and the region of attraction includes* $\mathcal{R}$*.*

Proof. The compact set $\mathcal{R} \subset E_R$, where $R = \alpha_1^{-1}(\mu)$. The function V_h in (4.11) is a hybrid Lyapunov candidate function for the pair $(\mathcal{H}, \mathcal{A})$. Consider the event-trigger (the sets C and D) designed in (4.8)-(4.9). Given a quantizer that satisfies (4.19)-(4.24), the following hold.

$$\langle \nabla V_h(\xi), F(\xi) \rangle < 0,\ \forall\, \xi \in C \cap \mathcal{R} \setminus \mathcal{A}$$

$$V_h(G(\xi)) - V_h(\xi) \leq 0,\ \forall\, \xi \in D \cap \mathcal{R} \setminus \mathcal{A}$$

where the first relation follows from Lemma 4.1, and the second from the fact that the quantizer function q ensures satisfiability of (4.17). Hence, for every $c > 0$ no

complete solution remains in the compact set $\{\xi \in \mathbb{R}^n \times \Omega : V_h(\xi) = c\} \cap \mathcal{R}$. Recall the definition of $\mathcal{R}$, (4.14). The function $V(x)$ decreases monotonously during flows and does not change during jumps. The constraints (4.19) and (4.21) imply that $|x_q| \leq R$ at all times. Hence, $\mathcal{R}$ is forward-invariant[2] and every maximal solution that starts in $\mathcal{R}$ is a complete solution. Therefore, Theorem 23 in [74] implies that the set $\mathcal{A}$ is asymptotically stable and the region of attraction includes the set $\mathcal{R}$. □

Corollary 4.1. *Suppose in addition to assumptions (A4.1), (A4.2) the functions f and κ are Lipschitz on compact sets. Then, there exists a constant $\tau_d > 0$ such that for all solutions starting in $\mathcal{R} \setminus \mathcal{A}$ the jumps are separated by at least an amount of time τ_d.*

Proof. Outside the set $\mathcal{A}$, $x_q^+ \neq x_q$ and x_q^+ is given by the second case of (4.24). Further, (4.23) implies that after a jump $x \in \overline{C_\rho^k}$, where k is such that $x_q^+ = \omega^k$. Therefore, $|x_q^+ - x|/(W_R|x|) \leq \rho < 1$. The rest of the proof follows from an analysis similar to that in [14]. □

In Theorem 4.2, the set $\mathcal{A}$ is globally asymptotically stable if W_R is a global constant. Notice that in event-triggered control, the measurement error is reset to zero at triggering instants. However, in the proposed discrete-event controller $|x_q^+ - x| \neq 0$ and instead satisfies $|x_q^+ - x| \leq \rho W|x|$, which is not zero in general. This is the reason why hysteresis is required in the quantizer, to avoid chattering.

Next, we demonstrate that a quantizer satisfying (4.19)-(4.24) indeed exists,

[2]See [74] for the definitions of the terms 'forward invariance', 'maximal solution' and 'complete solution'.

and construct a minimal set of generating points Ω that satisfy (4.19)-(4.23). For the sake of clarity, we first outline the design process for $n = 1$, that is, for nonlinear systems (4.2) that are one dimensional.

4.4.1 Design of Ω in One Dimensional Systems

Now, we invert the problem and ask: given a point in the region of interest what are the values ω^k, (4.19), can take such that C^k, (4.20), contains that point. If the point is 0 then it is contained in C^0. Also, all cells other than C^0 are intervals. Therefore, we ask the more specific question: given $r_k^u \neq 0$ such that $|r_k^u| \leq R$, what should ω^k be such that $|\omega^k| \leq |r_k^u|$ and $|\omega^k - r_k^u| = \rho W_R |r_k^u|$, where $0 < \rho < 1$ is a constant. Thus, r_k^u is the upper or the outer extreme of the interval C_ρ^k (see Figure 4.1) and ρ is a parameter that allows us to over-design. The inverse problem has the unique solution

$$\omega^k = (1 - \rho W_R) r_k^u \tag{4.25}$$

Then the inner or lower extreme of the interval C_ρ^k is

$$r_k^l = \frac{\omega^k}{1 + \rho W_R} \tag{4.26}$$

Therefore, the interval C_ρ^k is the open interval (r_k^l, r_k^u) or (r_k^u, r_k^l) depending on whether r_k^u is positive or negative, respectively. The points r_k^u and r_k^l are in the set C^k (see Figure 4.1). If we now set $r_{k+2}^u = r_k^l$ then we can recursively determine the

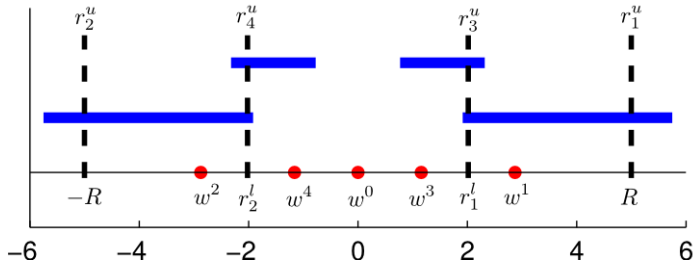

Figure 4.1: Design of Ω for 1-D systems. The blue lines indicate the actual quantization cells or intervals, while r_k^u and r_k^l indicate the extremities of the over-designed quantization cells $\overline{C_\rho^k}$.

set Ω. Following this procedure, we arrive at the following

$$\begin{aligned}
&\omega^0 = 0, \quad r_1^u = R, \quad r_2^u = -R \\
&\omega^k = (1 - \rho W_R) r_k^u, \quad \forall k \in \{1, 2, \ldots\} \\
&r_k^l = \frac{\omega^k}{1 + \rho W_R}, \quad \forall k \in \{1, 2, \ldots\} \\
&r_{k+2}^u = r_k^l, \quad \forall k \in \{1, 2, \ldots\} \\
&\omega^{k+2} = \frac{1 - \rho W_R}{1 + \rho W_R} \omega^k, \quad \forall k \in \{1, 2, \ldots\}
\end{aligned} \tag{4.27}$$

Note the symmetry in the positive and negative generators ω^k. Simple calculations give the quantization density as

$$\eta_q = \frac{2}{\ln\left(\frac{(1+\rho W_R)}{(1-\rho W_R)}\right)} \tag{4.28}$$

Thus, the proposed quantizer is a finite density logarithmic quantizer. The design process is summarized in Figure 4.1.

4.4.2 Design of Ω in Two Dimensional Systems

The design process for two dimensional systems is based on that of one dimensional systems, though there are also some significant differences. In 1-D systems there is only one type of cell (other than C^0). In 2-D systems, there is a larger variety of cells. More specifically, in 2-D systems there are three types of cells, other than C^0. These are shown in Figure 4.2. The state variable x is the vector $[x_1; x_2]$. The χ_1 and χ_2 axes are the lines $x_1 = x_2$ and $x_1 = -x_2$, respectively. Type 1 cells are the ones that lie completely within one of the quadrants of the χ_1-χ_2 axes. Type 2 cells are the ones whose generators lie on either χ_1 or χ_2 axis. Type 3 cells are those whose generators do not lie on the χ_1-χ_2 axes and yet the cell lies in more than one of χ_1-χ_2 quadrants.

To describe the different types of cells algebraically, let us define *Type 1 blocks* as (for arbitrary n)

$$S_i(\omega) \triangleq \{x \in \mathbb{R}^n : |\omega - x| < \rho W_R |x_i|\},\ i \in \{1, 2, \ldots, n\}$$

Every cell C_ρ^k is the union of the n Type 1 blocks

$$C_\rho^k = \bigcup_{i=1}^{n} S_i(\omega^k)$$

A cell C_ρ^k is of Type 1 if and only if it satisfies

$$C_\rho^k = S_i(\omega^k),\ \text{for some } i \in \{1, 2, \ldots, n\} \tag{4.29}$$

A cell $\overline{C_\rho^k}$ is of Type 2 if $|\omega^1| = |\omega^2| = \ldots = |\omega^n|$. A Type 3 cell is one that is neither of Type 1 nor Type 2. However, Type 3 cells can be approximated by

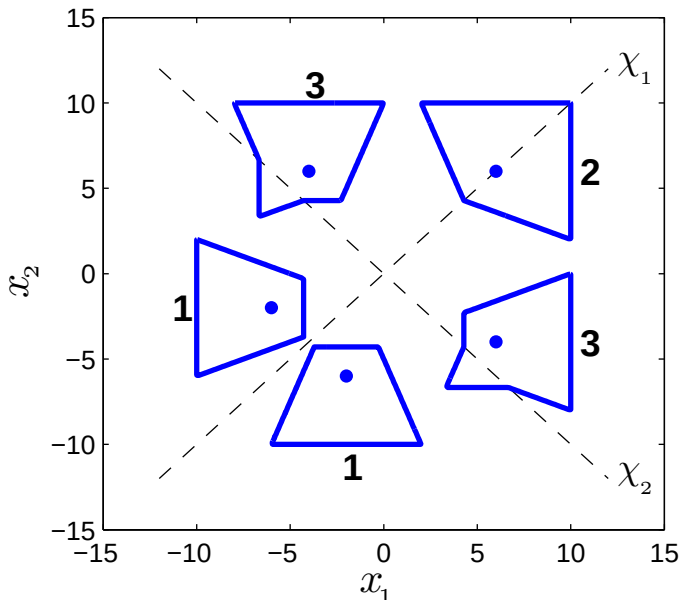

Figure 4.2: Possible types of cells in 2-D systems, excluding C^0. The dots are the generators of the quantization cells, whose boundaries are represented by the polygons.

appropriate Type 1 blocks, which have the same shape as Type 1 cells. Note that similar statements hold for the quantization cells C^k with $\rho = 1$.

Figure 4.3 shows the geometry of Type 1 cells, C^k_ρ. They have two parallel sides, which are in turn parallel to either x_1 or x_2 axes. Each cell is completely determined by the lengths a and b, which are given as

$$a = \frac{\rho W_R}{(1-\rho W_R)}|\omega^k|, \quad b = \frac{\rho W_R}{(1+\rho W_R)}|\omega^k|$$

Note that a and b depend only on $|\omega^k|$. Also, the magnitude of the slope of the non-parallel sides is equal to ρW_R, which is independent of ω^k. The two parallel sides of the of the cell are at $|\omega^k| + a$ and $|\omega^k| - b$ distances away from the origin.

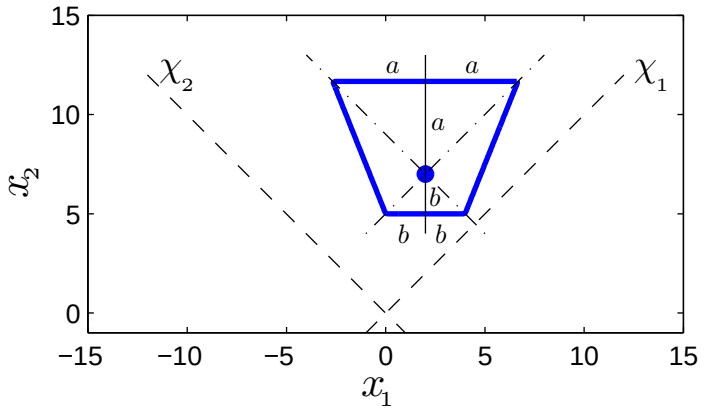

Figure 4.3: Geometry of Type 1 cells.

That is, the cell is part of an annulus (in the max norm sense) whose outer radius is $|\omega^k| + a$ and inner radius is $|\omega^k| - b$.

The information about the geometry can be used to solve the inverse problem: given the outer radius of the cell what should $|\omega^k|$ be? The solution is of course given by (4.27) with r_k^u, r_k^l and ω^k interpreted as the outer radius, the inner radius and $|\omega^k|$, respectively. Using these facts we design the quantization cells with Type 1, Type 2 cells and Type 1 approximation of Type 3 cells. The algorithm progresses in stages by covering recursively one annulus after another with quantization cells. The process of determining these annuli is similar to the 1-D case, with the difference that the procedure (4.27) now gives the inner and outer radii (in the max norm sense) of the overlapping annuli, Figure 4.4.

The design process is summarized in Figure 4.5. Figures 4.5(a) and 4.5(b) demonstrate the process to cover an annulus of a given outer radius. The outer radius of the annulus determines the radius at which the generators need to lie

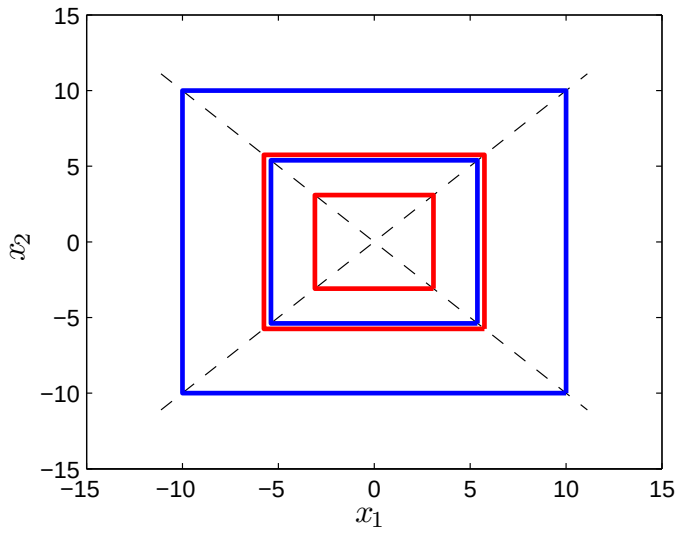

Figure 4.4: In the first stage of the design process, annuli are selected in a process analogous to (4.27) and Figure 4.1. The inner and outer boundaries of the first annulus are shown in blue, while those of the second annulus are shown in red.

according to the appropriate interpretation of (4.27). The generators are stacked equidistantly on a line to completely cover a quadrant of the annulus with the constraint that there be a generator on χ_1 and χ_2 axes. The process is repeated to cover each quadrant of the annulus. Then, the inner radius of the of the so covered annulus determines the outer radius of the next annulus. This process recursively designs the Ω set completely.

Simple calculations yield that

$$\text{Number of cells in an annulus } = 4\left\lceil \frac{1+\rho W_R}{\rho W_R} \right\rceil \tag{4.30}$$

where $\lceil . \rceil$ denotes the greatest integer function. Note that this number is independent of the outer or inner radius of the annulus. Of course the number of annuli required to cover a region is given by a number that is the same as in 1-D systems.

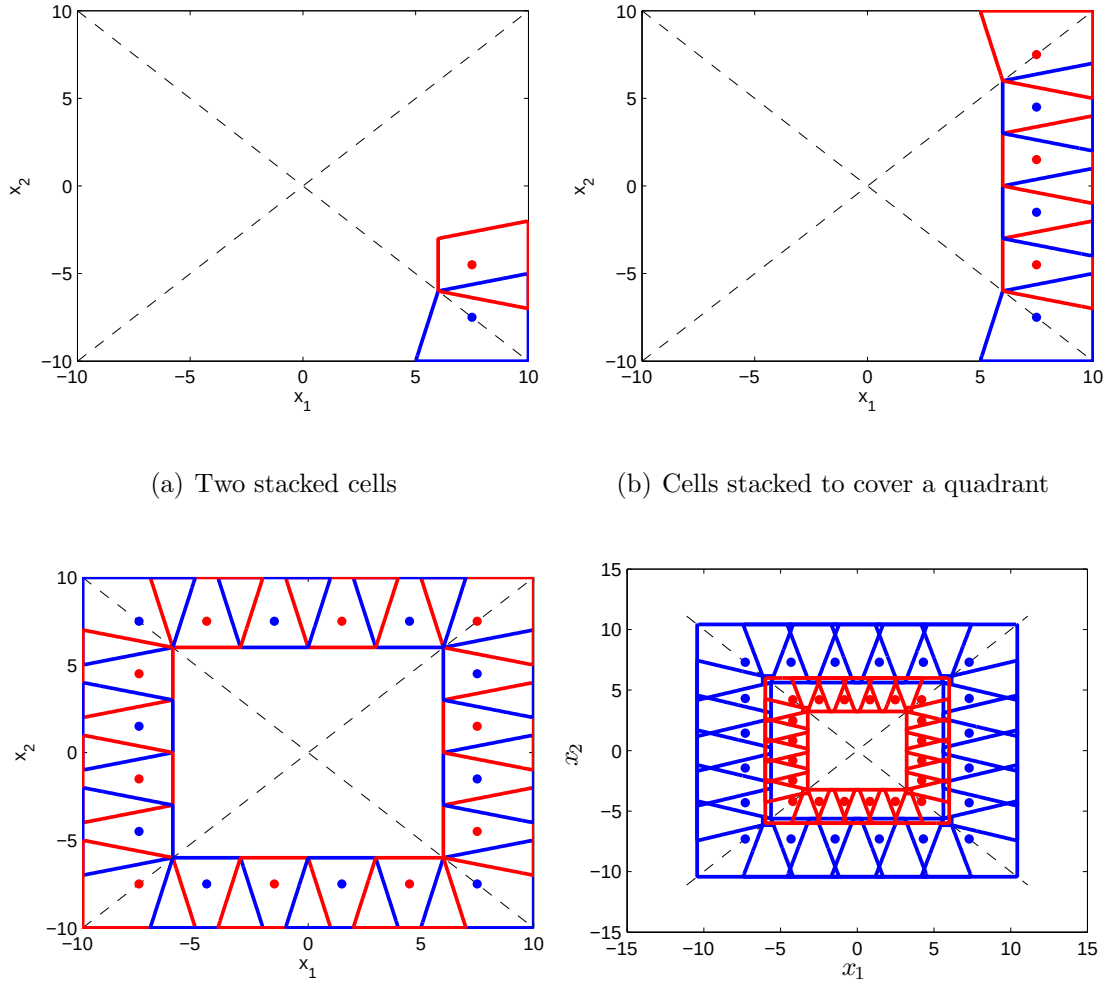

(a) Two stacked cells

(b) Cells stacked to cover a quadrant

(c) Annulus of a given outer radius

(d) Inner radius of the first annulus is the outer radius of the next one

Figure 4.5: Fig. 4.5(a) and Fig. 4.5(b) demonstrate the steps in covering an annulus. The dots indicate the generators of the quantization cells. Fig. 4.5(c) and Fig. 4.5(d) show that the procedure leads to a logarithmic quantizer in two dimensions.

Thus the quantization density in 2-D systems is

$$\eta_q = 4\left\lceil \frac{1+\rho W_R}{\rho W_R} \right\rceil \frac{1}{\ln\left(\frac{(1+\rho W_R)}{(1-\rho W_R)}\right)} \tag{4.31}$$

Hence, again the designed quantizer is a finite density logarithmic quantizer.

4.4.3 Design of Ω in n Dimensional Systems

The design in higher dimensional systems is similar to the two stage process for 2-D systems. In the first stage, an annulus of a given outer radius is covered and then the outer radius is updated, thus yielding Ω recursively. As in the 2-D case there are three main types of cells. Type 1 and Type 2 cells are similar to those in the 2-D case. However, Type 3 cells can be classified into multiple sub-types thus giving rise to much richer design options. In this chapter, we do not however investigate them further. We propose a direct adaptation of the 2-D case, that is using Type 1 approximation of Type 3 cells. This process gives the quantization density as

$$\eta_q = 2n \left\lceil \frac{1+\rho W_R}{\rho W_R} \right\rceil^{n-1} \frac{1}{\ln\left(\frac{(1+\rho W_R)}{(1-\rho W_R)}\right)} \tag{4.32}$$

This is a finite density logarithmic quantizer. However, it is very inefficient as the density grows exponentially with the dimension of the system. Hence, efficient design in higher dimensions is a topic of future research.

4.5 Example

In this section, the proposed emulation based controller is illustrated through an example. Consider the second order nonlinear system

$$\begin{aligned} \dot{x}_1 &= x_2 \\ \dot{x}_2 &= \frac{1}{l}(g\sin(x_1) + u). \end{aligned} \tag{4.33}$$

Let the control input be given as

$$u = \kappa(x) = -l\lambda x_2 - g\sin(x_1) - K(x_2 + \lambda x_1). \tag{4.34}$$

where $K > 0$ and $\lambda > 0$. Let the Lyapunov function in assumptions (A4.1) be

$$V(x) = \frac{l}{2}(x_2 + \lambda x_1)^2 + \lambda K x_1^2. \tag{4.35}$$

Routine calculations yield

$$\frac{\partial V}{\partial x} f(x, \kappa(x+e)) \leq -\alpha_3(|x|) + L\beta(|x|)|e| \tag{4.36}$$

where

$$\alpha_3(|x|) = \min(K, K\lambda^2)|x|^2$$

$$\beta(|x|) = \sqrt{2}\sqrt{\lambda^2+1}|x|$$

$$L = \sqrt{2}\sqrt{(\lambda K + g)^2 + (K + \lambda l)^2}$$

Let us choose the constant W in the sets C and D as

$$W = W_r = \frac{\sigma \min\{K, K\lambda^2\}}{L\sqrt{2}\sqrt{\lambda^2+1}}, \quad 0 < \sigma < 1$$

Then, it is clear that if $|e| \leq W|x|$ then

$$\frac{\partial V}{\partial x} f(x, \kappa(x+e)) \leq -(1-\sigma)\alpha_3(|x|) = \alpha(|x|)$$

that is assumption (A4.1) is satisfied. Further, since W_r is a global constant (independent of r), the discrete-event controller guarantees global asymptotic stability of the set $\mathcal{A}$ in the hybrid system $\mathcal{H}$, (4.6).

The quantizer designed as in Section 4.4 with $\sigma = 0.99$ and $\rho = 0.9$ has a density ≈ 2582. Figure 4.6 shows the evolution of $|x|$ and $|e|/W$ for a sample trajectory. In the simulations the parameters g, l, K and λ were chosen as 10, 0.2, 1 and 1, respectively, from which $W = 0.0447$ is obtained. The number of jumps or

equivalently the number of control updates was observed to be 165 in the simulated time, giving an average update frequency of 33Hz. The minimum inter-update time was observed to be 0.0011s.

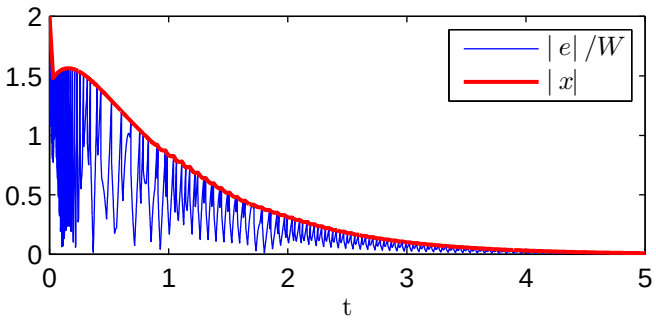

Figure 4.6: Evolution of $|x|$ and $|e|/W$.

4.6 Discussion and Conclusions

This chapter revisits the problem of control under data-rate constraints. Specifically, we have combined the ideas of event-triggered control and coarsest quantization to propose a method for co-designing the event-trigger and the quantizer in emulation based controllers for stabilization tasks. The resulting quantizer is a finite density logarithmic quantizer, applicable to general multi-input and multi-dimensional continuous-time nonlinear systems. To the best of our knowledge, this work is the first to look at the co-design of the event-trigger and the quantizer in emulation based discrete-event controllers. The proposed design algorithm results in a controller that guarantees semi-global asymptotic stability of the origin of the system with a specified arbitrary compact region of attraction. In case a certain Lipschitz

constant is global, the origin is globally asymptotically stable. If only semi-global practical stability is desired, with any specified compact region of attraction and ultimate bound, the quantizer has a finite number of cells. This makes the sensing and control system very simple, and by storing the control values for each cell in memory, the control response can be made significantly faster.

Several extensions are possible, such as treating W itself as a state, that is updated during the jumps along with the quantized state. In the quantizer design process, W_R need not be held fixed. Instead, for each annulus R and hence W_R can be appropriately re-defined. This is possible only in nonlinear systems, and it will lead to lower density quantizers than otherwise. Some future directions of research are the use of coordinate transformations as pre and post processing stages for lower density quantizers, and improvements to the design process in three and higher dimensions. Finally, as mentioned in Section 4.3, the proposed design easily extends to a case with a weaker assumption than the ISS one.

Part III

Utility Driven Event-Triggering for Trajectory Tracking

Chapter 5

Utility Driven Sampled Data Control for Trajectory Tracking

5.1 Introduction

In this chapter, we investigate an event triggered control algorithm for trajectory tracking. Tracking a time varying trajectory or even a set-point is of tremendous practical importance in many control applications. In these applications, the goal is to make the state of the system follow a reference or desired trajectory, which is usually specified as an exogenous input to the system. In this chapter, the reference trajectory is generated by a reference system. The majority of the previous works in the event-triggered control literature assumed a state feedback control strategy with no exogenous input, some exceptions being [12, 15, 18, 19, 21, 41, 75], where unknown disturbances appear as exogenous inputs. However, in this chapter, we consider exogenous inputs that are available to the controller through measurements, namely the reference trajectory and the input to the reference system.

5.1.1 Contributions

The main contribution of this chapter is the design of event-triggered controllers for trajectory tracking in nonlinear systems, which is a special case of nonlinear systems with exogenous inputs. It is assumed that the reference trajectory and the exogenous input to the reference system are uniformly bounded. Given a nonlinear system and

a continuous-time controller that ensures global uniform asymptotic tracking of the desired trajectory, the proposed algorithm provides an event based controller that guarantees uniform ultimate boundedness of the tracking error and ensures that the inter-event times of the controller are bounded away from zero. In the special case that the derivative of the exogenous input to the reference system is also uniformly bounded, an arbitrarily small ultimate bound for the tracking error can be designed. In this chapter, unlike in the event-triggered control literature, the continuous-time control law is assumed to render the closed loop system asymptotically stable rather than ISS with respect to measurement errors. Although on compact sets the latter condition can be arrived at from the former, our choice allows a direct and clear procedure for designing an event-triggering condition with time-varying components that results in fewer controller updates. The results in this chapter for nonlinear systems have appeared in [32, 33].

The rest of the chapter is organized as follows. In Section 5.2 we set up the problem and introduce the notation used in the chapter. Subsequently, in Section 5.3, the basic design procedure is highlighted for the special case of linear systems. Then in Section 5.4 the general case of nonlinear systems is addressed and results for three different classes of reference trajectories are presented. The theoretical results in the chapter are illustrated through numerical simulations of a second order nonlinear system in Section 5.5. Finally, the results are summarized in Section 5.6.

5.2 Problem statement and notation

Consider a nonlinear system of the form

$$\dot{x} = f(x, u), \quad x \in \mathbb{R}^n,\ u \in \mathbb{R}^m \tag{5.1}$$

which has to track a reference trajectory defined implicitly by the dynamical system

$$\dot{x}_d = f_r(x_d, v), \quad x_d \in \mathbb{R}^n,\ v \in \mathbb{R}^q \tag{5.2}$$

where the external signal v and the initial condition of the signal x_d determine the specific reference trajectory. Let the tracking error be defined as $\tilde{x} \triangleq x - x_d$. In general, a controller for tracking a reference trajectory depends on both the tracking error as well as the reference trajectory. Hence, we assume that the control signal is of the form

$$u = \gamma(\xi), \quad \text{where} \quad \xi \triangleq [\tilde{x}; x_d; v] \tag{5.3}$$

where the notation $[a_1; a_2; a_3]$ denotes the column vector formed by the concatenation of the vectors a_1, a_2 and a_3. Consequently, the closed loop system that describes the tracking error is given as

$$\dot{\tilde{x}} = f(\tilde{x} + x_d, \gamma(\xi)) - \dot{x}_d. \tag{5.4}$$

Now, consider a controller that updates the control only intermittently and not continuously in time. Let t_i for $i = 0, 1, 2, \ldots$ be the time instants at which the control is computed and updated. Then, the tracking error evolves as

$$\dot{\tilde{x}} = f\big(\tilde{x} + x_d, \gamma(\xi(t_i))\big) - \dot{x}_d, \quad \text{for } t \in [t_i, t_{i+1}). \tag{5.5}$$

The above dynamical system can also be viewed as a continuously updated control system, albeit with an error in the measurement of the state and the exogenous input. By defining the measurement error as

$$e \triangleq \begin{bmatrix} \tilde{x}_e \\ x_{d,e} \\ v_e \end{bmatrix} \triangleq \xi(t_i) - \xi \triangleq \begin{bmatrix} \tilde{x}(t_i) - \tilde{x} \\ x_d(t_i) - x_d \\ v(t_i) - v \end{bmatrix}, \ t \in [t_i, t_{i+1}) \tag{5.6}$$

the system in (5.5) can be rewritten as

$$\dot{\tilde{x}} = \big[f(\tilde{x} + x_d, \gamma(\xi)) - \dot{x}_d\big] + \big[f(\tilde{x} + x_d, \gamma(\xi + e)) - f(\tilde{x} + x_d, \gamma(\xi))\big] \tag{5.7}$$

where we have expressed the above system as a perturbed version of the dynamical system (5.4).

Our objective is to develop an event based controller for tracking a trajectory within a desired ultimate bound. To this end, we assume that when the control is updated continuously in time, the state x tracks the desired trajectory asymptotically, that is, there exists γ such that system (5.4) satisfies $\tilde{x} \to 0$ as $t \to \infty$. Then a utility driven event-triggered trajectory tracking control mechanism is proposed that (i) guarantees the tracking error to be uniformly ultimately bounded (within a desired bound), and (ii) ensures a positive lower bound for control update times.

5.3 Linear Systems

Before we address the problem for general nonlinear systems, we first describe the design procedure for linear systems. Thus, the plant and the reference system are

given by

$$\dot{x} = Ax + Bu, \quad x \in \mathbb{R}^n, \quad u \in \mathbb{R}^m \tag{5.8}$$

$$\dot{x}_d = A_r x_d + B_r v, \quad x_d \in \mathbb{R}^n, \ v \in \mathbb{R}^q \tag{5.9}$$

where A, B, A_r and B_r are matrices of appropriate dimensions. Letting $\tilde{x} \triangleq x - x_d$ and $\xi \triangleq [\tilde{x}; x_d; v]$, we assume that the control signal is of the form

$$u = G\xi = G_{\tilde{x}}\tilde{x} + G_{x_d}x_d + G_v v \tag{5.10}$$

where $G \in \mathbb{R}^m \times \mathbb{R}^{2n+q}$ is a matrix while $G_{\tilde{x}}$, G_{x_d} and G_v are appropriately defined block matrices of G. In the sequel, each of the two forms is used depending on the requirement. As a result, the closed loop system that describes the tracking error is given as

$$\dot{\tilde{x}} = A\tilde{x} + BG\xi + (A - A_r)x_d - B_r v. \tag{5.11}$$

Then, the sampled data control system in terms of the measurement error, (5.6), is given as

$$\dot{\tilde{x}} = \left[A\tilde{x} + BG\xi + (A - A_r)x_d - B_r v\right] + BGe. \tag{5.12}$$

Now, we state the main assumption that the continuous-time control law renders the origin of the closed loop system, (5.11), globally asymptotically stable.

(A5.1) Suppose $[\tilde{x}; x_d; v] \equiv 0$ is an equilibrium solution for the dynamical system in (5.4). Further, suppose that there exists a quadratic Lyapunov function, $V = \tilde{x}^T P \tilde{x}$, where P is a symmetric positive definite matrix, such that for all

admissible x_d and v,

$$a_1\|\tilde{x}\|^2 \leq V(\tilde{x}) \leq a_2\|\tilde{x}\|^2 \tag{5.13}$$

$$2\tilde{x}^T P\big[A\tilde{x} + BG\xi + (A - A_r)x_d - B_r v\big] \leq -a_3\|\tilde{x}\|^2 \tag{5.14}$$

where a_1, a_2, and a_3 are positive constants.

The notation $\|.\|$ denotes the Euclidean norm of a vector. In the sequel, it is also used to denote the induced Euclidean norm of a matrix. Note that (5.13) is technically not required as it follows from the positive definiteness of the matrix P. However, its purpose in the assumption is to collect all the relevant notation in a single place. Also note that the meaning of 'admissible x_d and v' in (A5.1) differs in each of our main results, where in each case it is specified precisely.

Consider the Lyapunov function, $V(.)$, in assumption (A5.1) as a candidate Lyapunov function for the system (5.12). The time derivative of $V(\tilde{x})$, along the flow of the tracking error system, (5.12), is given by

$$\begin{aligned}
\dot{V} &= 2\tilde{x}^T P\big[A\tilde{x} + BG\xi + (A - A_r)x_d - B_r v\big] + 2\tilde{x}^T PBGe \\
&\leq -a_3\|\tilde{x}\|^2 + 2\tilde{x}^T PBGe \\
&\leq -a_3\|\tilde{x}\|^2 + \|\tilde{x}\|L^T|e|
\end{aligned} \tag{5.15}$$

where where $|e|$ denotes the vector of the absolute values of the components of e and $L \in \mathbb{R}^{2n+q}$ is a non-zero vector, with non-negative elements, given by

$$L = \begin{bmatrix} \|c_1(2PBG)\| & \|c_2(2PBG)\| & \dots & \|c_{2n+q}(2PBG)\| \end{bmatrix} \tag{5.16}$$

where the notation $c_i(.)$ denotes the i^{th} column of the matrix argument. Then,

(5.15) suggests the following triggering condition.

$$t_0 = \min\{t \geq 0 : \|\tilde{x}\| \geq r > 0\}, \text{ and}$$

$$t_{i+1} = \min\{t \geq t_i : L^T|e| - \sigma a_3\|\tilde{x}\| \geq 0, \ \|\tilde{x}\| \geq r\} \tag{5.17}$$

where $\sigma \in (0,1)$ and $r > 0$ are design parameters. The parameter r determines the ultimate bound of the tracking error. It is necessary to update the control only when $\|\tilde{x}\| \geq r$, for some $r > 0$, else it may result in the accumulation of control update times. Notice that each update instant t_{i+1} is defined implicitly with respect to t_i. Hence, the initial update instant t_0 has been specified separately. As the proposed triggering condition does not allow the control to be updated whenever $\|\tilde{x}\| < r$, the first update instant, t_0, need not be at $t = 0$. Therefore, it is assumed that $u = 0$ for $t \in (0, t_0)$.

We now show that the triggering condition (5.17) ensures uniform ultimate boundedness of the tracking error under suitable conditions. The first of the conditions is the following assumption on the reference trajectory.

(A5.2) For all time $t \geq 0$, $\|[x_d; v]\| \leq d$ for some $d \geq 0$ and v is piecewise continuous.

The following lemma that the event-triggering condition (5.17) ensures that the tracking error is ultimately bounded, provided the sequence of control execution times does not exhibit *Zeno behavior* (accumulation of inter-event times), in other words either the sequence of control execution times is finite or $\lim_{i\to\infty} t_i = \infty$.

Lemma 5.1. *Consider the event-triggered system given by* (5.12) *and* (5.17)*. Suppose that assumptions* (A5.1) *and (A5.2) are satisfied. If the sequence of control*

execution times does not exhibit Zeno behavior, then the tracking error, $\tilde{x}$, is uniformly ultimately bounded by a ball of radius $r_1 = \sqrt{\frac{a_2}{a_1}}r$.

Proof. The assumption that the sequence of control execution times does not exhibit Zeno behavior implies that the triggering condition, (5.17), is well defined $\forall t \in [0, \infty)$ (if there are finitely many control updates, that is $i \in \{0, 1, \ldots, N\}$, then $t_{N+1} = \infty$). As a result, (5.15) and (5.17) imply that

$$\dot{V} \leq -(1-\sigma)a_3\|\tilde{x}\|^2 \leq -(1-\sigma)a_3 r^2 < 0, \quad \forall \tilde{x} \in \{\tilde{x} \in \mathbb{R}^n : \|\tilde{x}\| \geq r\} \tag{5.18}$$

Thus, given any initial condition $\tilde{x}(0)$, there is a finite time (dependent on the initial condition) in which the solution enters the set $\{\tilde{x} : V(\tilde{x}) \leq a_2 r^2, \|[x_d; v]\| \leq d\}$ and stays there. Therefore, the tracking error, $\tilde{x}$, is uniformly ultimately bounded by a ball of radius $r_1 = \sqrt{\frac{a_2}{a_1}}r$. □

Now we show that, under suitable conditions, the inter-event times resulting from (5.17) have a positive lower bound guaranteeing the non-occurrence of Zeno behavior. For the first result, we need the following additional assumption.

(A5.3) For all time $t \geq 0$, v is differentiable and $\|\dot{v}\| \leq c$ for some $c \geq 0$.

Theorem 5.1. *Consider the event-triggered system given by* (5.12) *and* (5.17). *Suppose that assumptions* (A5.1), *(A5.2) and (A5.3) are satisfied. Then, the tracking error, $\tilde{x}$, is uniformly ultimately bounded by a ball of radius* $r_1 = \sqrt{\frac{a_2}{a_1}}r$, *and the inter-event times $(t_{i+1} - t_i)$ for $i \in \{0, 1, 2, \ldots\}$ are uniformly bounded below by a positive constant that depends on the bound of the initial tracking error.*

Proof. Uniform ultimate boundedness of the tracking error automatically follows from Lemma 5.1 if the existence of a positive lower bound for the inter-event times is shown. Note that for each i, $\|e(t_i)\| = 0$ and $\|\tilde{x}(t_i)\| \geq r$. Further, note that $L^T|e| \leq \|L\|\|e\|$ for all e. Hence, the triggering condition (5.17) implies that the inter-event times, $(t_{i+1} - t_i) \geq T$, where T is the time it takes $\|e\|$ to grow from 0 to $\frac{\sigma a_3}{\|L\|} r \leq \frac{\sigma a_3}{\|L\|}\|\tilde{x}\|$. If we show that $T > 0$, then the proof is complete.

From (5.12), (5.9), (5.10) and triangle inequality property, we observe that

$$\|\dot{\tilde{x}}\| \leq \|(A + BG_{\tilde{x}})\tilde{x}\| + \|(A - A_r + BG_{x_d})x_d + (BG_v - B_r)v\| + \|BGe\|$$

$$\|\dot{x}_d\| \leq \|A_r x_d + B_r v\|$$

Now, note that the triggering condition (5.17) implies that $\|\tilde{x}(t_0)\| \geq r$ and (5.18) implies that for all time $t \geq t_0$, $\|x(t)\| \leq \mu_0$, where

$$\mu_0 = \sqrt{\frac{a_2}{a_1}}\|\tilde{x}(t_0)\|$$

Thus, letting

$$P_1 = \|(A + BG_{\tilde{x}})\|, \quad P_2 = \left\|\begin{bmatrix}(A - A_r + BG_{x_d}) & (BG_v - B_r)\end{bmatrix}\right\|, \quad P_e = \|BG\|$$

$$P_3 = \left\|\begin{bmatrix}A_r & B_r\end{bmatrix}\right\|$$

(A5.2) implies that

$$\|\dot{\tilde{x}}\| \leq P_1\|\tilde{x}\| + P_2\|[x_d; v]\| + P_e\|e\|$$

$$\leq P_1\mu_0 + P_2 d + P_e\|e\|$$

and $\|\dot{x}_d\| \leq P_3 d$, while (A5.3) implies $\|\dot{v}\| \leq c$. Then, by letting $P_0 = P_1\mu_0 + (P_2 +$

$P_3)d$ and from the definition $\dot{e} = -[\dot{\tilde{x}}; \dot{x}_d; \dot{v}]$ it follows that

$$\frac{\mathrm{d}\|e\|}{\mathrm{d}t} \leq \|\dot{e}\| \leq P_e\|e\| + P_0 + c \tag{5.19}$$

Note that for $\|e\| = 0$, the first inequality holds for all the directional derivatives of $\|e\|$. Then, according to the Comparison Lemma [45]

$$\|e\| \leq \frac{P_0 + c}{P_e}(\mathrm{e}^{P_e(t-t_i)} - 1), \quad \text{for} \quad t \geq t_i. \tag{5.20}$$

Thus, the inter-event times are uniformly lower bounded by T, which satisfies

$$T \geq \frac{1}{P_e} \log\left(1 + \frac{\sigma a_3 r P_e}{\|L\|(P_0 + c)}\right). \tag{5.21}$$

Thus, we conclude that the uniform positive lower bound for the inter-event times, T, is positive. □

In the next section, the event-triggering condition and the corresponding results for nonlinear systems are given. We also demonstrate two additional results, where the assumption (A5.3) is relaxed to include piecewise continuous v.

5.4 Nonlinear Systems

In this section, we address the problem for general nonlinear systems. We start by stating the main assumptions.

(A5.4) Suppose $f(0, \gamma(0)) - f_r(0, 0) = 0$ and that there exists a C^1 Lyapunov function for the dynamical system in (5.4), $V : \mathbb{R}^n \to \mathbb{R}$, such that for all admissible x_d

and v,

$$\alpha_1(\|\tilde{x}\|) \leq V(\tilde{x}) \leq \alpha_2(\|\tilde{x}\|)$$
$$\frac{\partial V}{\partial \tilde{x}}\big[f(\tilde{x}+x_d,\gamma(\xi)) - f_r(x_d,v)\big] \leq -\alpha_3(\|\tilde{x}\|)$$

where $\alpha_1(.)$, $\alpha_2(.)$, and $\alpha_3(.)$ are class $\mathcal{K}_\infty$ functions[1].

(A5.5) The functions f, γ and f_r are Lipschitz on compact sets.

The notation $\|.\|$ denotes the Euclidean norm of a vector. In the sequel, it is also used to denote the induced Euclidean norm of a matrix. Note that the meaning of 'admissible x_d and v' in (A5.4) differs in each of our main results, where in each case it is specified precisely. At this stage, it is enough to know that (A5.2) is satisfied in each case. Now, consider the following family of compact sets:

$$S(R) = \{\xi : V(\tilde{x}) \leq \alpha_2(R),\ \|[x_d; v]\| \leq d\}$$
$$\delta S(R) = \{\xi : V(\tilde{x}) = \alpha_2(R),\ \|[x_d; v]\| \leq d\} \tag{5.22}$$

Note that for each $R \geq 0$, the sets $S(R)$ and $\delta S(R)$ include all the admissible reference signals, x_d and v. For each set $S(R)$ there exists, by assumption (A5.5), a non-zero vector $L(R) \in \mathbb{R}^{2n+q}$, with non-negative elements, such that

$$\|f(\tilde{x}+x_d,\gamma(\xi+e)) - f(\tilde{x}+x_d,\gamma(\xi))\|$$
$$\leq L(R)^T|e| \leq \|L(R)\|\|e\|, \quad \forall\ \xi,\ (\xi+e) \in S(R) \tag{5.23}$$

[1] A continuous function $\alpha : [0,\infty) \to [0,\infty)$ is said to belong to the class $\mathcal{K}_\infty$ if it is strictly increasing, $\alpha(0) = 0$ and $\alpha(r) \to \infty$ as $r \to \infty$ [45].

where $|e|$ denotes the vector of the absolute values of the components of e. Without loss of generality, it may be assumed that each component of $L(R)$ is a non-decreasing function of R. In the sequel, we use the notation S_i, δS_i and L_i to denote $S(\|\tilde{x}(t_i)\|)$, $\delta S(\|\tilde{x}(t_i)\|)$ and $L(\|\tilde{x}(t_i)\|)$, respectively. Next, we define a continuous function, $\beta(.)$, that satisfies

$$\beta(R) \geq \max_{\|w\| \leq R} \left|\left| \frac{\partial V(w)}{\partial w} \right|\right|, \quad \forall R \geq 0 \tag{5.24}$$

We now derive the triggering condition that determines the time instants t_i at which the control is updated.

Consider the Lyapunov function, $V(.)$, in assumption (A5.4) as a candidate Lyapunov function for the system (5.5). The time derivative of $V(\tilde{x})$, along the flow of the tracking error system, $\dot{V} = (\partial V/\partial \tilde{x})\dot{\tilde{x}}$, may be obtained through the measurement error interpretation, (5.7).

$$\begin{aligned}
\dot{V} &= \frac{\partial V}{\partial \tilde{x}}\big[f(\tilde{x}+x_d,\gamma(\xi)) - \dot{x}_d\big] + \frac{\partial V}{\partial \tilde{x}}\big[f(\tilde{x}+x_d,\gamma(\xi+e)) - f(\tilde{x}+x_d,\gamma(\xi))\big] \\
&\leq -\alpha_3(\|\tilde{x}\|) + \frac{\partial V}{\partial \tilde{x}}\big[f(\tilde{x}+x_d,\gamma(\xi+e)) - f(\tilde{x}+x_d,\gamma(\xi))\big] \\
&\leq -\alpha_3(\|\tilde{x}\|) + \beta(\|\tilde{x}\|)L(R)^T|e|, \quad \forall\ \xi,\ (\xi+e) \in S(R)
\end{aligned} \tag{5.25}$$

where the second last equation is obtained from assumption (A5.4), and (5.25) is then obtained from (5.22)-(5.24). Then, (5.25) suggests a triggering condition.

Consider the following **triggering condition** (for the sake of clarity, the complete system description including the state equation and the triggering condition

are given).

$$\dot{\tilde{x}} = f\big(\tilde{x} + x_d, \gamma(\xi(t_i))\big) - \dot{x}_d, \quad \forall t \in [t_i, t_{i+1}) \tag{5.26}$$

$t_0 = \min\{t \geq 0 : \|\tilde{x}\| \geq r > 0\}$, and

$$t_{i+1} = \min\{t \geq t_i : L_i^T |e| - \frac{\sigma\alpha_3(\|\tilde{x}\|)}{\beta(\|\tilde{x}\|)} \geq 0, \ \|\tilde{x}\| \geq r\} \tag{5.27}$$

where $0 < \sigma < 1$ and $r > 0$ is a design parameter that determines the ultimate bound of the tracking error. It is necessary to update the control only when $\|\tilde{x}\| \geq r$, for some $r > 0$, else it may result in the accumulation of control update times. Notice that each update instant t_{i+1} is defined implicitly with respect to t_i. Hence, the initial update instant t_0 has been specified separately. As the proposed triggering condition does not allow the control to be updated whenever $\|\tilde{x}\| < r$, the first update instant, t_0, need not be at $t = 0$. Therefore, it is assumed that $u = 0$ for $0 \leq t < t_0$.

Under assumptions (A5.2), (A5.4) and (A5.5), the following lemma demonstrates that the event-triggering condition (5.27) ensures $\xi \in S_i$ for all $t \in [t_i, t_{i+1})$, for each i. Moreover, the lemma also demonstrates that the event-triggering condition (5.27) renders the tracking error ultimately bounded, provided the sequence of control execution times does not exhibit *Zeno behavior* (accumulation of inter-event times), in other words either the sequence of control execution times is finite or $\lim_{i\to\infty} t_i = \infty$.

Lemma 5.2. *Consider the system (5.4). Suppose that assumptions (A5.2), (A5.4) and (A5.5) are satisfied. Then, in the event-triggered system (5.26)-(5.27), for each i, $\xi \in S_i$ for all $t \in [t_i, t_{i+1})$. Further, if the initial condition is bounded and the*

sequence of control execution times does not exhibit Zeno behavior, then the tracking error, $\tilde{x}$, is uniformly ultimately bounded by a ball of radius $r_1 = \alpha_1^{-1}(\alpha_2(r))$.

Proof. First, we establish by contradiction that for each i, $\xi \in S_i$ for all $t \in [t_i, t_{i+1})$. Note that by definition, $(\xi + e) = \xi(t_i) \in S_i$ and the triggering condition enforces $\|\tilde{x}(t_i)\| \geq r$. Further, since $\|\tilde{x}(t_i)\| \geq r$, the open r-ball is a proper subset of and is contained within the interior of S_i (that is, its intersection with δS_i is an empty set). Also note that sets S_i and δS_i (see (5.22) and the text following (5.23)) are essentially a sub-level set and a level set, respectively, of the Lyapunov function V. Now, let us assume that ξ does escape S_i during the interval $[t_i, t_{i+1})$. Then, since the tracking error $\tilde{x}$ is continuous as a function of time, there exists a $t_i^* \in [t_i, t_{i+1})$ such that $\xi(t_i^*) \in \delta S_i \subset S_i$ and $\dot{V}|_{t=t_i^*} > 0$ (where $\dot{V}|_{t=t_i^*}$ denotes $\dot{V}$ evaluated at $t = t_i^*$). However, as $\xi(t_i^*) \in \delta S_i \subset S_i$, (5.25) and (5.27) imply $\dot{V}|_{t=t_i^*} \leq -(1 - \sigma)\alpha_3(\|\tilde{x}(t_i^*)\|) < 0$. Thus, having arrived at a contradiction, we conclude that no such t_i^* exists and that the first claim of the lemma is true. Consequently, (5.25) and (5.27) again imply that the derivative $\dot{V}$ along the flow of the system satisfies

$$\dot{V} \leq -(1 - \sigma)\alpha_3(\|\tilde{x}\|) < 0, \ \forall t \in [t_i, t_{i+1}), \ \|\tilde{x}(t)\| \geq r \tag{5.28}$$

and further, for each $R \geq r$ it is true that any solution that enters the set $S(R)$ does not leave it subsequently.

The assumption that $\tilde{x}(0)$ is bounded and the definition of t_0 imply that $\tilde{x}(t_0)$ is also bounded. Then, the assumption that the sequence of control execution times does not exhibit Zeno behavior implies that the triggering condition, (5.27), is well defined and that $\dot{V} \leq -(1 - \sigma)\alpha_3(\|\tilde{x}\|) < 0$, $\forall t \in [0, \infty)$ s.t. $\|\tilde{x}(t)\| \geq r$ (if there are

finitely many control updates, that is $i \in \{0, 1, \ldots, N\}$, then $t_{N+1} = \infty$). Then, in fact, it is true that $S(R)$ is positively invariant for each $R \geq r$. In particular, S_0 is positively invariant. Then, (5.28) implies that $\dot{V} \leq -(1-\sigma)\alpha_3(r) < 0$ for all $\xi \in S_0$ such that $\|\tilde{x}\| \geq r$. Hence all solutions, ξ, with bounded initial conditions enter the set $S(r)$ in finite time and as $S(r)$ is positively invariant, the solutions stay there. Therefore the tracking error, $\tilde{x}$, is uniformly ultimately bounded by the closed ball of radius $r_1 = \alpha_1^{-1}(\alpha_2(r))$. □

Looking back at (5.27), it is clear that the functions α_3 and β play a crucial role in determining how often an event is triggered or in computing a lower bound for the inter-event times. Specifically, the following definition is useful.

$$\Delta_{s_1}^{s_2} \triangleq \min_{s_1 \leq \|\tilde{x}\| \leq s_2} \sigma\alpha_3(\|\tilde{x}\|)/\beta(\|\tilde{x}\|) \tag{5.29}$$

where $s_2 \geq s_1 > 0$ are any positive real numbers, the functions α_3 and β are as defined in (A5.4) and (5.24), respectively. Since α_3 and β are continuous positive definite functions, $\Delta_{s_1}^{s_2}$ is well defined and positive for any given $s_2 \geq s_1 > 0$.

Now we present the first main result of the chapter. It demonstrates, for a particular class of reference trajectories, that in the event-triggered system (5.26)-(5.27) the inter-event times are uniformly bounded away from zero while the tracking error is uniformly ultimately bounded.

Theorem 5.2. *Consider the system (5.4). Suppose that assumptions* (A5.2), (A5.3), (A5.4) *and* (A5.5) *are satisfied. Then, for the event-triggered system (5.26)-*(5.27), *the tracking error, $\tilde{x}$, is uniformly ultimately bounded by a ball of radius $r_1 = \alpha_1^{-1}(\alpha_2(r))$, and the inter-event times $(t_{i+1} - t_i)$ for $i \in \{0, 1, 2, \ldots\}$ are uniformly*

bounded below by a positive constant that depends on the bound of the initial tracking error.

Proof. Uniform ultimate boundedness of the tracking error follows from Lemma 5.2. Only the existence of a positive lower bound for the inter-event times remains to be shown. Note that for each i, $\|e(t_i)\| = 0$ and $\|\tilde{x}(t_i)\| \geq r$. Hence, the triggering condition (5.27) implies that the i^{th} inter-update time, $(t_{i+1} - t_i)$, is at least equal to the time it takes $\|L_i\|\|e\|$ to grow from 0 to $\sigma\alpha_3(\|\tilde{x}\|)/\beta(\|\tilde{x}\|)$. Recall from the proof of Lemma 5.2 that every solution, ξ, stays in the set S_0 for all $t \in [t_0, t_i)$, for each i. Thus, $\|L_i\| \leq \|L_0\|$ for each i. Notice

$$S_0 \subset \{\xi : \|\tilde{x}\| \leq \mu_0,\ \|[x_d; v]\| \leq d\} \tag{5.30}$$

where $\mu_0 = \alpha_1^{-1}(\alpha_2(\|\tilde{x}(t_0)\|))$. Then, (5.29) implies $t_{i+1} - t_i \geq T$, where T is the time it takes $\|e\|$ to grow from 0 to $\Delta_r^{\mu_0}/\|L_0\|$. If we show that $T > 0$, then the proof is complete.

From (5.7), and triangle inequality property, we observe that

$$\|\dot{\tilde{x}}\| \leq \|f(\tilde{x} + x_d, \gamma(\xi)) - \dot{x}_d\| + \|f(\tilde{x} + x_d, \gamma(\xi + e)) - f(\tilde{x} + x_d, \gamma(\xi))\| \tag{5.31}$$

From (5.23), the second term is bounded by $L_0^T|e| \leq \|L_0\|\|e\|$ on the set S_0. Since, according to (A5.4), $f(0, \gamma(0)) - f_r(0, 0) = 0$, (A5.5) then implies that there exist Lipschitz constants $P_1 \geq 0$ and $P_2 \geq 0$ such that

$$\begin{aligned}\|\dot{\tilde{x}}\| &\leq P_1\|\tilde{x}\| + P_2\|[x_d; v]\| + L_0^T|e| \\ &\leq P_1\mu_0 + P_2 d + \|L_0\|\|e\|\end{aligned}$$

where the second inequality is obtained from (5.30). Assumptions (A5.5)-(A5.2) imply that there exists a constant $P_3 \geq 0$ such that $\|\dot{x}_d\| \leq P_3 d$ and (A5.3) implies $\|\dot{v}\| \leq c$. Then, by letting $P_0 = P_1\mu_0 + (P_2 + P_3)d$ and from the definition $\dot{e} = -[\dot{\tilde{x}}; \dot{x}_d; \dot{v}]$ it follows that

$$\frac{\mathrm{d}\|e\|}{\mathrm{d}t} \leq \|\dot{e}\| \leq \|L_0\|\|e\| + P_0 + c \tag{5.32}$$

Note that for $\|e\| = 0$, the first inequality holds for all the directional derivatives of $\|e\|$. Then, according to the Comparison Lemma [45]

$$\|e\| \leq \frac{P_0 + c}{\|L_0\|}(\mathrm{e}^{\|L_0\|(t-t_i)} - 1), \quad \text{for} \quad t \geq t_i. \tag{5.33}$$

Thus, the inter-event times are uniformly lower bounded by T, which satisfies

$$T \geq \frac{1}{\|L_0\|} \log\left(1 + \frac{\Delta_r^{\mu_0}}{P_0 + c}\right). \tag{5.34}$$

As $\|L_0\|$ is finite and $\Delta_r^{\mu_0} > 0$, we conclude that the inter-event times have a uniform positive lower bound, T. □

In the next result, the conditions on the reference trajectory are relaxed by no longer requiring it to satisfy assumption (A5.3). Instead, to ensure the absence of Zeno behavior, a new assumption is made - that d_v, the uniform bound on $\|v\|$, is no larger than a quantity determined by $\Delta_r^{\mu_0}$ and L_0. The new assumptions, in contrast to Theorem 5.2, lead to a constraint on the choice of the radius r in the triggering condition and ensure only local uniform ultimate boundedness of the trajectory tracking error. Let $L(R) \triangleq [Q(R); M(R)]$ and $L_i \triangleq [Q_i; M_i]$ where $Q(R), Q_i \in \mathbb{R}^{2n}$ and $M(R), M_i \in \mathbb{R}^q$. Now, the second main result is presented.

Theorem 5.3. *Consider the system defined by (5.4). Suppose that the assumptions (A5.2), (A5.4) and (A5.5) hold. Also, for some $R_0 \geq r$ suppose that $\Delta_r^{\mu_0} - 2d_v\|M(R_0)\| > 0$, where $\mu_0 = \alpha_1^{-1}(\alpha_2(R_0))$, $\Delta_r^{\mu_0}$ is given by (5.29) and d_v is the uniform bound on $\|v\|$. If $\|\tilde{x}(0)\| \leq R_0$, then in the event-triggered system (5.26)-(5.27), the tracking error, $\tilde{x}$, is uniformly ultimately bounded by a ball of radius $r_1 = \alpha_1^{-1}(\alpha_2(r))$, and the inter-update times $(t_{i+1} - t_i)$ for $i \in \{0, 1, 2, \ldots\}$ are uniformly bounded below by a positive constant that depends on R_0.*

Proof. The proof is very similar to that of Theorem 5.2, and hence only the essential steps are described here. According to Lemma 5.2 each solution, ξ, with $\|\tilde{x}(0)\| \leq R_0$ stays in the set $S(R_0)$. Hence, $\|M_i\| \leq \|M(R_0)\|$ and $\|Q_i\| \leq \|Q(R_0)\|$ for each i. Since $\|v\|$ is uniformly bounded by d_v it follows that for each i, $M_i^T|v_e| \leq \|M_i\|\|v_e\| \leq 2d_v\|M(R_0)\|$, where $v_e = v(t_i) - v$ and $|v_e|$ denotes the component-wise absolute value of the vector v_e. The definitions of Q_i and M_i imply that $L_i^T|e| = Q_i^T|[\tilde{x}_e; x_{d,e}]| + M_i^T|v_e| \leq Q_i^T|[\tilde{x}_e; x_{d,e}]| + 2d_v\|M(R_0)\|$.

Note that for each i, $r \leq \|\tilde{x}(t_i)\| \leq \mu_0$. Thus, the triggering condition in (5.27) implies that for each i, $L_{i-1}^T|e(t_i^-)| \geq \Delta_r^{\mu_0}$, or equivalently, $Q_{i-1}^T|[\tilde{x}_e(t_i^-); x_{d,e}(t_i^-)]| \geq \delta \triangleq \Delta_r^{\mu_0} - 2d_v\|M(R_0)\| > 0$, the last inequality being one of the assumptions. Hence, the inter-event times $t_{i+1} - t_i \geq T$, where T is the time it takes $\|[\tilde{x}_e; x_{d,e}]\|$ to grow from 0 to $\delta/\|Q(R_0)\|$. If we show that $T > 0$, then the proof is complete.

Following steps similar to those in the proof of Theorem 5.2, we know that there exists a finite $P_0 \geq 0$ such that $\dfrac{\mathrm{d}\|[\tilde{x}_e; x_{d,e}]\|}{\mathrm{d}t} \leq \|Q_0\|\|[\tilde{x}_e; x_{d,e}]\| + P_0 + 2d_v\|M(R_0)\|$. Note that for $\|[\tilde{x}_e; x_{d,e}]\| = 0$, the inequality holds for all the directional derivatives.

Thus, the inter-event times are uniformly lower bounded by T, which satisfies

$$T \geq \frac{1}{\|Q_0\|} \log \left(1 + \frac{\Delta_r^{\mu_0} - 2d_v}{P_0 + 2d_v \|M(R_0)\|} \right). \tag{5.35}$$

As $\|Q_0\|$ is finite, we conclude that the inter-event times have a lower bound, T, that is greater than zero. □

Theorem 5.3 is somewhat conservative because only the uniform bound on $\|v\|$ is utilized in determining the ultimate bound and the lower bound on the inter-event times. A more useful result is obtained by imposing only slightly stricter constraints on v - that jumps in v are separated in time by $T_v > 0$, that the magnitude of each jump is upper bounded by a known constant and that v is Lipschitz between jumps. This is expressed formally in the following assumption.

(A5.6) There exist constants $c \geq 0$, $T_v \geq 0$ and $J_v \geq 0$ such that for all $t, s \geq 0$, the following holds: $\|v(t) - v(s)\| \leq c|t - s| + \left\lceil \frac{|t-s|}{T_v} \right\rceil J_v$, where $\lceil . \rceil$ is the ceiling function.

Now the final result is presented.

Theorem 5.4. *Consider the system defined by (5.4). Suppose that the assumptions (A5.2), (A5.4), (A5.5) and (A5.6) hold. Also, for some $R_0 \geq r$ suppose that $\Delta_r^{\mu_0} - J_v \|M(R_0)\| > 0$, where $\mu_0 = \alpha_1^{-1}(\alpha_2(R_0))$ and $\Delta_r^{\mu_0}$ is given by (5.29). If $\|\tilde{x}(0)\| \leq R_0$, then in the event-triggered system (5.26)-(5.27), the tracking error, $\tilde{x}$, is uniformly ultimately bounded by a ball of radius $r_1 = \alpha_1^{-1}(\alpha_2(r))$, and the inter-update times $(t_{i+1} - t_i)$ for $i \in \{0, 1, 2, \ldots\}$ are uniformly bounded below by a positive constant that depends on R_0.*

Proof. Let $e^* \triangleq [e_{\tilde{x}}; e_{x_d}; e_{v^*}]$, where $e_{v^*} \triangleq c(t-t_i)$ for $t \in [t_i, t_{i+1})$ and each i. Then, by (A5.6), $\|e\| \leq \|e^*\| + \left\lceil \frac{|t-t_i|}{T_v} \right\rceil J_v$. Now, let T_k be the time it takes $\|e^*\|$ to grow from zero to $(\Delta_r^\mu - kJ_v\|M(R_0)\|)/\|L_0\|$. Then, a lower bound on the inter-event times is given by

$$\max_{k\in\{1,2,\ldots,N\}} \{\min\{kT_v, T_k\}\}, \quad N = \left\lfloor \frac{\Delta_r^\mu}{J_v\|M(R_0)\|} \right\rfloor \tag{5.36}$$

where $\lfloor . \rfloor$ denotes the floor function. Following the proof of Theorem 5.2, T_k is estimated as

$$T_k \geq \frac{1}{\|L_0\|} \log\left(1 + \frac{\Delta_r^\mu - kJ_v\|M(R_0)\|}{P_0 + c}\right). \tag{5.37}$$

Note that $T_k > 0$ for $k \in \{1, \ldots, N-1\}$ and $T_N \geq 0$. Further, $\{kT_v\}$ is an increasing sequence of positive numbers while $\{T_k\}$ is a decreasing sequence. Thus the lower bounded on inter-event times given by (5.36) is positive. The ultimate boundedness of the tracking error follows from Lemma 5.2. □

Remark 5.1. *Notice from (5.23) that in order to compute $L_i = L(\|\tilde{x}(t_i)\|)$ it is necessary to compute the set $S_i = S(\|\tilde{x}(t_i)\|)$ or at least a set of which S_i is a subset, such as $B_i \triangleq \{\xi : \|\tilde{x}\| \leq \alpha_1^{-1}(\alpha_2(\|\tilde{x}(t_i\|)), \|[x_d; v]\| \leq d\}$. However, if $\|\tilde{x}(t_i)\| \geq \|\tilde{x}(t_{i-1})\|$ then clearly some components of L_i may be greater than those of L_{i-1}. But from Lemma 5.2, we know that $S_i \subset S_{i-1}$ for each i, so at time instant t_i instead of computing L_i based on B_i, we can let $L_i = L_{i-1}$. Following this rule, the sequence $\{L_i\}$ can be chosen to be component-wise non-increasing. The triggering condition and the estimates of lower bounds on the inter-update times depend critically on L and hence using a time-varying L lowers the overall average*

update rate. Computing L is in general a computationally costly task and it is not useful to update L continuously in time like $\alpha_3(\|\tilde{x}\|)$ *and* $\beta(\|\tilde{x}\|)$.

In the next section our theoretical results are illustrated through simulations.

5.5 Examples and simulation results

The theoretical results developed in the previous sections are illustrated through simulations.

5.5.1 Nonlinear System Example

First, we present the simulation results for the following second order nonlinear system.

$$\dot{x} = \begin{bmatrix} \dot{x}_1 \\ \dot{x}_2 \end{bmatrix} = \begin{bmatrix} 0 & 1 \\ 0 & -1 \end{bmatrix} x + \begin{bmatrix} 0 \\ -x_1^3 \end{bmatrix} + \begin{bmatrix} 0 \\ 1 \end{bmatrix} u$$
$$= Ax + \begin{bmatrix} 0 \\ -x_1^3 \end{bmatrix} + Bu \tag{5.38}$$

The desired trajectory is a solution of the system $[\dot{x}_{d,1}; \dot{x}_{d,2}] = [x_{d,2}; v]$, where v is an exogenous input, which along with the initial conditions of the state of the reference system, $x_d = [x_{d,1}; x_{d,2}]$, determines the specific trajectory. The control function is chosen as

$$\gamma(\xi) = K\tilde{x} + v + (\tilde{x}_1 + x_{d,1})^3 + x_{d,2} \tag{5.39}$$

where $K = [k_1; k_2]^T$ is a 2×1 row vector such that $\tilde{A} = (A + BK)$ is Hurwitz, and $\tilde{x} = [\tilde{x}_1; \tilde{x}_2]$ is the tracking error. Then, the closed-loop tracking error system with

event-triggered control can be written as

$$\dot{\tilde{x}}_1 = \tilde{x}_2$$

$$\dot{\tilde{x}}_2 = -(\tilde{x}_2 + x_{d,2}) - (\tilde{x}_1 + x_{d,1})^3 + \gamma(\xi + e) - v. \tag{5.40}$$

Now, consider the quadratic Lyapunov function $V = \tilde{x}^T P \tilde{x}$ where P is a positive definite matrix that satisfies the Lyapunov equation $P\tilde{A} + \tilde{A}^T P = -H$, where H is a given positive definite matrix. The time derivative of V along the flow defined by (5.40) can be shown to satisfy

$$\begin{aligned} \dot{V} &\leq -\tilde{x}^T H \tilde{x} + 2\tilde{x}^T PB[\gamma(\xi + e) - \gamma(\xi)] \\ &\leq -\sigma a \|\tilde{x}\|^2 + \beta(\|\tilde{x}\|) L(R)^T |e|, \ \forall \xi, (\xi + e) \in S(R) \end{aligned} \tag{5.41}$$

where $a > 0$ is the minimum eigenvalue of H, $\beta(\|\tilde{x}\|) = 2\|PB\|\|\tilde{x}\|$ and

$$L(R) = \left[3(\mu + d_1)^2 + |k_1|; |k_2|; 3(\mu + d_1)^2; 1; 1\right] \tag{5.42}$$

where $\mu = \alpha_1^{-1}(\alpha_2(R))$ and $d_1 \leq d$ is the uniform bound on $x_{d,1}$. If d_1 is not known explicitly then d from assumption (A5.2) may be used instead. Note that B has been absorbed in β rather than in $L(R)$, as it should have been according to their definitions. This makes the β function point-wise lower. The vectors L_i were computed according to the procedure in Remark 5.1. Finally, given a desired ultimate bound for the trajectory tracking error, the parameter r in the triggering condition can be designed. Next, we present simulation results for two cases corresponding to the two main classes of reference trajectories considered in this chapter.

Case I: The signals $x_{d,1}$, $x_{d,2}$, and v were chosen as sinusoidal signals with peak-to-peak amplitude 2. This was done by choosing $[x_{d,1}(0), x_{d,2}(0); v(0)] =$

$[\pi/3; 1; 0]$ and $\dot{v} = -\cos(t)$. The initial condition of the plant was $[x_1(0); x_2(0)] = [5; -1]$. The parameter d_1 was chosen as 2.5 while the actual uniform bounds on $x_{d,1}$ and $\|[x_d; v]\|$ were observed to be around 2 and 2.28, respectively. The parameters in the controller were chosen as $K = -[20; 20]^T$, $\sigma = 0.95$ and H was chosen as the identity matrix. According to Theorem 5.2, we chose $r = 0.0154$ in the triggering condition to achieve an ultimate bound of $r_1 = 0.1$ in the tracking error.

The simulation results are shown in Figure 5.1(a). The Figure shows the norm of the tracking error, the radius r in the triggering condition, the desired ultimate bound r_1 and $W_i^T|e|$, where $W_i = (2\|PB\|L_i)/(\sigma a)$. The figure demonstrates that the tracking error is ultimately bounded, and well below the desired bound. We recall that according to the triggering condition (5.27), the control is not updated when $\|\tilde{x}\| < r$. Hence, as long as $\|\tilde{x}\| \geq r$, the weighted measurement error, $W_i^T|e|$, is bounded above by the norm of the tracking error, $\|\tilde{x}\|$, and an event is triggered (control is updated) each time $W_i^T|e| \geq \|\tilde{x}\|$. However, when $\|\tilde{x}\| < r$, $W_i^T|e|$ may exceed $\|\tilde{x}\|$. A zoomed version of the plot in Figure 5.1(a) is shown in Figure 5.1(b), where it is clearly seen that the tracking error is only ultimately bounded.

The number of control executions in the simulated time duration was 301, and the minimum inter-event time was observed to be 0.005s. The observed average frequency of control updates was around 30Hz. Since most of the updates occur before $\tilde{x}$ first enters the ball of radius r, it is important to also consider the average frequency for this time period, and in this simulation it was found to be around 46Hz. If L is kept constant then these average frequencies are much higher at 943Hz and 1586Hz, respectively, with almost no change in the rate of convergence.

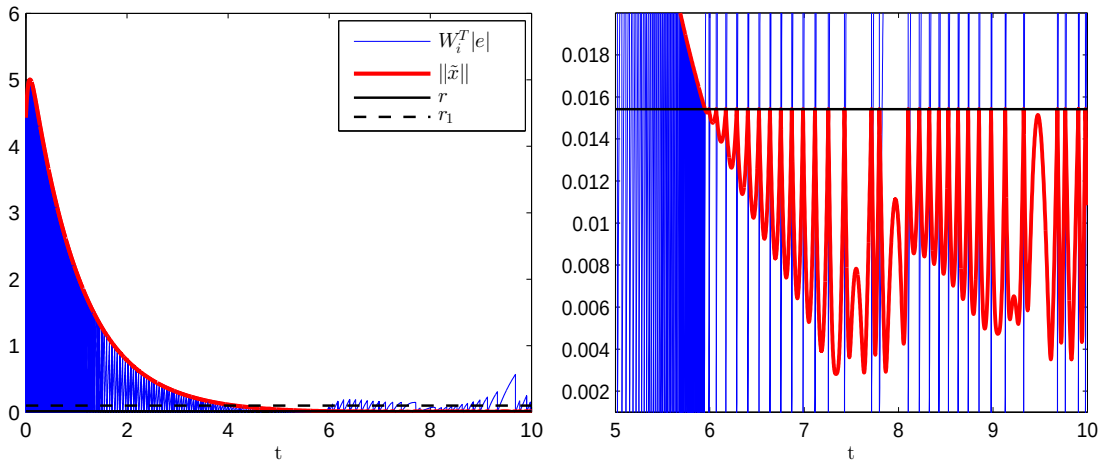

(a) Case I (b) Case I (zoom)

Figure 5.1: Simulation results for Case I.

The theoretical estimate of the minimum inter-event time is around 6×10^{-8}s, which is orders of magnitude lower than the observed value.

Case II: In this case the result in Theorem 5.4 is illustrated, where the input signal v is piecewise continuous. In the simulations it was defined as the piecewise constant function, taking values in the set $\mathcal{Q} = \{0, \pm 0.1, \pm 0.2, \ldots\}$ and defined as

$$v(t) = \arg\min_{k \in \mathcal{Q}} \{| - \sin(t) - k|\}.$$

For the time instants when $(-\sin(t))$ equals an odd multiple of 0.05, $v(t)$ is chosen as the higher or the lower of the two possible values based on whether the time derivative of $(-\sin(t))$ is positive or negative, respectively. In the context of Theorem 5.4, the constants $c = 0$ and $J_v = 0.1$.

The initial condition of the reference system was $[x_{d,1}(0); x_{d,2}(0); v(0)] = [1; 1.003; 0]$. From Theorem 5.4, we know that Δ_r^μ has to be greater than $J_v = 0.1$, which implies that r has to be greater than 0.0075. For the example system here, R_0 in Theorem

5.4 can assume any value. Thus, as in CASE I, $r = 0.0154$ was chosen. The rest of the parameters were the same as in Case I. Figure 5.2 shows the simulation results. The number of control updates were observed to be 304, with the minimum exe-

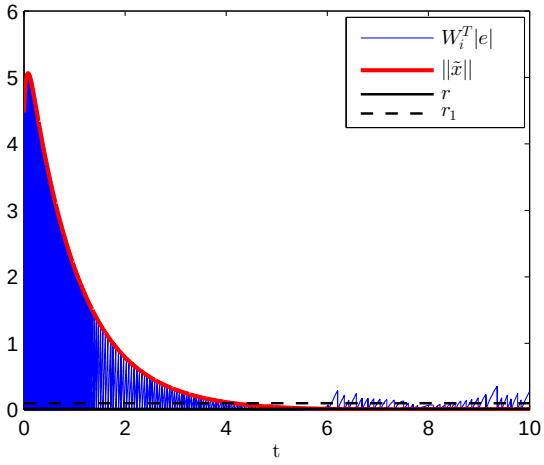

Figure 5.2: Simulation results for Case II.

cution time at around 0.005s. The observed average frequencies of control updates were found to be around 30Hz and 46Hz for the simulated time duration and the time duration that $\tilde{x}$ takes to first enter the ball of radius r, respectively. These average frequencies are comparable to those in Case I. The theoretical estimate of the minimum inter-event time is around 3×10^{-8}s, which is very conservative.

5.5.2 Linear System Example

In this example, the plant and the reference system are given by (5.8)-(5.9) with

$$A = A_r = \begin{bmatrix} 0 & 1 \\ 0 & 0 \end{bmatrix}, \qquad B = B_r = \begin{bmatrix} 0 \\ 1 \end{bmatrix}$$

The control gain was chosen as

$$G = \begin{bmatrix} -2 & -3 & 0 & 0 & 1 \end{bmatrix}$$

Thus, in the notation of (5.10),

$$G_{\tilde{x}} = \begin{bmatrix} -2 & -3 \end{bmatrix}$$

From (5.12), the tracking error is seen to evolve as

$$\dot{\tilde{x}} = (A + BG_{\tilde{x}})\tilde{x} + BGe$$

The gain matrix $G_{\tilde{x}}$ has been chosen so that the eigenvalues of $\bar{A} = (A + BG_{\tilde{x}})$ are at $\{-1, -2\}$. Thus, consider the candidate Lyapunov function

$$V(\tilde{x}) = \tilde{x}^T P \tilde{x}$$

where P is the symmetric positive definte matrix satisfying

$$P\bar{A} + \bar{A}^T P = -I_2$$

where I_2 is a 2×2 identity matrix. In the simulations, $\sigma = 0.95$, $r_1 = 0.1$ have been chosen, giving $L = [1.414; 2.121; 0; 0; 0.707]$, $\sigma * a_3 = 0.95$ and $r = 0.038$. The initial condition of the plant $x(0) = [5; 0]$ has been chosen. The reference trajectory and the input to the reference system were chosen as

$$[x_d; v] = [\cos(\omega t); -\omega \sin(\omega t); -\omega^2 \cos(\omega t)]$$

Then, a number of simulations, parametrized by ω, were performed. The parameter ω was varied from 1 to 10 in steps of 0.1. Notice that

$$\begin{aligned} \|[x_d; v]\| &= \sqrt{\cos^2(\omega t) + \omega^2 \sin^2(\omega t) + \omega^4 \cos^2(\omega t)} \\ &= \sqrt{(1 + w^4 - w^2)\cos^2(\omega t) + w^2} \leq \sqrt{1 + w^4} = d \end{aligned}$$

and

$$\|\dot{v}\| \leq w^3 = c$$

Thus, the theoretical lower bound on inter-event times may be computed, (5.21) as a function of w, which is shown in Figure 5.3. In each of the simulation, the initial

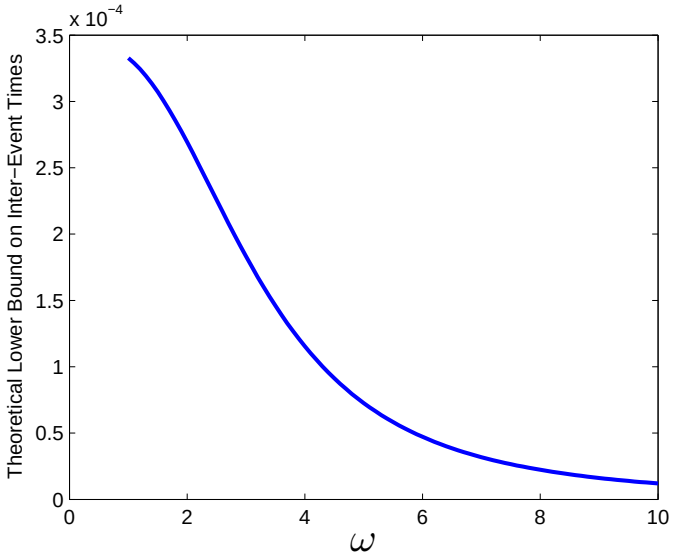

Figure 5.3: Theoretical lower bound on inter-event times for the linear system example.

tracking error is $\tilde{x}(0) = [4; 0]$. Each simulation was performed until the time it took the trajectory to reach the r-ball. In the corresponding time duration, the minimum and the average inter-event times were found. The resulting relationship with w is shown in Figure 5.4. Clearly, the the theoretical lower bound for the inter-event times in Figure 5.3 is very conservative. However, Figure 5.4 clearly demonstrates one of the most significant advantages of the utility driven event-triggered control - the ability to adjust to the sampling rate according to the requirement.

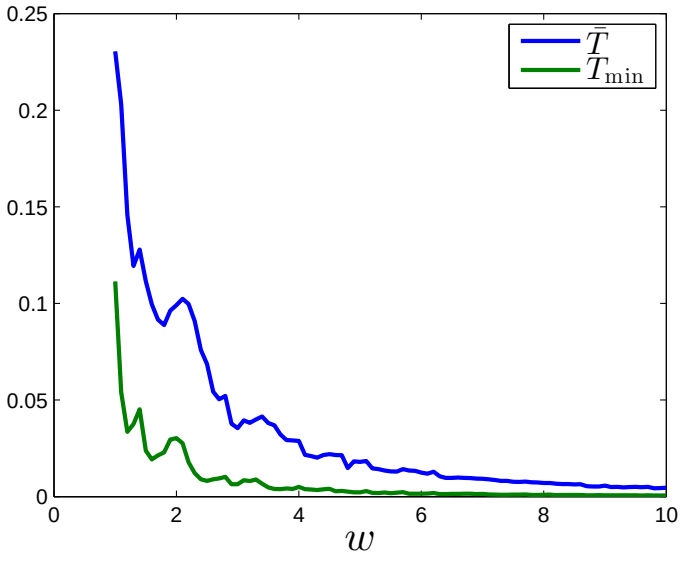

Figure 5.4: Observed average ($\bar{T}$) and minimum ($T_{\min}$) inter-event times observed in the simulations parametrized by ω.

5.6 Conclusions

In this chapter, we developed an event based control algorithm for trajectory tracking in nonlinear systems. It was demonstrated that given a nonlinear dynamical system, and a continuous-time controller that ensures uniform asymptotic tracking of the desired trajectory, an event based controller can be designed that not only guarantees uniform ultimate boundedness of the tracking error, but also ensures that the inter-event times for the control algorithm are uniformly bounded away from zero. The first result demonstrated that uniform boundedness with an arbitrary ultimate bound for the tracking error can be achieved, provided the reference trajectory, the exogenous input to the reference system, and its derivative are all uniformly bounded. However, the minimum *guaranteed* inter-event time decreases

along with the ultimate bound. In the second and third results, we relaxed the assumption on the derivative of the input to the reference system, and demonstrated that the tracking error is uniformly ultimately bounded. In these cases, the analytical results show that it may not be feasible to reduce the ultimate bound below a certain threshold and moreover, the result is only local in general.

The theoretical results were demonstrated through simulations of a second order nonlinear system. The theoretical lower bounds on inter-update times have been found to be very conservative. This is partially due to the fact that the estimates are based on the rate of change of $\|e\|$ (made necessary by the presence of exogenous signals) rather than that of $\|\tilde{x}\|/\|e\|$ as in [14]. Thus, there is significant room for improvement in these estimates and how they are computed. Numerical simulations indicated that the ultimate bound on the tracking error is much lower than the desired value, which is another area for improvement of the theoretical predictions. Finally, it is important to extend these results to output feedback systems.

Chapter 6

Utility Driven Sampled Data Adaptive Control for Tracking in Robot Manipulators

6.1 Introduction

Many of the utility driven *event-triggered* controllers in the literature are essentially sampled data versions of continuous time controllers, with the sampling instants determined by state based triggering conditions. While utility driven event-triggered controllers implicitly guarantee stability, they have a drawback. These controllers rely critically on the knowledge of a good model of the system. For example, the results in [14, 32] are general enough to hold for robotic manipulators when perfect knowledge of the system is available. However, building a model of high accuracy is a time consuming process and in many cases, it may not even be possible. Therefore, it is important to extend the design of implicitly verified event based controllers to cases where only a poor model of the system is available. This is specially important in the field of robotics, where adaptive and robust controllers are often used.

It is our opinion that event-triggered controllers can have a significant impact in the field of robotics. For example, many industrial robotics applications use visual feedback, which inherently works at a low rate. Hence, we are interested in introducing specific event-triggered controllers for robotics. Therefore, in this chap-

ter we develop a specific event-triggered adaptive controller for trajectory tracking in robotic manipulators. That is, we incorporate adaptation in the proposed controller. The controller is demonstrated through simulations and experiments on a two-link planar robotic manipulator.

6.1.1 Contributions

The contribution of this chapter is twofold. In this chapter, we design a specific event-triggered controller applicable in the field of robotics. In addition, the proposed controller incorporates adaptation. The only other reference in the event-triggered control literature that explores adaptation is [76], where in a Kalman filter like approach was adopted to estimate the system parameters of a discrete time linear system. We explore the problem of adaptation for continuous-time trajectory tracking in nonlinear robotic systems. Finally, this work adds to the limited body of work on event-triggered implementations in experiments [5, 12, 22, 77–80]. By incorporating adaptation, we allow for larger modelling errors and thus make safe experimentation of event-triggered controllers more feasible.

The rest of the chapter is organized as follows. In Section 6.2, an event-triggered implementation of the controller of [81] is presented under the assumption that the controller has exact knowledge of the robot dynamics. Then in Section 6.3, the adaptive controller of [81] is introduced, and the design of the proposed event based adaptive controller is described. In Section 6.4 the dynamic model of a planar two-link robot is presented. The simulation and experimental results are presented

in Section 6.5. Finally, some concluding remarks are made in Section 6.6 and some future directions of work are proposed.

6.2 Event-Triggered Control

In this section we introduce the idea of event-triggered control, and design an event-triggered controller for trajectory tracking in robotic manipulators through a process similar to that in [32]. Secondly, in this section we provide motivation for incorporating adaptation in the event-triggered controller. Consider a standard n-degree of freedom rigid robot model of the form, [82],

$$M(q)\ddot{q} + C(q,\dot{q})\dot{q} + G(q) = u, \quad q \in \mathbb{R}^n,\ u \in \mathbb{R}^n \tag{6.1}$$

where $M : \mathbb{R}^n \longrightarrow \mathbb{R}^{n\times n}$, $C : \mathbb{R}^n \times \mathbb{R}^n \longrightarrow \mathbb{R}^{n\times n}$ and $G : \mathbb{R}^n \longrightarrow \mathbb{R}^n$. Let $x_d \triangleq [q_d; \dot{q}_d] \in \mathbb{R}^n \times \mathbb{R}^n$ be the state of the desired trajectory that the robot has to track. Here the notation $[a_1; a_2]$ denotes the column vector formed by concatenating the vectors a_1 and a_2. This notation is used in this chapter to refer to various concatenated vectors. Let $\tilde{q} \triangleq q - q_d$, then the tracking error is defined as $\tilde{x} \triangleq [\tilde{q}; \dot{\tilde{q}}]$. Let $u = \gamma(\xi) \in \mathbb{R}^m$ be a known continuous-time control law for trajectory tracking, where ξ is the data that the controller depends on. For example in the passivity based Slotine-Li controller [83] or in the controller of [81],

$$\xi = [\tilde{x}; x_d; \ddot{q}_d] \tag{6.2}$$

More specifically, consider the controller of [81], an event-triggered implementation of which is proposed controller in this chapter.

$$\begin{aligned} u = \gamma(\xi) &= M(q)\ddot{q}_d + C(q,\rho)\dot{q}_d + G(q) - K_d\dot{\tilde{q}} - K_p\tilde{q} \\ &= Y(q,\rho,\dot{q}_d,\ddot{q}_d)\theta - K_d\dot{\tilde{q}} - K_p\tilde{q} \end{aligned} \tag{6.3}$$

where $\rho \triangleq \dot{q} - \lambda\tilde{q}$, $K_d = K_d^T > 0$ and $K_p = K_p^T > 0$. Additionally

$$\lambda = \frac{\lambda_0}{1 + \|\tilde{q}\|} \tag{6.4}$$

where λ_0 is a positive constant and $\|.\|$ denotes the Euclidean norm. The second relation in (6.3) is a result of the well-known fact that the Lagrangian robot dynamics are linearly parametrizable [82]. In the sequel, $Y(q,\rho,\dot{q}_d,\ddot{q}_d)$ is nearly always shortened to Y to make the notation compact.

(A6.1) Assume that the controller gains are chosen such that

$$\lambda_0 < \min\left\{\frac{K_{d,m}}{3M_M + 2C_M}, \frac{4K_{p,m}}{K_{d,M} + K_{d,m}}\right\} \tag{6.5}$$

where $K_{d,m} \equiv \sigma_m(K_d)$, $K_{d,M} \equiv \sigma_M(K_d)$, $K_{p,m} \equiv \sigma_m(K_p)$, with $\sigma_m(.)$, $\sigma_M(.)$ the minimum and maximum eigenvalues respectively. The constants M_m, M_M and C_M satisfy

$$0 < M_m \leq \|M(q)\| \leq M_M \tag{6.6}$$

$$\|C(q,w)\| \leq C_M\|w\|, \quad \text{for all } w \tag{6.7}$$

where w denotes an arbitrary vector.

The following result shows that when Assumption (A6.1) is satisfied the robot manipulator asymptotically tracks the desired trajectory. The result as well as its proof are taken from [81].

Proposition 6.1 (Prop. 2.1, [81]). *Suppose that assumption* (A6.1) *holds. Then the closed loop system (6.1, 6.3) is globally convergent, that is* $\tilde{q}$ *and* $\dot{\tilde{q}}$ *asymtptotically converge to zero, and all the internal signals are bounded.*

Proof. The proof strongly relies on the following well known properties of $C(q,.)$.

$$C(q,x)y = C(q,y)x \tag{6.8}$$

$$C(q,x+\alpha y) = C(q,x) + \alpha C(q,y) \tag{6.9}$$

for all $x, y, q \in \mathbb{R}^n$ and $\alpha \in \mathbb{R}$.

Using (6.9), the closed loop system given by (6.1) and (6.3) can be shown to satisfy

$$M(q)\ddot{\tilde{q}} + C(q,\dot{q})\dot{\tilde{q}} + \lambda C(q,\tilde{q})\dot{q}_d + K_d\dot{\tilde{q}} + K_p\tilde{q} = 0 \tag{6.10}$$

Consider the positive-definite candidate Lyapunov function

$$V(\tilde{q},\dot{\tilde{q}}) = \frac{1}{2}\psi^T M(q)\psi + \frac{1}{2}\tilde{q}^T K_p \tilde{q} \tag{6.11}$$

where $\psi = \dot{\tilde{q}} + \lambda\tilde{q}$. The time derivative of the candidate Lyapunov function along the flow of the system (6.10) is given by

$$\dot{V} = \psi^T[\lambda M(q)\dot{\tilde{q}} + \dot{\lambda}M(q)\tilde{q} + \lambda C(q,\dot{q})\tilde{q} - \lambda C(q,\tilde{q})\dot{q}_d - K_d\dot{q} - K_p\tilde{q}] + \dot{\tilde{q}}^T K_p\tilde{q}$$

where (6.9) and the skew-symmetry of $\dot{M}(q) - 2C(q,\dot{q})$ [82] have been used. Further, applying (6.8) and (6.9) yields

$$\dot{V} = -\psi^T[K_d - \lambda M(q)]\dot{\tilde{q}} + \dot{\lambda}\psi^T M(q)\tilde{q} + \lambda\psi^T C(q,\dot{\tilde{q}})\tilde{q} - \lambda\tilde{q}^T K_p\tilde{q} \tag{6.12}$$

Now we introduce a new variable, namely,

$$\psi_1 = \dot{\tilde{q}} + \frac{\lambda}{2}\tilde{q}$$

Then, (6.12) can be rewritten as

$$\begin{aligned}\dot{V} =& -\psi_1^T\big[K_d - \lambda M(q)\big]\psi_1 + \dot{\lambda}\psi^T M(q)\tilde{q} + \lambda\psi^T C(q,\dot{\tilde{q}})\tilde{q} \\ & - \left(\frac{\lambda\tilde{q}}{2}\right)^T \left[4\frac{K_p}{\lambda} - (K_d - \lambda M(q))\right]\left(\frac{\lambda\tilde{q}}{2}\right)\end{aligned} \tag{6.13}$$

Now we establish a bound on the second term

$$\begin{aligned}\dot{\lambda}\psi^T M(q)\tilde{q} =& -\frac{\lambda\tilde{q}^T\dot{\tilde{q}}}{\|\tilde{q}\|(1+\|\tilde{q}\|)}\psi^T M(q)\tilde{q} \\ =& -\frac{\lambda\tilde{q}^T(\psi_1 - \frac{\lambda}{2}\tilde{q})}{\|\tilde{q}\|(1+\|\tilde{q}\|)}(\psi_1 + \frac{\lambda}{2}\|\tilde{q}\|)^T M(q)\tilde{q} \\ \leq& \frac{\lambda M_M\|\tilde{q}\|}{1+\|\tilde{q}\|}\left(\|\psi_1\|^2 + 2\|\psi_1\|\left(\frac{\lambda}{2}\tilde{q}\right) + \left\|\frac{\lambda}{2}\tilde{q}\right\|^2\right) \\ \leq& \frac{2\lambda M_M\|\tilde{q}\|}{1+\|\tilde{q}\|}\left(\|\psi_1\|^2 + \left\|\frac{\lambda}{2}\tilde{q}\right\|^2\right) \\ \leq& 2\lambda_0 M_M\left(\|\psi_1\|^2 + \left\|\frac{\lambda}{2}\tilde{q}\right\|^2\right)\end{aligned} \tag{6.14}$$

and on the third term

$$\begin{aligned}\lambda\psi^T C(q,\dot{\tilde{q}})\tilde{q} =& \lambda\left(\psi_1 + \frac{\lambda}{2}\tilde{q}\right)^T C(q,\tilde{q})\left(\psi_1 - \frac{\lambda}{2}\tilde{q}\right) \\ \leq& \lambda C_M\|\tilde{q}\|\left(\|\psi_1\|^2 + 2\|\psi_1\|\left(\frac{\lambda}{2}\tilde{q}\right) + \left\|\frac{\lambda}{2}\tilde{q}\right\|^2\right) \\ \leq& 2\lambda C_M\|\tilde{q}\|\left(\|\psi_1\|^2 + \left\|\frac{\lambda}{2}\tilde{q}\right\|^2\right) \\ \leq& 2\lambda_0 C_M\left(\|\psi_1\|^2 + \left\|\frac{\lambda}{2}\tilde{q}\right\|^2\right)\end{aligned} \tag{6.15}$$

where (6.8) and (6.7) have been used in the first and the second steps, respectively.

Replacing these bounds in (6.13) and rearranging terms we obtain

$$\dot{V}(\tilde{q},\dot{\tilde{q}}) \leq -k_1\|\psi_1\|^2 - k_2\left\|\frac{\lambda}{2}\tilde{q}\right\|^2 \tag{6.16}$$

where

$$k_1 = K_{d,m} - 3\lambda_0 M_M - 2\lambda_0 C_M \tag{6.17}$$

$$k_2 = 4\lambda_0^{-1} K_{p,m} - K_{d,M} - 2\lambda_0 M_M - 2\lambda_0 C_M \tag{6.18}$$

The condition (6.5) ensures that k_1 and k_2 are positive. Thus $V(\tilde{q}, \dot{\tilde{q}})$ is a non-increasing function bounded from below. The definition of $V(\tilde{q}, \dot{\tilde{q}})$, (6.11), then implies that $\psi, \tilde{q} \in \mathcal{L}_\infty^n$, and consequently $\dot{\tilde{q}}, \psi_1 \in \mathcal{L}_\infty^n$. Further, since $\lambda \in \mathcal{L}_\infty$, (6.16) implies that $\psi_1, \tilde{q} \in \mathcal{L}_2^n$. From square integrability of $\tilde{q}$ and the fact that $\dot{\tilde{q}} \in \mathcal{L}_\infty^n$ we conclude that $\tilde{q}$ asymptotically converges to zero. Also notice that $\dot{\tilde{q}} \in \mathcal{L}_2^n$ and that the tracking error dynamics (6.10) implies $\ddot{\tilde{q}} \in \mathcal{L}_\infty^n$. Thus, $\dot{\tilde{q}}$ also asymptotically converges to zero. □

Now let us consider the event-triggered implementation of the controller (6.3). Recall the notation, from Section 1.3, used to denote the sampled data versions of different signals in the system. The sampled data version of any signal ζ (which can be a scalar, a vector or a matrix) is denoted by ζ_s. In particular, the data sampled by the controller is denoted by ξ_s, and is defined as

$$\xi_s(t) = \xi(t_i), \quad \text{for all } t \in [t_i, t_{i+1}), \quad \text{for each } i \tag{6.19}$$

where t_i are the sampling instants. All the other sampled data signals are similarly defined. The 'measurement error' of the sampled data is denoted by

$$e \triangleq \xi_s - \xi = \xi(t_i) - \xi, \quad \text{for } t \in [t_i, t_{i+1}),\ i \in \{0, 1, 2, ...\} \tag{6.20}$$

The sampled data controller is then given as

$$u_s = \gamma(\xi_s) = Y_s\theta - K_d\dot{\tilde{q}}_s - K_p\tilde{q}_s \tag{6.21}$$

Utilizing the measurement error view, the closed loop tracking error system can be written as a perturbation of (6.10).

$$M(q)\ddot{\tilde{q}} + C(q,\dot{q})\dot{\tilde{q}} + \lambda C(q,\tilde{q})\dot{q}_d + K_d\dot{\tilde{q}} + K_p\tilde{q} =$$

$$(Y_s - Y)\theta - K_d(\dot{\tilde{q}}_s - \dot{\tilde{q}}) - K_p(\tilde{q}_s - \tilde{q}) \tag{6.22}$$

Before we describe the event-triggering condition we state the **assumptions** that are made regarding the desired trajectory and the robot.

(A6.2) The desired trajectory $[q_d; \dot{q}_d]$, and its first two derivatives are uniformly bounded by known constants. That is, q_d, $\dot{q}_d$, $\ddot{q}_d$ and $\dddot{q}_d$ exist for all time, and are uniformly bounded by known constants d_0, d_1, d_2 and d_3, respectively.

(A6.3) The matrices $M(.)$, $C(.,.)$ and $G(.)$ are globally Lipschitz.

The following lemma is used to bound the terms on the right hand side of (6.22). In the sequel, the notation $|.|$ denotes the component-wise absolute value of a vector or matrix. A *Lipschitz vector* is similar to a Lipschitz constant. More specifically, it is a vector of non-negative elements other than the zero vector.

Lemma 6.1. *Suppose that assumptions* (A6.2),(A6.3) *and conditions* (6.6), (6.7) *hold. Also assume that* $K_p = K_p^T > 0$ *and* $K_d = K_d^T > 0$. *Then, there exist Lipschitz vectors* L_Y *and* D *that depend only on the sampled data, and the uniform bound on* $\dot{q}_d$ *such that*

$$\|(Y_s - Y)\theta\| \leq L_Y^T|e| \tag{6.23}$$

$$\|K_d(\dot{\tilde{q}}_s - \dot{\tilde{q}}) + K_p(\tilde{q}_s - \tilde{q})\| \leq D^T|e| \tag{6.24}$$

Proof. Equation (6.24) is satisfied with $D = [K_{p,M}\mathbf{1}_n; K_{d,M}\mathbf{1}_n; \mathbf{0}_{3n}]$, where $\mathbf{1}_n$ is an n dimensional vector of 1's and $\mathbf{0}_{3n}$ is a vector of zeros of dimension $3n$. Next, by (6.6) and assumption (A6.3), there exist constants M_M and L_M, respectively, such that

$$\begin{aligned}\|M(q_s)\ddot{q}_{d,s} - M(q)\ddot{q}_d\| &= \|(M(q_s) - M(q))\ddot{q}_{d,s} + M(q)(\ddot{q}_{d,s} - \ddot{q}_d)\| \\ &\leq L_M\|\ddot{q}_{d,s}\|\|q_s - q\| + M_M\|\ddot{q}_{d,s} - \ddot{q}_d\|\end{aligned}$$

Again, by (6.7) and assumption (A6.3), there exist constants C_M and L_C, respectively such that

$$\begin{aligned}\|C(q_s, \rho_s)\dot{q}_{d,s} - C(q, \rho)\dot{q}_d\| &= \|C(q_s, \dot{q}_{d,s})\rho_s - C(q, \dot{q}_d)\rho\| \\ &= \|(C(q_s, \dot{q}_{d,s}) - C(q, \dot{q}_d))\rho_s + C(q, \dot{q}_d)(\rho_s - \rho)\| \\ &\leq L_C\|\rho_s\|(\|q_s - q\| + \|\dot{q}_{d,s} - \dot{q}_d\|) + C_M d_1\|(\rho_s - \rho)\|\end{aligned}$$

where $\rho = \dot{q} - \lambda\tilde{q}$, ρ_s the sampled version of ρ and d_1 is a known upper bound for $\|\dot{q}_d\|$ from assumption (A6.1). Next, note that

$$\begin{aligned}\|(\rho_s - \rho)\| &= \|(\dot{q}_s - \lambda_s\tilde{q}_s) - (\dot{q} - \lambda\tilde{q})\| \\ &\leq \|\dot{q}_s - \dot{q}\| + \|\tilde{q}_s\||\lambda_s - \lambda| + \lambda\|\tilde{q}_s - \tilde{q}\|\end{aligned}$$

Now, note that

$$\begin{aligned}|\lambda_s - \lambda| &= \lambda_0\left|\frac{1}{1 + \|\tilde{q}_s\|} - \frac{1}{1 + \|\tilde{q}\|}\right| \leq \lambda_s\Big|\|\tilde{q}_s\| - \|\tilde{q}\|\Big| \\ &\leq \lambda_s\|\tilde{q}_s - \tilde{q}\|\end{aligned}$$

Noting that $\lambda \leq \lambda_0$, for all $\tilde{q}$, we see that

$$\begin{aligned}\|(\rho_s - \rho)\| &\leq \|\dot{q}_s - \dot{q}\| + \lambda_s \|\tilde{q}_s\| \|\tilde{q}_s - \tilde{q}\| + \lambda_0 \|\tilde{q}_s - \tilde{q}\| \\ &\leq L_\rho^T |e|\end{aligned}$$

where L_ρ is a vector that depends only on the sampled data. Finally, assumption (A6.3) also guarantees a constant L_G such that

$$\|G(q_s) - G(q)\| \leq L_G \|q_s - q\|$$

By the linear parametrizability of robot dynamics, we know that

$$Y(q, \rho, \dot{q}_d, \ddot{q}_d)\theta = M(q)\ddot{q}_d + C(q, \rho)\dot{q}_d + G(q)$$

Hence, there exists a Lipschitz vector L_Y that depends only on the sampled data such that

$$\|(Y_s - Y)\theta\| \leq L_Y^T |e|$$

□

Notice that the process of computing the Lipschitz vectors is simplified considerably by allowing them to depend on the sampled data. For example, the approach adopted in Chapter 5 requires an appropriate set to be defined first over which a Lipschitz vector is computed. Such a Lipschitz vector holds for any two points in the set. However, we only need to estimate the 'error' in a function with respect to a fixed sampled value. Using this fact, for the system under consideration in this chapter, it is possible to find a Lipschitz vector in terms of the sampled data that

holds 'globally' - in the sense that one of the points where the function is evaluated at is the fixed sample point while the other can be any arbitrary point. As seen from the results in the sequel, such a formulation simplifies the analysis considerably compared to that in Chapter 5.

Now let

$$\alpha(\tilde{x}) = k_1 \left|\left| \dot{\tilde{q}} + \frac{\lambda}{2}\tilde{q} \right|\right|^2 + k_2 \left|\left| \frac{\lambda}{2}\tilde{q} \right|\right|^2 \tag{6.25}$$

$$\beta(\tilde{x}) = \|\psi\| = \|\dot{\tilde{q}} + \lambda \tilde{q}\| \tag{6.26}$$

where k_1 and k_2 are given by (6.17) and (6.18), respectively. Then we define the sampling or control execution instants implicitly with an event-triggering condition in the following way.

$$t_0 = 0$$

$$t_{i+1} = \min\{t \geq t_i : \beta(\tilde{x}) L^T |\xi(t_i) - \xi(t)| \geq \sigma \alpha(\tilde{x})\} \tag{6.27}$$

where $\sigma \in (0, 1)$ is a design parameter, $L = L_Y + D$ with L_Y and D satisfying Lemma 6.1. Notice that each update instant t_{i+1} is defined implicitly with respect to t_i. Hence, the initial update instant t_0 has been specified separately. Given this event-trigger, the following result demonstrates the global convergence of the tracking error to zero.

Theorem 6.2. *Under assumptions* (A6.1)-(A6.3) *and dynamics* (6.1), (6.21), (6.27), *the tracking error,* $\tilde{x} = [\tilde{q}; \dot{\tilde{q}}]$ *globally asymptotically converges to zero.*

Proof. Consider the candidate Lyapunov function.

$$V(\tilde{q}, \dot{\tilde{q}}) = \frac{1}{2}\psi^T M(q)\psi + \frac{1}{2}\tilde{q}^T K_p \tilde{q}$$

Through the measurement error view of (6.22) and the analysis of 6.1, it can be shown that the derivative of the candidate Lyapunov function along the flow of the closed loop system (6.1), (6.21), (6.27) satisfies the following.

$$\begin{aligned}\dot{V} &\leq -\alpha(\tilde{x}) + \psi^T\left[(Y_s - Y)\theta - K_d(\dot{\tilde{q}}_s - \dot{\tilde{q}}) - K_p(\tilde{q}_s - \tilde{q})\right] \\ &\leq -\alpha(\tilde{x}) + \beta(\tilde{x})L^T|e|\end{aligned}$$

where the second step is obtained using the definitions of β, (6.26) and L. The triggering condition (6.27) ensures that $\beta(\tilde{x})L^T|e| \leq \sigma\alpha(\tilde{x})$, which then implies that

$$\dot{V} \leq -(1-\sigma)\alpha(\tilde{x})$$

Then, asymptotic convergence of $\tilde{q}$ and $\dot{\tilde{q}}$ to zero follows from arguments used in the proof of Proposition 6.1. □

Now, it must be pointed out that both the control law (6.21) and the triggering condition (6.27) (through L) depend on the knowledge of a good model of the robot system. However, in many applications an accurate model is not available. If only a poor model is available then the tracking performance may deteriorate. It would be useful for practical applications to incorporate adaptation in the event-triggered controller. In the next section, we present the methodology for accomplishing this goal.

6.3 Event Based Adaptive Control

In this section, the adaptive controller from [81] for tracking in robot manipulators is introduced, and a utility driven event-triggered implementation of it is developed.

Consider the following controller and adaptation law from [81]

$$u = \hat{M}(q)\ddot{q}_d + \hat{C}(q, \dot{q} - \lambda\tilde{q})\dot{q}_d + \hat{G}(q) - K_d\dot{\tilde{q}} - K_p\tilde{q}$$

$$= Y(q, \dot{q} - \lambda\tilde{q}, \dot{q}_d, \ddot{q}_d)\hat{\theta} - K_d\dot{\tilde{q}} - K_p\tilde{q} \tag{6.28}$$

$$\dot{\hat{\theta}} = -\Gamma^{-1}Y^T(q, \dot{q} - \lambda\tilde{q}, \dot{q}_d, \ddot{q}_d)\psi \tag{6.29}$$

where $Y(.)$ is a regressor matrix, $\psi = \dot{\tilde{q}} + \lambda\tilde{q}$, Γ is an arbitrary positive definite matrix and $\hat{\theta}$ is a vector of estimates of the true system parameters θ, which depend on parameters such as link masses and link lengths. Then, the following result can be proven, which is taken from [81] and stated here without proof.

Proposition 6.3 (Prop. 3.1, [81]). *Suppose that assumption* (A6.1) *holds. Then the adaptive system (6.1, 6.28, 6.29) is globally convergent, that is $\tilde{q}$ and $\dot{\tilde{q}}$ asymtptotically converge to zero, and all the internal signals are bounded.*

The proof of this proposition is similar to Proposition 6.1 and relies on the candidate Lyapunov function

$$V(\tilde{q}, \dot{\tilde{q}}, \tilde{\theta}) = \frac{1}{2}\psi^T M(q)\psi + \frac{1}{2}\tilde{q}^T K_p\tilde{q} + \frac{1}{2}\tilde{\theta}^T\Gamma\tilde{\theta} \tag{6.30}$$

where $\Gamma = \Gamma^T$ is a positive definite matrix and $\tilde{\theta} \triangleq \hat{\theta} - \theta$ is the parameter estimation error.

Now, we develop an event-triggered adaptive controller based on (6.28)-(6.29). First, we make the following assumption

(A6.4) An upper bound on each of the parameters θ_i is known, that is, $\bar{\theta}$ is known such that $\theta_i \leq \bar{\theta}_i$.

Note that the conditions (6.6), (6.7), (A6.3) on the one hand and (A6.4) on other are not entirely independent. However, (A6.4) is a convenient form to base our design on.

Now, the complete system including the robot dynamics, the event-triggered controller and the adaptation law are as follows.

$$M(q)\ddot{q} + C(q,\dot{q})\dot{q} + G(q) = u_s, \quad q \in \mathbb{R}^n \tag{6.31}$$

$$u_s = Y_s\hat{\theta}_s - K_d\dot{\tilde{q}}_s - K_p\tilde{q}_s = \gamma(\xi_s), \quad \text{if } t \geq t_0 \tag{6.32}$$

$$\xi \triangleq [\tilde{q}; \dot{\tilde{q}}; q_d; \dot{q}_d; \ddot{q}_d; \hat{\theta}] \tag{6.33}$$

$$\xi_s(t) = \xi(t_i), \quad \text{for all } t \in [t_i, t_{i+1}), \quad \text{for each } i$$

$$t_0 = 0$$

$$t_{i+1} = \min\{t \geq t_i : \beta(\tilde{x})L^T|\xi(t_i) - \xi(t)| \geq \sigma\alpha(\tilde{x})\} \tag{6.34}$$

$$\dot{\hat{\theta}} = -\Gamma^{-1}Y_s^T\psi, \quad \text{if } t \geq t_0 \tag{6.35}$$

where $\sigma \in (0,1)$ is a design parameter. Notice that the data required by the controller is, ξ, now additionally includes $\hat{\theta}$ compared to that in Section 6.2. Equations (6.32)-(6.34) provide a complete description of the event-triggered controller. The condition that implicitly defines the sampling instants (6.34) is the event-trigger. The functions α and β are given by (6.25) and (6.26), respectively. The vector $L = L_Y + D + N$, where L_Y and D satisfy Lemma 6.1 (with e defined appropriately to include $\hat{\theta}_s - \hat{\theta}$) whereas N is a Lipschitz vector that satisfies

$$\|Y_s(\hat{\theta}_s - \hat{\theta})\| \leq N^T|e|$$

More specifically, $N = [\mathbf{0}^T, \text{ Column-wise sum of } |Y_s|\,]^T$, where $\mathbf{0}$ is a vector of zeros

of appropriate dimension. Given this complete system, the following result demonstrates the global convergence of the tracking error to zero.

Theorem 6.4. *Under assumptions* (A6.1)-(A6.3) *and dynamics* (6.31)-(6.35)*, the tracking error,* $\tilde{x} = [\tilde{q}; \dot{\tilde{q}}]$ *globally asymptotically converges to zero.*

Proof. Using the measurement error approach, the tracking error dynamics can be shown to satisfy

$$\begin{aligned} &M(q)\ddot{\tilde{q}} + C(q,\dot{q})\dot{\tilde{q}} + \lambda C(q,\tilde{q})\dot{q}_d + K_d\dot{\tilde{q}} + K_p\tilde{q} \\ &= (Y_s\hat{\theta}_s - Y\theta) - K_d(\dot{\tilde{q}}_s - \dot{\tilde{q}}) - K_p(\tilde{q}_s - \tilde{q}) \end{aligned}$$

which is essentially a perturbed version of (6.10). Now, consider the candidate Lyapunov function (6.30). Again, following the analysis in Proposition 6.1, the derivative of the Lyapunov function along the flow of the closed loop system (6.31)-(6.35) can be shown to satisfy

$$\begin{aligned} \dot{V} &\leq -\alpha(\tilde{x}) + \tilde{\theta}^T\Gamma\dot{\tilde{\theta}} + \psi^T\left[(Y_s\hat{\theta}_s - Y\theta) - K_d(\dot{\tilde{q}}_s - \dot{\tilde{q}}) - K_p(\tilde{q}_s - \tilde{q})\right] \\ &= -\alpha(\tilde{x}) + \tilde{\theta}^T\Gamma\dot{\tilde{\theta}} + \psi^T\left[(Y_s - Y)\theta + Y_s(\hat{\theta}_s - \hat{\theta}) + Y_s\tilde{\theta} - K_d(\dot{\tilde{q}}_s - \dot{\tilde{q}}) - K_p(\tilde{q}_s - \tilde{q})\right] \\ &= -\alpha(\tilde{x}) + \psi^T\left[(Y_s - Y)\theta + Y_s(\hat{\theta}_s - \hat{\theta}) - K_d(\dot{\tilde{q}}_s - \dot{\tilde{q}}) - K_p(\tilde{q}_s - \tilde{q})\right] + \tilde{\theta}^T\left[\Gamma\dot{\tilde{\theta}} + Y_s^T\psi\right] \\ &= -\alpha(\tilde{x}) + \beta(\tilde{x})L^T|e| + 0 \end{aligned}$$

where the last step is obtained using the definition of β, (6.26), the definition of L and the adaptation law (6.35). The event-trigger (6.34) ensures that $\beta(\tilde{x})L^T|e| \leq \sigma\alpha(\tilde{x})$, which then implies that

$$\dot{V} \leq -(1-\sigma)\alpha(\tilde{x}) < 0$$

The rest of the proof is similar to that of Proposition 6.1. □

Notice that in our treatment so far, the implementation aspects arising out of implicitly defined sampling instants given by (6.34) have not been discussed. For example, implicitly defined inter-sample times may exhibit zeno behavior - sampling infinitely many times in a finite time period, which is something not realistically implementable. Ideally, it is good to have a positive lower bound between every two consecutive sample times. Given that sampling the complete system data involves sampling an external desired trajectory as well as parameter estimates resulting from adaptation along with the state of the robot system, it is not easy to provide analytical bounds that hold globally, semi-globally or even over significant regions of the state space. Therefore, in the following subsection, we provide a method to analytically estimate the inter-sample time as a function of only the tracking error, independent of the robot parameter estimation error.

6.3.1 Inter-sample times

The basic idea behind the method we have adopted to estimate the inter-sampling times is to estimate an upper bound on $\|e\|$, and a lower bound on $\frac{\sigma\alpha(\tilde{x})}{\|L\|\beta(\tilde{x})}$ as functions of time since the last sample. Then, from (6.34) it is seen that, the time required for the above two quantities to equal each other provides a lower estimate of the inter-sample time. As a first step, we provide estimates of $\alpha(\tilde{x})$ and $\beta(\tilde{x})$ as functions of $\|\tilde{x}\|$.

$$\alpha(\tilde{x}) = k_1\Big(\dot{\tilde{q}} + \frac{\lambda}{2}\tilde{q}\Big)^T\Big(\dot{\tilde{q}} + \frac{\lambda}{2}\tilde{q}\Big) + k_2\Big(\frac{\lambda}{2}\tilde{q}\Big)^T\Big(\frac{\lambda}{2}\tilde{q}\Big)$$
$$= [\tilde{q}; \dot{\tilde{q}}]^T \begin{bmatrix} \frac{\lambda^2}{4}(k_1+k_2)I_n & \frac{\lambda}{2}k_1 I_n \\ \frac{\lambda}{2}k_1 I_n & k_1 I_n \end{bmatrix} [\tilde{q}; \dot{\tilde{q}}]$$

where I_n is a $n \times n$ identity vector and $[\tilde{q}; \dot{\tilde{q}}]$ is a concatenated column vector. The two distinct eigenvalues of the matrix are given by

$$s_\alpha = \frac{\lambda^2(k_1+k_2)+4k_1}{8} \pm \frac{\sqrt{\big(\lambda^2(k_1+k_2)-4k_1\big)^2 + 16\lambda^2 k_1^2}}{8}$$

Note $\lambda = \dfrac{\lambda_0}{1+\|\tilde{q}\|}$ is a function of $\|\tilde{q}\|$ and so are the eigenvalues s_α. Now, since $\lambda_0 > 0$, $\lambda > 0$ for any finite value of $\|\tilde{q}\|$. Thus, both the eignevalues, s_α, are strictly positive for any finite value of $\|\tilde{q}\|$ and the smaller eigenvalue converges to 0 as $\|\tilde{q}\|$ converges to ∞. We denote the smaller of the eigenvalues s_α as

$$a(\tilde{q}) \triangleq \frac{\lambda^2(k_1+k_2)+4k_1}{8} - \frac{\sqrt{\big(\lambda^2(k_1+k_2)-4k_1\big)^2 + 16\lambda^2 k_1^2}}{8} \tag{6.36}$$

Thus for any finite $\tilde{x}$,

$$a(\tilde{q})\|\tilde{x}\|^2 \leq \alpha(\tilde{x}) \tag{6.37}$$

Similarly,

$$\beta(\tilde{x}) = \|\psi\| = \sqrt{(\dot{\tilde{q}} + \lambda\tilde{q})^T(\dot{\tilde{q}} + \lambda\tilde{q})}$$
$$= \sqrt{\begin{bmatrix} \tilde{q} & \dot{\tilde{q}} \end{bmatrix} \begin{bmatrix} \lambda^2 I_n & 2\lambda I_n \\ 2\lambda I_n & I_n \end{bmatrix} \begin{bmatrix} \tilde{q} \\ \dot{\tilde{q}} \end{bmatrix}}$$

The $2n \times 2n$ matrix in the above equation has only two distinct eigenvalues, which are given by

$$s_\beta = \frac{(\lambda^2+1) \pm \sqrt{(\lambda^2+1)^2 + 12\lambda^2}}{2}$$

The largest eigenvalue is an increasing function of λ and since $\lambda \leq \lambda_0$ for all $\tilde{q}$, the following quantity is an upper bound for the eigenvalues s_β.

$$b^2 = \frac{(\lambda_0^2+1) + \sqrt{(\lambda_0^2+1)^2 + 12\lambda_0^2}}{2} \tag{6.38}$$

Then,

$$\beta(\tilde{x}) = \|\psi\| \leq b\|\tilde{x}\| \tag{6.39}$$

The next step in the procedure is to estimate an upper bound on the rate of change of $\|e\|$. Notice that $e = \xi_s - \xi = \xi(t_i) - \xi$, for $t \in [t_i, t_{i+1})$ and each i, where ξ is the data given in (6.33). Therefore, $\dot{e} = -\dot{\xi}$. Hence, we look at how the derivative of each of the components of ξ (see (6.33)) can be bounded, starting with that of $\tilde{\theta}$. From (6.35), we see that

$$\frac{\mathrm{d}\|\tilde{\theta}\|}{\mathrm{d}t} \leq \|\Gamma^{-1} Y_s^T \psi\| \leq b\|\Gamma^{-1} Y_s^T\|.\|\tilde{x}\| \tag{6.40}$$

where (6.39) has been used to obtain the second inequality. The rate of change of the desired trajectory, and its derivatives is provided by Assumption (A6.2). In fact, only the constant d_3 is required here, as seen in the following equation.

$$\frac{\mathrm{d}}{\mathrm{d}t}\begin{bmatrix} \|q_d\| \\ \|\dot{q}_d\| \\ \|\ddot{q}_d\| \end{bmatrix} = \begin{bmatrix} 0 & 1 & 0 \\ 0 & 0 & 1 \\ 0 & 0 & 0 \end{bmatrix}\begin{bmatrix} \|q_d\| \\ \|\dot{q}_d\| \\ \|\ddot{q}_d\| \end{bmatrix} + \begin{bmatrix} 0 \\ 0 \\ d_3 \end{bmatrix} \tag{6.41}$$

Next, from the robot dynamics (6.31) and the sampled data controller (6.32), the equation of motion can be written as

$$
\begin{aligned}
&M(q)\ddot{q} + C(q,\dot{q})\dot{q} + G(q) \\
&= Y\theta + (Y_s\hat{\theta}_s - Y\theta) - K_d\dot{\tilde{q}}_s - K_p\tilde{q}_s \\
&= M(q)\ddot{q}_d + C(q,\rho)\dot{q}_d + G(q) + (Y_s\hat{\theta}_s - Y\theta) - K_d\dot{\tilde{q}}_s - K_p\tilde{q}_s
\end{aligned}
$$

After rearranging terms we obtain

$$
M(q)\ddot{\tilde{q}} + C(q,\dot{q})\dot{\tilde{q}} + C(q,\lambda\tilde{q})\dot{q}_d = (Y_s - Y)\theta + Y_s(\hat{\theta}_s - \hat{\theta}) + Y_s\tilde{\theta} - K_d\dot{\tilde{q}}_s - K_p\tilde{q}_s
$$

where $\tilde{\theta} = \hat{\theta} - \theta$. Thus,

$$
\ddot{\tilde{q}} = M^{-1}(q)[-C(q,\dot{q})\dot{\tilde{q}} - C(q,\lambda\tilde{q})\dot{q}_d + (Y_s - Y)\theta + Y_s(\hat{\theta}_s - \hat{\theta}) + Y_s\tilde{\theta} - K_d\dot{\tilde{q}}_s - K_p\tilde{q}_s]
$$

Then by assumption (A6.1) and Lemma 6.1, it follows that

$$
\frac{\mathrm{d}\|\ddot{\tilde{q}}\|}{\mathrm{d}t} \leq \frac{1}{M_m}\left[C_M\|\dot{q}\|\|\dot{\tilde{q}}\| + C_M\|\lambda\tilde{q}\|\|q_d\| + \|L\|\|e\| + \|Y_s\|\|\tilde{\theta}\| + K_d\|\dot{\tilde{q}}_s\| + K_p\|\tilde{q}_s\|\right] \tag{6.42}
$$

Now, we introduce two new variables. Let $e_{\tilde{x}}$ and e_d be the measurement error in the tracking error $\tilde{x}$ and the rest of the data, respectively. That is,

$$
e_{\tilde{x}} = \tilde{x}_s - \tilde{x} \tag{6.43}
$$

$$
e_d = [q_{d,s}; \dot{q}_{d,s}; \ddot{q}_{d,s}; \hat{\theta}_s] - [q_d; \dot{q}_d; \ddot{q}_d; \hat{\theta}] \tag{6.44}
$$

Hence, $e = [e_{\tilde{x}}; e_d]$. From (6.40)-(6.42) along with the facts that $\dot{e} = -\dot{\xi}$ and $\xi = \xi_s - e$, we see that

$$
\frac{\mathrm{d}}{\mathrm{d}t}\begin{bmatrix}\|e_{\tilde{x}}\| \\ \|e_d\|\end{bmatrix} \leq A\begin{bmatrix}\|e_{\tilde{x}}\| \\ \|e_d\|\end{bmatrix} + B_1\frac{C_M\|\dot{q}\|\|\dot{\tilde{q}}\|}{M_m} + B_2 \tag{6.45}
$$

where A and B_2 are matrices that depend on sampled data and system constants, and $B_1 = [1; 0]$. Thus, for any finite ξ_s, the matrices A, B_1 and B_2 are finite. However, we still have a nonlinear term. To simplify the analysis let us consider a ball in $\mathbb{R}^{2n}$ centred around $\tilde{x}_s$. More specifically, if we let $R_s \triangleq \|\tilde{x}_s\|$, then consider the ball defined by $\mathcal{R}_s^h \triangleq \{\tilde{x} : \|e_{\tilde{x}}\| \leq hR_s\}$ for any arbitrary $h > 0$. On this set $\|\dot{\tilde{q}}\| \leq (1+h)R_s$ and hence it is possible to obtain a linear differential equation as follows

$$\frac{\mathrm{d}}{\mathrm{d}t}\begin{bmatrix}\|e_{\tilde{x}}\| \\ \|e_d\|\end{bmatrix} \leq A_1 \begin{bmatrix}\|e_{\tilde{x}}\| \\ \|e_d\|\end{bmatrix} + B_3, \quad \forall\, e \text{ s.t. } \|e_{\tilde{x}}\| \leq hR_s \tag{6.46}$$

where A_1 and B_3 depend on sampled data and are finite for any finite ξ_s. At any given sample instants t_i, $\xi_s = \xi = \xi(t_i)$. Hence, $\|e\| = 0$ at $t = t_i$ for each i. Therefore, by using the Comparison Lemma [45] and (6.46) it is possible to estimate the time it takes for $\|e_{\tilde{x}}\|$ to grow from 0 to hR_s. Let this time be T_1. Therefore, (6.46) is useful for further analysis only over this time period.

The triggering condition ensures that

$$\|e\| \leq \frac{\alpha(\tilde{x})}{\|L\|\beta(\tilde{x})}$$

and the inter-sample time is lower bounded by the time it takes $\|e\|$ to grow from 0 to $\dfrac{\alpha(\tilde{x})}{\|L\|\beta(\tilde{x})}$. The estimation of this time can be simplified in the following way. On the set $\mathcal{R}_s^h = \{\tilde{x} : \|e_{\tilde{x}}\| \leq hR_s\}$, $a(\|\tilde{q}\|)$ attains a minimum, which we denote by a_s^h. Thus on this set,

$$\frac{\alpha(\tilde{x})}{\|L\|\beta(\tilde{x})} \geq \frac{a_s^h\|\tilde{x}\|^2}{\|L\|b\|\tilde{x}\|} = \frac{a_s^h(\|\tilde{x}_s - e_{\tilde{x}}\|)}{\|L\|b} \tag{6.47}$$

Notice that this equation is well defined for all $\tilde{x} \neq 0$. Now let T_2 be the time defined as

$$T_2 = \min\{(t - t_i) > 0 : b\|L\|\|e\| = a_s^h(\|\tilde{x}_s\| - \|e_{\tilde{x}}\|)\} \tag{6.48}$$

This time T_2 can be found numerically or estimated analytically from (6.46). Then, the inter-sample time $t_{i+1} - t_i \geq \min\{T_1, T_2\}$ when $\xi_s = \xi(t_i)$. Clearly, this inter-sample time is greater than zero if $\tilde{x}_s \neq 0$. However, the analysis presented so far is not powerful enough to provide an explicit and non-conservative lower bound for inter-sample times over a region of interest. We believe numerical analysis would reveal such bounds much more efficiently. Note, however, finding estimates of T_1 and T_2 for any given sampling point doesn't require the exact knowledge of the robot parameters, which is a significant advantage from a practical perspective.

In the next section, we present a dynamic model of a two-link planar manipulator on which we have performed simulations and conducted experiments.

6.4 Two Link Planar Manipulator

In this section we describe the dynamic model of a planar two-link revolute joint arm, with both the joints driven by motors mounted at the base. We choose this model because of a similar driving mechanism in PHANToM Omni. A schematic of the arm is shown along with the generalized coordinates in Figure 6.1. The $M(q)$, $C(q, \rho)$ and $G(q)$ matrices can be easily found from the Euler-Lagrange equations,

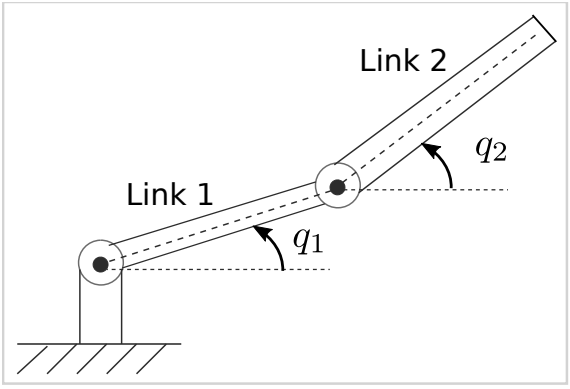

Figure 6.1: A schematic of a two link planar revolute manipulator with the second link remotely driven from base of Link 1.

and are given as follows.

$$M(q) = \begin{bmatrix} m_1 l_{c_1}^2 + m_2 l_1^2 + I_1 & m_2 l_1 l_{c_2} \cos(q_2 - q_1) \\ m_2 l_1 l_{c_2} \cos(q_2 - q_1) & m_2 l_{c_2}^2 + I_2 \end{bmatrix}$$

$$C(q, \rho)$$

$$= \begin{bmatrix} 0 & -m_2 l_1 l_{c_2} \sin(q_2 - q_1)\rho_2 \\ m_2 l_1 l_{c_2} \sin(q_2 - q_1)\rho_1 & 0 \end{bmatrix}$$

$$G(q) = \begin{bmatrix} (m_1 l_{c_1} + m_2 l_1) g cos(q_1) \\ m_2 l_{c_2} g cos(q_2) \end{bmatrix}$$

where m_i, l_i, l_{c_i} and I_i are the mass, length, distance of the center of mass from the joint, and moment of inertia about the center of mass of the i^{th} link, respectively.

Thus, the regressor matrix is given as

$$
\begin{aligned}
&Y(q, \rho, \dot{q}_d, \ddot{q}_d)^T \\
&= \begin{bmatrix}
\ddot{q}_{d,1} & 0 \\
\ddot{q}_{d,2}\cos(q_2 - q_1) - \dot{q}_{d,2}\sin(q_2 - q_1)\rho_2 & \ddot{q}_{d,1}\cos(q_2 - q_1) + \dot{q}_{d,1}\sin(q_2 - q_1)\rho_1 \\
0 & \ddot{q}_{d,2} \\
\cos(q_1) & 0 \\
0 & \cos(q_2)
\end{bmatrix}
\end{aligned}
$$

and the vector of parameters is given as

$$
\theta = \begin{bmatrix}
m_1 l_{c_1}^2 + m_2 l_1^2 + I_1 \\
m_2 l_1 l_{c_2} \\
m_2 l_{c_2}^2 + I_2 \\
(m_1 l_{c_1} + m_2 l_1) g \\
m_2 l_{c_2} g
\end{bmatrix} \tag{6.49}
$$

The vector L_Y is given as

$$L_Y = \begin{bmatrix} \bar{\theta}_2(\phi_{s,1} + d_1\phi_{s,2}) + \bar{\theta}_4 \\ \bar{\theta}_2(\phi_{s,1} + d_1\phi_{s,2}) + \bar{\theta}_5 \\ \bar{\theta}_2 d_1 \\ \bar{\theta}_2 d_1 \\ \bar{\theta}_2\phi_{s,1} + \bar{\theta}_4 \\ \bar{\theta}_2\phi_{s,1} + \bar{\theta}_5 \\ \bar{\theta}_2(|\rho_{s,1}| + d_1) \\ \bar{\theta}_2(|\rho_{s,2}| + d_1) \\ \bar{\theta}_1 + \bar{\theta}_2 \\ \bar{\theta}_3 + \bar{\theta}_2 \\ \mathbf{0} \end{bmatrix} \tag{6.50}$$

$$\phi_{s,1} = |\rho_{s,1}\dot{q}_{d,s,1}| + |\rho_{s,2}\dot{q}_{d,s,2}| + |\ddot{q}_{d,s,1}| + |\ddot{q}_{d,s,2}|$$

$$\phi_{s,2} = \lambda_s(1 + 2|\tilde{q}_{s,1}| + 2|\tilde{q}_{s,2}|)$$

where $\rho_{s_k} = \dot{q}_{s,k} - \lambda_s\tilde{q}_{s,k}$, for $k = 1, 2$, $\mathbf{0}$ is a vector of zeros of appropriate dimension and $\bar{\theta}_i$ are from (A6.4). As in section 6.3, $L = L_Y + N + D$. Notice that most of the elements in these vectors are constants or easily computable functions of the sampled data. Of course when a good model of the system is available (the system parameters θ_i are known with good accuracy), $\bar{\theta}_i$ in the definition of L_Y may simply be replaced with θ_i. In the next section we present the simulation and experimental results.

6.5 Results

In both the simulation and experimental results presented here, the position variables of the desired trajectory was chosen as

$$q_{d,1} = -0.4(\cos(0.8t) - 1.1)$$

$$q_{d,2} = -0.4(\cos(0.3\pi t) - 1) - (\pi/2)$$

The signals $\dot{q}_d$, $\ddot{q}_d$ and $\dddot{q}_d$ were defined simply as the corresponding derivatives of q_d. The control gains and the parameters were chosen as

$$\lambda_0 = 0.7, \quad K_d = 0.03, \quad K_p = 0.7, \quad \sigma \in \{0.95, 0.6, 0.2\}$$

$$\Gamma = \text{diag}([30, 40, 50, 10, 10]^T)$$

$$d_2 = 0.5$$

where d_2 is the uniform upper bound on $|\dot{q}_{d,1}|$ and $|\dot{q}_{d,2}|$. The initial condition of the robot was chosen as

$$[q_1, q_2, \dot{q}_1, \dot{q}_2]^T(0) = [0, -\pi/2, 0, 0]^T$$

6.5.1 Simulation Results

In the simulations, the true robot parameters were assumed to be the following.

$$m_1 = 0.065, \quad m_2 = 0.065, \quad I_1 = 10^{-5}, \quad I_2 = 10^{-5}$$

$$l_1 = 0.14, \quad l_2 = 0.2, \quad l_{c,1} = 0.07, \quad l_{c,2} = 0.09, \quad g = 9.8$$

thus giving $\theta = [0.0016; 0.0008; 0.0005; 0.1338; 0.0573]$.

In the first set of simulations, we avoid adaptation and show the effect of an inaccurate knowledge of the parameters θ_i. In these set of simulations $\sigma = 0.95$ was chosen. Figure 6.2 shows the results when the controller has exact knowledge of the robot parameters (Figure 6.2(a)), and when the controller has an inaccurate knowledge of the robot parameters (Figure 6.2(b)). These figures show the norm of the tracking error, $\|\tilde{x}\|$. In addition, the former figure also shows the measurement error scaled such that it equals $\|\tilde{x}\|$ whenever the equality is satisfied in the triggering condition (6.27). In the first case, the norm of the tracking error converges to zero very quickly while in the latter case the tracking error does not converge even after a long time. In the second case, the controller assumes robot parameters

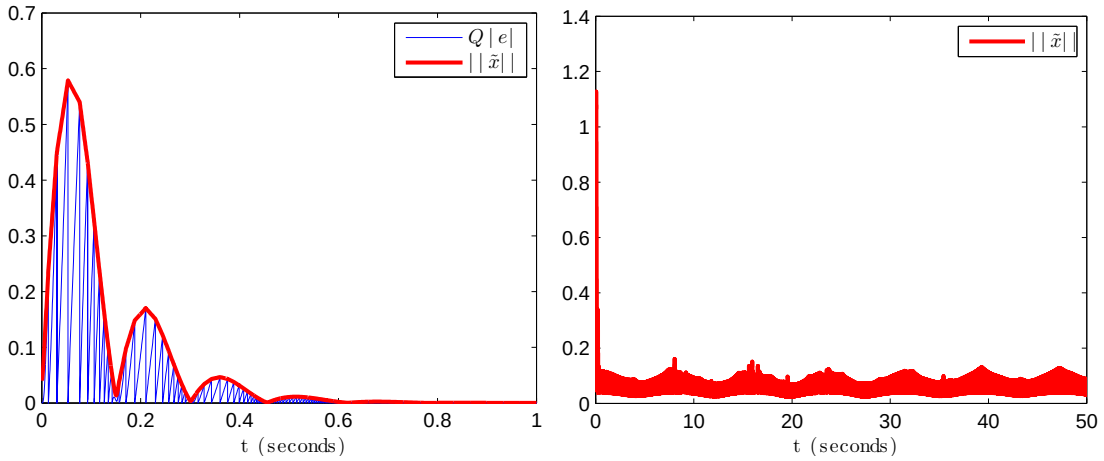

(a) (b)

Figure 6.2: (a) Controller has exact knowledge of the robot parameters. The figure shows norm of the tracking error and the scaled measurement error. (b) Controller has inaccurate knowledge of the robot parameters. The figure shows norm of the tracking error.

to be $\hat{\theta} = [0.0019; 0.0010; 0.0004; 0.1605; 0.0459]$ while the actual parameters were

$\theta = [0.0016; 0.0008; 0.0005; 0.1338; 0.0573]$, which represents a plus/minus 20% error in each of the parameters.

For the simulations with adaptation, we first assumed

$$\bar{\theta} = [0.0035, 0.0035, 0.002, 0.2, 0.1]^T, \quad h_l = 10^{-8}$$

where h_l is a lower bound on $(\theta_1\theta_3 - \theta_2^2)$, which can be easily shown to be positive for a two link manipulator. Using these quantities, M_M, M_m and C_M can be estimated as

$$M_M = \frac{\bar{\theta}_1 + \bar{\theta}_3 + \sqrt{\left(\bar{\theta}_1 + \bar{\theta}_3\right)^2 - 4h_l}}{2}$$
$$M_m = \frac{\bar{\theta}_1 + \bar{\theta}_3 - \sqrt{\left(\bar{\theta}_1 + \bar{\theta}_3\right)^2 - 4h_l}}{2}$$
$$C_M = \bar{\theta}_2$$

Finally, the initial system parameter estimates have been chosen as

$$\hat{\theta}(0) = [0.0001, 0.0001, 0.0001, 0.01, 0.001]^T$$

The choice of such low initial values for $\hat{\theta}$ is motivated by the fact that initial torques will be lower in the absence of knowledge of the system parameters.

Figure 6.3 shows, for the cases of $\sigma = 0.6$ and $\sigma = 0.95$, the norm of the tracking error, $\|\tilde{x}\| = \|[\tilde{q}; \dot{\tilde{q}}]\|$. As expected, the convergence is faster for the case with the smaller $\sigma = 0.6$. Figure 6.4 shows the desired and the actual joint positions as functions of time.

The observed minimum inter-update times and average frequency in simulations are reported in Table 6.1.

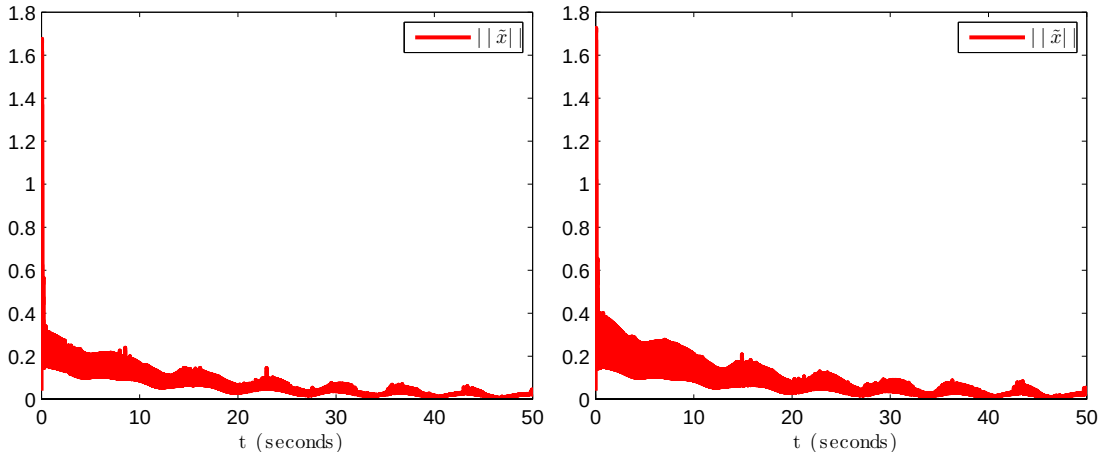

(a) (b)

Figure 6.3: The norm of the tracking error and the scaled measurement error. (a) $\sigma = 0.6$ (b) $\sigma = 0.95$

Table 6.1: The observed minimum inter-update times and average frequency in simulations.

σ	Observed minimum inter-update time (s)	Observed average Frequency (Hz)
0.6	0.0017	28
0.95	0.0028	26.5

Next, we present the experimental results of the algorithm on a PHANToM Omni.

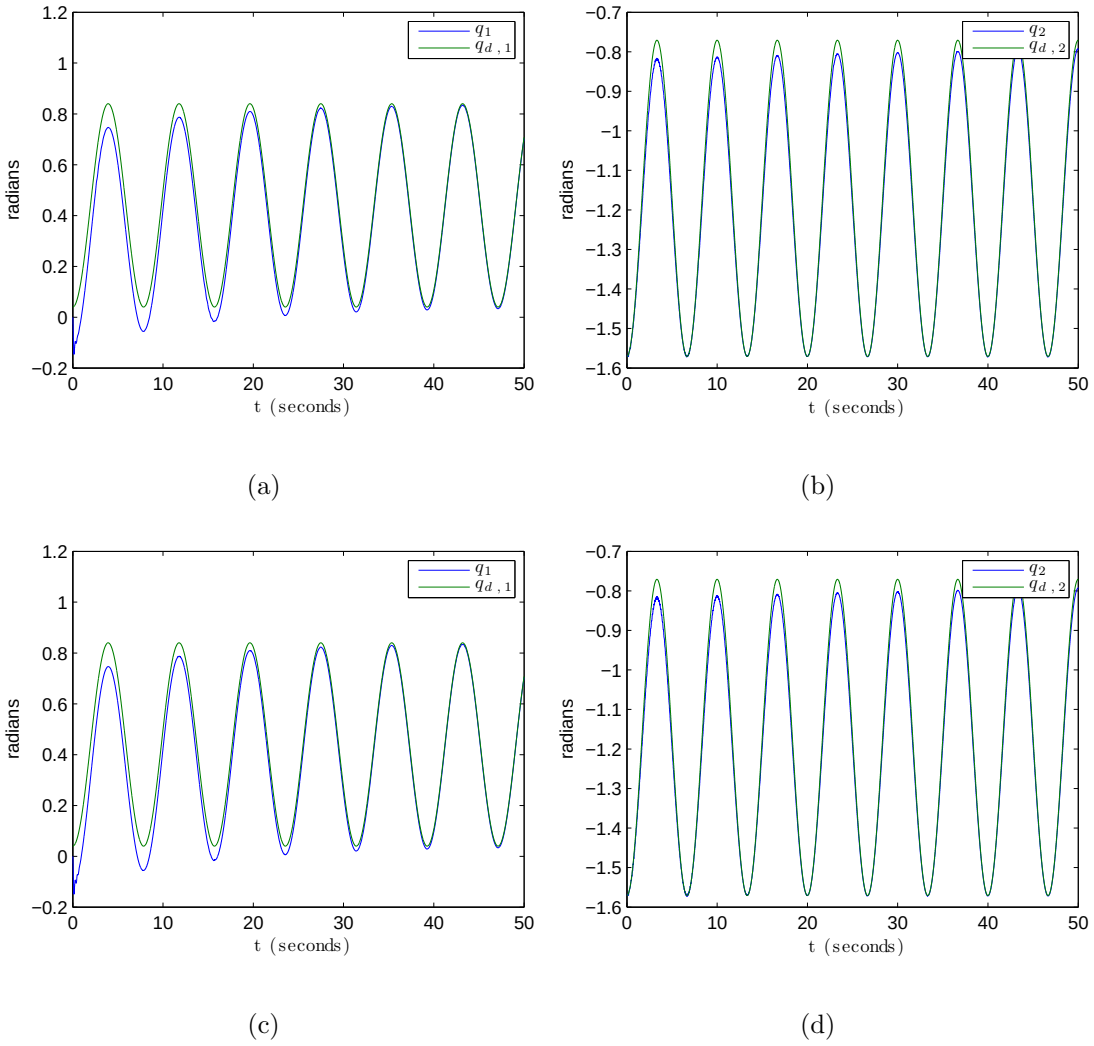

Figure 6.4: The desired joint positions and the actual positions of the robot. (a), (b) $\sigma = 0.6$, (c), (d) $\sigma = 0.95$

6.5.2 Experimental Results

PHANToM Omni, a picture shown in Figure 6.5, is a 6 degree of freedom robotic manipulator. It uses IEEE-1394 Firewire to communicate with a computer. The OpenHaptics 3.0 [84] is an API that allows one to program the PHANToM Omni and one can perform tasks such as reading the sensors and controlling the joint

torques.

Figure 6.5: PHANToM Omni^{TM}

For the experiments presented here, only the second and third joint have been kept active. The first joint was never actuated, and the remaining joints were either removed or constrained to a fixed position. Hence, this provides a simple test bed for the event-triggered controller developed in the previous sections.

The OpenHaptics 3.0 API does not provide the capability to arbitrarily choose the sampling and control update instants. The API samples the sensors and updates the control torques at a roughly constant inter-tick period of 1 milli-seconds. Figure 6.6 shows the cumulative frequency distribution of the inter-tick times for a typical experiment. As can be seen most of the ticks occur with a 1 milli-second period or a frequency of 1000Hz. Hence, in the experiments the event-triggering condition was checked at a roughly constant frequency of 1000Hz.

The experimental results are presented in Figure 6.7. Joint 2 tracking is comparable to the simulation results, though with more error near the peaks. In the beginning of the experiment, Joint 1 tracking error converges to zero faster compared to the simulation results. This is because of the physical joint limits, due to which Joint 1 is at equilibrium in the beginning of the experiment. On the other

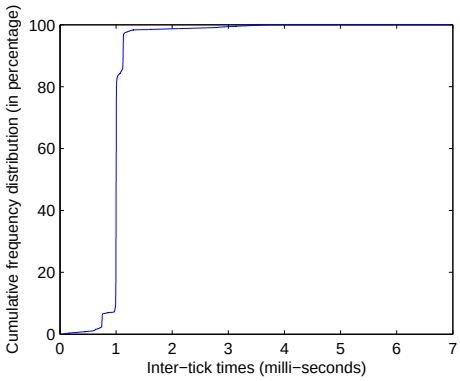

Figure 6.6: The cumulative frequency distribution of the inter-tick times of the PHANToM Omni$^{\text{TM}}$.

hand, in the simulation, joint limits are not considered, and hence Link 1 is in free fall in the beginning, which contributes to the sharp rise in the tracking error and slightly slower convergence of Joint 1 tracking error. In experiments, there are also unmodeled factors such as friction which contribute to the persisting tracking error, specially near the peaks and troughs of the $q_{d,1}$ and $q_{d.2}$.

The observed minimum inter-update times and average frequency in simulations are reported in Table 6.2. The observed minimum inter-update time is, however, partly determined by the roughly fixed sampling and control update frequency inherent in the Phantom Omni system. Figure 6.8 shows the cumulative distribution of the control inter-update times. The maximum inter-update time was around 0.6s and 0.98s, in the experiments with $\sigma = 0.6$ and $\sigma = 0.95$, respectively.

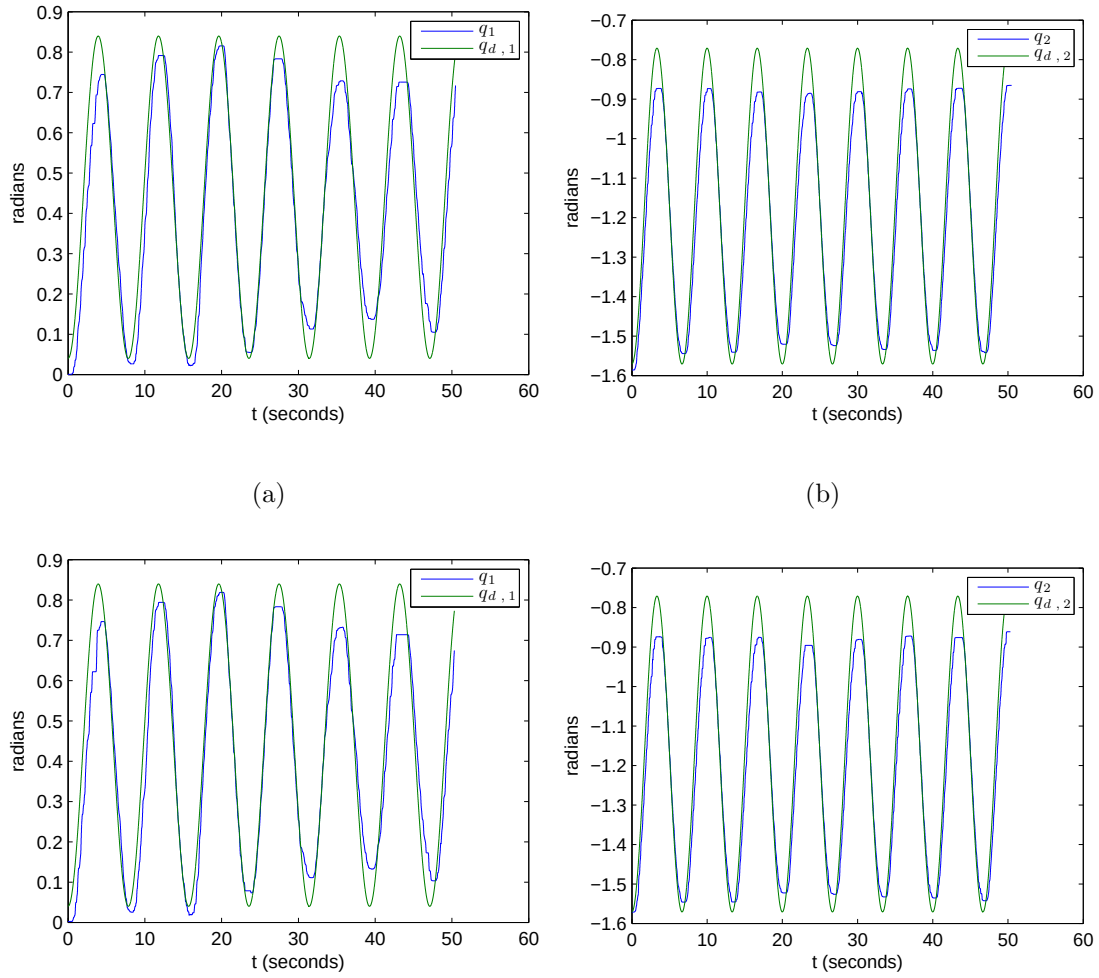

Figure 6.7: The desired joint positions and the actual positions of the robot. (a), (b) $\sigma = 0.6$, (c), (d) $\sigma = 0.95$

6.6 Conclusions

A major drawback of the event-triggered control paradigm is that it requires an accurate model of the system, which is not always possible to obtain. Motivated by this challenge to the practical utility of event-triggered control, we seek to design event based adaptive controllers. In this chapter, an event based implementation

Table 6.2: The observed minimum inter-update times and average frequency in experiments.

σ	Observed minimum inter-update time (s)	Observed average Frequency (Hz)
0.6	9.8×10^{-4}	50
0.95	9.8×10^{-4}	34

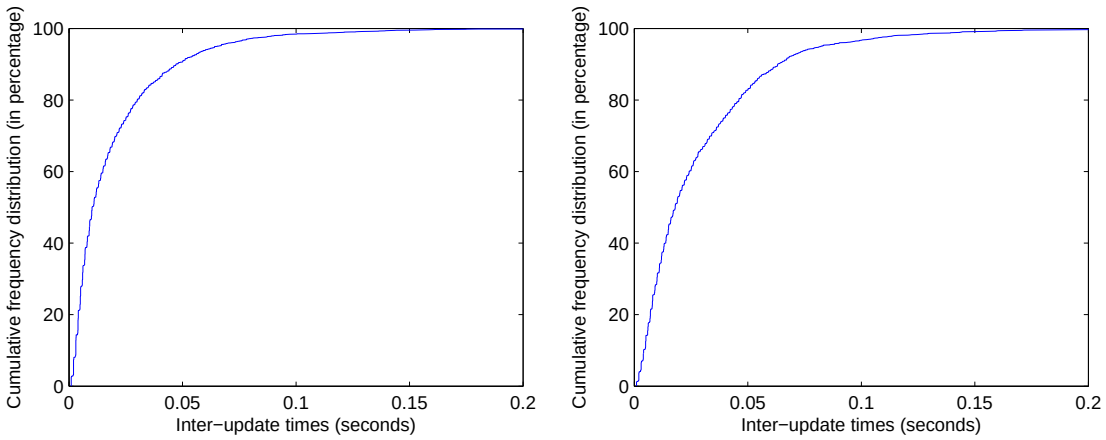

(a) (b)

Figure 6.8: The cumulative frequency distribution of the control inter-update times in the experiments. (a) $\sigma = 0.6$, (b) $\sigma = 0.95$

of an adaptive controller for trajectory tracking in robot manipulators has been presented. More precisely, an existing continuous-time adaptive controller from the literature was chosen and an event-trigger was designed in a manner similar to that in [32] for trajectory tracking applications. Then, simulation and experimental results on a two-link planar manipulator were presented demonstrating the efficacy

of the algorithm. Both simulation and experimental results demonstrate the promise that event based algorithms hold in robotic applications. Future work will include improving the event-triggering and adaptation to obtain better results and numerical analysis necessary for estimating the inter-update times.

Chapter 7

Conclusions

This dissertation is motivated by the need to design efficient sampled data controllers through utility driven event-triggering. Much of the existing literature in the area is applicable for fixed-point stabilization under full state feedback. This dissertation explores a few important classes of problems where only imperfect information, of different kinds, is available.

The dissertation is broadly divided into three parts. The first part of the dissertation is utility driven event-triggering under partial state information. Much of the existing literature on event-triggered control assumes the availability of the full state information to the event-trigger. This assumption fails to be satisfied in two very important scenarios - decentralized control systems and dynamic output feedback control. The first scenario is addressed in Chapter 2, where in a control system with distributed sensors and a central controller is considered. The decentralized sensors together are assumed to sense the complete state of the system, which however transmit data to the central controller intermittently and asynchronously at time instants determined by local utility driven event-triggers. We were able to approach this problem with less restrictive assumptions than in some of the references. Unlike in the literature, we were also able to guarantee semi-global asymptotic stability for nonlinear systems and global asymptotic stability for linear systems without the

sensors having to listen to the controller. However, in the nonlinear case the design is conservative. Thus, we also proposed a modification, wherein the sensors occasionally receive updates from the controller.

Chapter 3 addressed the scenario where a system inherently lacks full state feedback and an output feedback dynamic (for example, observer based) controller has to be used. This chapter is concerned solely with Multi Input Multi Output (MIMO) Linear Time Invariant (LTI) systems. This problem naturally extends to the case where the sensors are decentralized and not co-located with the controller. In this chapter, we in fact progress from a centralized architecture where the sensors, controller and the actuators are co-located to a fully decentralized control system - a Sensor-Controller-Actuator Network (SCAN). Again, unlike in the existing literature, we were able to guarantee global asymptotic stability. Even in the most general of the architectures considered in this chapter, Sensor-Controller-Actuator Network (SCAN), the assumptions on the system matrices are fairly simple. In future, the ideas used in these two chapters will be utilized to design schemes to decentralize sophisticated centralized event-triggers.

The second part expands the definition of utility driven sampling to include sampling in both time and space. The fields of event-triggered control and coarsest quantization have very similar motivations, although they are aimed at 'coarse sampling' in time and space, respectively. In Chapter 4, we exploit the common principle behind the two fields, which is robustness/tolerance to measurement errors, to design implicitly verified discrete-event emulation based controllers for asymptotic stabilization of general nonlinear systems. In comparison to the coarsest quantization

literature, our quantizer design holds for general multi-input nonlinear continuous time systems.

The third part is on utility driven sampled data control for trajectory tracking. Tracking a time varying trajectory or even a set-point is of tremendous practical importance in many control applications. In these applications, the goal is to make the state of the system follow a reference or desired trajectory, which is usually specified as an exogenous input to the system. In Chapter 5, a method for designing utility driven event-triggered controllers for trajectory tracking in nonlinear systems is proposed.

In Chapter 6, we propose a utility driven sampled data implementation of an adaptive controller for trajectory tracking in robot manipulators. This is motivated by the fact that commonly, utility driven event-triggered controllers such as the one presented in Chapter 5 rely on the knowledge of an accurate model of the system. However, building a model of high accuracy is a time consuming process and in many cases, it may not even be possible. Therefore, it is important to extend the design of implicitly verified event based controllers to cases where only a poor model of the system is available. In this work, we propose an event-triggered emulation of an adaptive controller from the existing literature.

Bibliography

[1] P. Ellis. Extension of phase plane analysis to quantized systems. *IRE Transactions on Automatic Control*, 4(2):43–54, 1959.

[2] R. Dorf, M. Farren, and C. Phillips. Adaptive sampling frequency for sampled-data control systems. *IRE Transactions on Automatic Control*, 7(1):38–47, 1962.

[3] A.M. Phillips and M. Tomizuka. Multirate estimation and control under time-varying data sampling with applications to information storage devices. In *American Control Conference*, volume 6, pages 4151–4155, 1995.

[4] D. Seto, J.P. Lehoczky, L. Sha, and K.G. Shin. On task schedulability in real-time control systems. In *rtss*, page 13. Published by the IEEE Computer Society, 1996.

[5] W.P.M.H. Heemels, R.J.A. Gorter, A. van Zijl, P.P.J. Van den Bosch, S. Weiland, W.H.A. Hendrix, and M.R. Vonder. Asynchronous measurement and control: a case study on motor synchronization. *Control Engineering Practice*, 7(12):1467–1482, 1999.

[6] K.J. Åström and B.M. Bernhardsson. Comparison of Riemann and Lebesgue sampling for first order stochastic systems. In *41st IEEE Conference on Decision and Control*, Las Vegas, USA, Dec 2002.

[7] K.J. Åström and B. Bernhardsson. Systems with Lebesgue sampling. In Anders Rantzer and Christopher Byrnes, editors, *Directions in Mathematical Systems Theory and Optimization*, volume 286 of *Lecture Notes in Control and Information Sciences*, pages 1–13. Springer Berlin / Heidelberg, 2003.

[8] D. Hristu-Varsakelis and P.R. Kumar. Interrupt-based feedback control over a shared communication medium. In *41st IEEE Conference on Decision and Control*, volume 3, pages 3223–3228, 2002.

[9] P. Tabuada and X. Wang. Preliminary results on state-trigered scheduling of stabilizing control tasks. In *45th IEEE Conference on Decision and Control*, pages 282–287, 2006.

[10] K.-E. Årzén. A simple event-based PID controller. In *Preprints 14th World Congress of IFAC*, Beijing, P.R. China, Jan 1999.

[11] M. Miskowicz. The event-triggered sampling optimization criterion for distributed networked monitoring and control systems. In *IEEE International Conference on Industrial Technology*, volume 2, pages 1083–1088, 2003.

[12] J.H. Sandee. *Event-driven control in theory and practice*. PhD thesis, Technische Universiteit Eindhoven, Eindhoven, Dec 2006.

[13] Ernesto Kofman and Julio H Braslavsky. Level crossing sampling in feedback stabilization under data-rate constraints. In *IEEE Conference on Decision and Control*, pages 4423–4428. IEEE, 2006.

[14] P. Tabuada. Event-triggered real-time scheduling of stabilizing control tasks. *IEEE Transactions on Automatic Control*, 52(9):1680–1685, 2007.

[15] W.P.M.H. Heemels, J.H. Sandee, and P.P.J. Van Den Bosch. Analysis of event-driven controllers for linear systems. *International Journal of Control*, 81(4):571–590, 2008.

[16] K.J. Åström. Event based control. In Alessandro Astolfi and Lorenzo Marconi, editors, *Analysis and Design of Nonlinear Control Systems: In Honor of Alberto Isidori*, pages 127–147. Springer Berlin Heidelberg, 2008.

[17] X. Wang and M.D. Lemmon. Event design in event-triggered feedback control systems. In *47th IEEE Conference on Decision and Control*, pages 2105–2110, 2008.

[18] X. Wang and M.D. Lemmon. Self-triggered feedback control systems with finite-gain $\mathcal{L}_2$ stability. *IEEE Transactions on Automatic Control*, 54:452–467, 2009.

[19] X. Wang and M.D. Lemmon. Self-triggering under state-independent disturbances. *IEEE Transactions on Automatic Control*, 55(6):1494–1500, 2010.

[20] Manel Velasco, Pau Martí, and Enrico Bini. On Lyapunov sampling for event-driven controllers. In *IEEE Conference on Decision and Control and Chinese Control Conference*, pages 6238–6243. IEEE, 2009.

[21] J. Lunze and D. Lehmann. A state-feedback approach to event-based control. *Automatica*, 46(1):211–215, 2010.

[22] M. D. Lemmon. Event-triggered feedback in control, estimation, and optimization. In Alberto Bemporad, Maurice Heemels, and Mikael Johansson, editors, *Networked Control Systems*, volume 406 of *Lecture Notes in Control and Information Sciences*, pages 293–358. Springer Berlin / Heidelberg, 2011.

[23] Peter JG Ramadge and W Murray Wonham. The control of discrete event systems. *Proceedings of the IEEE*, 77(1):81–98, 1989.

[24] A. Anta and P. Tabuada. Self-triggered stabilization of homogeneous control systems. In *American Control Conference*, pages 4129–4134, 2008.

[25] M. Lemmon, T. Chantem, X.S. Hu, and M. Zyskowski. On self-triggered full-information h-infinity controllers. *HSCC 2007*, 4416:371, 2007.

[26] A. Anta and P. Tabuada. Space-time scaling laws for self-triggered control. In *47th IEEE Conference on Decision and Control*, pages 4420–4425, 2008.

[27] M. Mazo Jr, A. Anta, and P. Tabuada. On self-triggered control for linear systems: Guarantees and complexity. In *European control conference*, 2009.

[28] A. Anta and P. Tabuada. To sample or not to sample: Self-triggered control for nonlinear systems. *IEEE Transactions on Automatic Control*, 55(9):2030–2042, 2010.

[29] P. Tallapragada and N. Chopra. Event-triggered dynamic output feedback control for LTI systems. In *IEEE Conference on Decision and Control*, pages 6597–6602, 2012.

[30] P. Tallapragada and N. Chopra. Event-triggered decentralized dynamic output feedback control for LTI systems. In *Estimation and Control of Networked Systems*, volume 3, pages 31–36, 2012.

[31] P. Tallapragada and N. Chopra. On co-design of event trigger and quantizer for emulation based control. In *American Control Conference*, pages 3772–3777, 2012.

[32] P. Tallapragada and N. Chopra. On event triggered trajectory tracking for control affine nonlinear systems. In *IEEE Conference on Decision and Control and European Control Conference*, pages 5377–5382, 2011.

[33] P. Tallapragada and N. Chopra. On event triggered tracking for nonlinear systems. *IEEE Transactions on Automatic Control*. Accepted.

[34] WPMH Heemels, Karl Henrik Johansson, and P Tabuada. An introduction to event-triggered and self-triggered control. In *IEEE Conference on Decision and Control*, pages 3270–3285. IEEE, 2012.

[35] M. Mazo Jr. and M. Cao. Decentralized event-triggered control with asynchronous updates. In *IEEE Conference on Decision and Control and European Control Conference*, pages 2547 –2552, 2011.

[36] M. Mazo Jr. and M. Cao. Decentralized event-triggered control with one bit communications. In *IFAC Conference on Analysis and Design of Hybrid Systems*, pages 52–57, 2012.

[37] Manuel Mazo Jr and Ming Cao. Asynchronous decentralized event-triggered control. *arXiv preprint arXiv:1206.6648v1 [math.OC]*, 2012.

[38] X. Wang and M. Lemmon. Event-triggering in distributed networked systems with data dropouts and delays. *Hybrid systems: Computation and control*, pages 366–380, 2009.

[39] X. Wang and M.D. Lemmon. Event triggering in distributed networked control systems. *IEEE Transactions on Automatic Control*, 56(3):586–601, 2011.

[40] M.C.F. Donkers and W.P.M.H. Heemels. Output-based event-triggered control with guaranteed $\mathcal{L}_\infty$-gain and improved and decentralized event-triggering. *Automatic Control, IEEE Transactions on*, 57(6):1362–1376, 2012.

[41] M.C.F. Donkers and W. Heemels. Output-based event-triggered control with guaranteed $\mathcal{L}_\infty$-gain and improved event-triggering. In *IEEE Conference on Decision and Control*, pages 3246–3251, 2010.

[42] D. Lehmann and J. Lunze. Event-based output-feedback control. In *Mediterranean Conference on Control & Automation*, pages 982–987, 2011.

[43] L. Li and M. Lemmon. Weakly coupled event triggered output feedback control in wireless networked control systems. In *Annual Allerton Conference on Communication, Control, and Computing*, pages 572–579, 2011.

[44] J. Almeida, C. Silvestre, and A. M. Pascoal. Observer based self-triggered control of linear plants with unknown disturbances. In *American Control Conference*, pages 5688–5693, 2012.

[45] H.K. Khalil. *Nonlinear systems*. Prentice Hall, third edition, 2002.

[46] M. Mazo Jr. and P. Tabuada. Decentralized event-triggered control over Wireless Sensor/Actuator Networks. *IEEE Transactions on Automatic Control*, 56(10):2456–2461, 2011.

[47] G.C. Walsh and H. Ye. Scheduling of networked control systems. *IEEE Control Systems Magazine*, 21(1):57–65, 2001.

[48] L. Li and M. Lemmon. Event-triggered output feedback control of finite horizon discrete-time multi-dimensional linear processes. In *IEEE Conference on Decision and Control*, pages 3221–3226, 2010.

[49] F. Dorfler, F. Pasqualetti, and F. Bullo. Continuous-time distributed observers with discrete communication. *Selected Topics in Signal Processing, IEEE Journal of*, 2013.

[50] G.N. Nair, F. Fagnani, S. Zampieri, and R.J. Evans. Feedback control under data rate constraints: an overview. *Proceedings of the IEEE*, 95(1):108–137, 2007.

[51] W.S. Wong and R.W. Brockett. Systems with finite communication bandwidth constraints. ii. stabilization with limited information feedback. *IEEE Transactions on Automatic Control*, 44(5):1049–1053, 1999.

[52] G.N. Nair and R.J. Evans. Stabilization with data-rate-limited feedback: tightest attainable bounds. *Systems & Control Letters*, 41(1):49–56, 2000.

[53] S. Tatikonda and S. Mitter. Control under communication constraints. *IEEE Transactions on Automatic Control*, 49(7):1056–1068, 2004.

[54] C. De Persis. n-bit stabilization of n-dimensional nonlinear systems in feedforward form. *IEEE Transactions on Automatic Control*, 50(3):299–311, 2005.

[55] Q. Ling, M.D. Lemmon, and H. Lin. Asymptotic stabilization of dynamically quantized nonlinear systems in feedforward form. *Journal of Control Theory and Applications*, 8(1):27–33, 2010.

[56] R.W. Brockett and D. Liberzon. Quantized feedback stabilization of linear systems. *IEEE Transactions on Automatic Control*, 45(7):1279–1289, 2000.

[57] D. Liberzon. Hybrid feedback stabilization of systems with quantized signals. *Automatica*, 39(9):1543–1554, 2003.

[58] D. Liberzon and J.P. Hespanha. Stabilization of nonlinear systems with limited information feedback. *IEEE Transactions on Automatic Control*, 50(6):910–915, 2005.

[59] D. Liberzon. Quantization, time delays, and nonlinear stabilization. *IEEE Transactions on Automatic Control*, 51(7):1190–1195, 2006.

[60] C. De Persis and A. Isidori. Stabilizability by state feedback implies stabilizability by encoded state feedback. *Systems & control letters*, 53(3-4):249–258, 2004.

[61] Daniel Lehmann and Jan Lunze. Event-based control using quantized state information. In *Estimation and Control of Networked Systems*, pages 1–6, 2010.

[62] Lichun Li, Xiaofeng Wang, and Michael Lemmon. Stabilizing bit-rates in quantized event triggered control systems. In *International Conference on Hybrid Systems: Computation and Control*, pages 245–254, 2012.

[63] N. Elia. Design of hybrid systems with guaranteed performance. In *39th IEEE Conference on Decision and Control*, volume 1, pages 993–998, 2000.

[64] N. Elia and S.K. Mitter. Stabilization of linear systems with limited information. *IEEE Transactions on Automatic Control*, 46(9):1384–1400, 2001.

[65] N. Elia and E. Frazzoli. Quantized stabilization of two-input linear systems: a lower bound on the minimal quantization density. *Hybrid Systems: Computation and Control*, pages 335–349, 2002.

[66] M. Fu and L. Xie. The sector bound approach to quantized feedback control. *IEEE Transactions on Automatic Control*, 50(11):1698–1711, 2005.

[67] C.Y. Kao and S.R. Venkatesh. Stabilization of linear systems with limited information multiple input case. In *American Control Conference*, volume 3, pages 2406–2411, 2002.

[68] H. Haimovich and M.M. Seron. On infimum quantization density for multiple-input systems. In *IEEE Conference on Decision and Control and European Control Conference*, pages 7692–7697, 2005.

[69] H. Haimovich, MM Seron, and GC Goodwin. Geometric characterization of multivariable quadratically stabilizing quantizers. *International Journal of Control*, 79(8):845–857, 2006.

[70] H. Haimovich and M.M. Seron. Multivariable quadratically-stabilizing quantizers with finite density. *Automatica*, 44(7):1880–1885, 2008.

[71] J. Liu and N. Elia. Quantized feedback stabilization of non-linear affine systems. *International Journal of Control*, 77(3):239–249, 2004.

[72] F. Ceragioli and C. De Persis. Discontinuous stabilization of nonlinear systems: Quantized and switching controls. *Systems & control letters*, 56(7-8):461–473, 2007.

[73] D. Liberzon. *Switching in systems and control*. Birkhäuser, 2003.

[74] R. Goebel, R. Sanfelice, and A. Teel. Hybrid dynamical systems. *IEEE Control Systems Magazine*, 29(2):28–93, 2009.

[75] H. Yu and P.J. Antsaklis. Event-triggered real-time scheduling for stabilization of passive and output feedback passive systems. In *American Control Conference*, pages 1674 –1679, 2011.

[76] Eloy Garcia and Panos J. Antsaklis. Parameter estimation in time-triggered and event-triggered model-based control of uncertain systems. *International Journal of Control*, 85(9):1327–1342, 2012.

[77] Toivo Henningsson and Anton Cervin. Comparison of LTI and event-based control for a moving cart with quantized position measurements. In *European Control Conference*, 2009.

[78] A. Camacho, P. Martí, M. Velasco, C. Lozoya, R. Villa, J.M. Fuertes, and E. Griful. Self-triggered networked control systems: an experimental case study. In *IEEE International Conference on Industrial Technology*, pages 123–128. IEEE, 2010.

[79] Sebastian Trimpe and Raffaello DAndrea. An experimental demonstration of a distributed and event-based state estimation algorithm. In *IFAC World Congress*, pages 8811–8818, 2011.

[80] D. Lehmann and J. Lunze. Extension and experimental evaluation of an event-based state-feedback approach. *Control Engineering Practice*, 19(2):101–112, 2011.

[81] H. Berghuis, R. Ortega, and H. Nijmeijer. A robust adaptive controller for robot manipulators. In *IEEE International Conference on Robotics and Automation*, pages 1876–1881, 1992.

[82] M.W. Spong, S. Hutchinson, and M. Vidyasagar. *Robot Modeling and Control*. John Wiley & Sons, Inc., New York, 2006.

[83] J. Slotine and L. Weiping. Adaptive manipulator control: A case study. *IEEE Transactions on Automatic Control*, 33(11):995–1003, 1988.

[84] SensAble Technologies *OpenHaptics Toolkit 3.0*, Jan 2009, http://www.sensable.com/products-openhaptics-toolkit.htm.